UNIVERSIDADE FEDERAL DO CEARÁ

INSTITUTO DE CIÊNCIAS DO MAR - LABOMAR

PROGRAMA DE PÓS-GRADUAÇÃO EM CIÊNCIAS MARINHAS TROPICAIS

MARIANY SOUSA CAVALCANTE

CARACTERIZAÇÃO DA MATÉRIA ORGÂNICA NATURAL NO ESTUÁRIO DO RIO JAGUARIBE EM DIFERENTES ESTAÇÕES CLIMÁTICAS EM ANOS DE SECA PROLONGADA

FORTALEZA

2019

MARIANY SOUSA CAVALCANTE

CARACTERIZAÇÃO DA MATÉRIA ORGÂNICA NATURAL NO ESTUÁRIO DO RIO JAGUARIBE EM DIFERENTES ESTAÇÕES CLIMÁTICAS EM ANOS DE SECA PROLONGADA

Tese apresentada ao Programa de Pós-Graduação em Ciências Marinhas Tropicais da Universidade Federal do Ceará, como requisito parcial à obtenção do título de Doutora em Ciências Marinhas Tropicais.

Orientadora: Profa. Dra. Rozane Valente Marins.

Fortaleza

2019

Dados Internacionais de Catalogação na Publicação
Universidade Federal do Ceará
Biblioteca Universitária
Gerada automaticamente pelo módulo Catalog, mediante os dados fornecidos pelo(a) autor(a)

C364c Cavalcante, Mariany.
Caracterização da matéria orgânica natural no estuário do rio Jaguaribe em diferentes estações climáticas em anos de seca prolongada / Mariany Cavalcante. – 2019.
125 f. : il. color.

Tese (doutorado) – Universidade Federal do Ceará, Instituto de Ciências do Mar, Programa de Pós-Graduação em Ciências Marinhas Tropicais, Fortaleza, 2019.
Orientação: Profa. Dra. Rozane Valente Marins.

1. carbono. 2. isótopos estáveis. 3. ultrafiltração. 4. aromaticidade. I. Título.

CDD 551.46

MARIANY SOUSA CAVALCANTE

CARACTERIZAÇÃO DA MATÉRIA ORGÂNICA NATURAL NO ESTUÁRIO DO RIO JAGUARIBE EM DIFERENTES ESTAÇÕES CLIMÁTICAS EM ANOS DE SECA PROLONGADA

Tese apresentada ao Programa de Pós-Graduação em Ciências Marinhas Tropicais da Universidade Federal do Ceará, como requisito parcial à obtenção do título de Doutora em Ciências Marinhas Tropicais.

Aprovada em: ____/___/_____.

BANCA EXAMINADORA

_____
Profa. Dra. Rozane Valente Marins (Orientadora)
Universidade Federal do Ceará (UFC)

_____
Prof. Dr. Carlos Eduardo de Rezende
Universidade Estadual do Norte Fluminense (UENF)

_____
Prof. Dr. Sergio Rossi
Università del Salento

_____
Prof. Dr. Tristan Rousseau
Universidade Federal do Ceará (UFC)

_____
Prof. Dr. Luiz Drude de Lacerda
Universidade Federal do Ceará (UFC)

A Deus.

À minha família, Avanatan, Marcos, Luciene, Lucas, Priscila, Breno e Benício.

Aos meus amigos.

AGRADECIMENTOS

À Professora Dra. Rozane Valente Marins, pela excelente orientação, apoio e incentivo para o desenvolvimento deste trabalho. Seus esforços foram além do seu dever como professora e eu reconheço e serei eternamente grata por isto. Ao professor Dr Luiz Drude de Lacerda, por estar sempre disposto a esclarecer minhas dúvidas e compartilhar seu conhecimento.

Aos professores participantes da banca examinadora Sergio Rossi, Carlos Eduardo de Rezende, Tristan Rousseau e Luiz Drude de Lacerda pela disponibidade, colaborações e sugestões para este trabalho.

Agradeço ao professor Carlos Eduardo de Rezende por me receber no Laboratório de Ciências Ambientais, da Universidade Estadual do Norte Fluminense Darcy Ribeiro (UENF), para realizar as análises de isótopos e lignina. Agradeço também a todos os amigos que fiz na UENF, que me auxiliaram nos campos e análises e que me deram suporte durante este período, como, Bráulio, Thiago, Fred, Beatriz, Vivian, Joviana, Jessica, Camila, Cinara, Emilane, Diegos, Jeffersson, Igor, Jomar e Karol.

Muito obrigada, professor Stéphane Mounier, por me receber no MIO de Toulon, França, para realização das análises de fluorescência da matéria orgânica. Agradeço também aos amigos que me acolheram e me ajudaram com as análises: Amonda, Deborah, Cyril, Sébastien e Nicolas.

À minha família, Avanatan, Marcos, Lucas, Priscila e Breno, e amigos pelo apoio, incentivo e compreensão.

Aos meus amigos do Laboratório de Biogeoquímica Costeira, Isabelle, Raisa, Ingra, Jessyca, Thays, Ana Paula, Victor, César, Leonardo, Ricarda, Richelle e Matheus por estarem sempre disponíveis a ajudar, a esclarecer dúvidas e ensinar algo novo. Especialmente à Raisa, que nunca mediu esforços a me ajudar na preparação e execução dos campos, bem como com a elaboração das figuras.

À FUNCAP (PRONEX PR2 - 0101 - 00052.01.00/15) pelo financiamento da pesquisa. À CAPES, pelo apoio financeiro com a manutenção da bolsa de auxílio. Ao Programa de Pós-graduação em Ciências Marinhas Tropicais pelo auxílio financeiro para o estágio realizado na França.

Obrigada!

“O Rio Jaguaribe é uma artéria aberta

por onde escorre

e se perde

o sangue do Ceará.

O mar não se tinge de vermelho

porque o sangue do Ceará

é azul ...”

Demócrito Rocha

RESUMO

Este trabalho avaliou como os fatores hidrodinâmicos e sazonais afetaram os fluxos, teores e origem da matéria orgânica natural (MON) no estuário do rio Jaguaribe, além da sua interação com metais dissolvidos, medidos por ICP MS. O período estudado foi de acentuada redução do aporte de água doce causada pela escassez de chuva e controle artificial do rio por barragens, levando o estuário a condições de hipersalinidade, em 2016. A composição isotópica ($\delta^{13}C$ e $\delta^{15}N$) e análises de fluorescência da MON mostraram que ela foi oriunda preponderantemente de fontes terrestres. No entanto, a contribuição da MON marinha também foi relevante, aumentando em anos mais secos devido à maior intrusão salina no estuário. Em concordância com a caracterização isotópica, o carbono orgânico dissolvido (COD) foi composto preponderantemente por substâncias húmicas e não mostrou correlação com a atividade biológica, provavelmente por ser refratário. Contudo, a diminuição não conservativa do COD e da aromaticidade da MON, representada pela absorbância UV específica em 254nm (SUVA), com o aumento da salinidade sugere que essa MON é quimicamente ativa. A matéria orgânica verdadeiramente dissolvida (<1 kDa) foi a principal fração de COD, correspondendo a 80 ± 2%. Observou-se uma redução no tamanho das partículas de MON com a mistura estuarina promovida provavelmente pela decomposição da MON. Os metais Cr, Fe, V, Al, Cu e Ni apresentaram correlação significativa com o COD e redução com o aumento da salinidade. A concentração da MON foi fortemente controlada pela hidrodinâmica estuarina, aumentando com o tempo de residência e o percentual de água doce. Entretanto, a redução do aporte de água doce para o estuário resultou em fluxos de carbono para o oceano inferiores aos esperados para a região tropical. A zona de mistura estuarina comportou-se como retentora de carbono durante a seca e como exportadora na estação chuvosa. É possível que estes resultados sejam um prognóstico das alterações ambientais estuarinas no clima tropical semiárido, resultantes da diminuição do aporte fluvial e maior intrusão marinha em cenário de mudanças climáticas globais.

Palavras-chave: carbono, isótopos estáveis, ultrafiltração, aromaticidade.

ABSTRACT

This work evaluated how seasonal and hydrodynamic factors affected the fluxes, contents, and origin of natural organic matter (NOM) in the Jaguaribe River estuary, as well as its interaction with dissolved metals, measured by ICP MS. The period was characterized by a strong reduction in freshwater input to the estuarine region caused by rainfall shortages and artificial river control by dams, leading the estuary to hypersalinity conditions in 2016. The isotopic composition ($\delta^{13}C$ and $\delta^{15}N$) and fluorescence analyzes of NOM showed that it originates mainly from terrestrial sources. However, the contribution of marine NOM was also relevant, increasing in drier years due to increased saline intrusion into the estuary. In agreement with the isotopic characterization, the dissolved organic carbon (DOC) was composed mainly of humic substances and showed no correlation with the biological activity, probably due to its refractory nature. However, the non-conservative decrease in COD and NOM aromaticity, represented by specific UV absorbance at 254 nm (SUVA), with increasing salinity suggests that this MON was chemically active. Truly dissolved organic matter (<1 kDa) was the main fraction of DOC, corresponding to 80 ± 2%. A reduction in NOM particle size was observed with the estuarine mixture, probably promoted by the decomposition of MON. Cr, Fe, V, Al, Cu and Ni presented a significant correlation with DOC and a concentration reduction with the increase of salinity. MON concentrations were controlled by the estuarine hydrodynamics, increasing with residence time and freshwater percentage. However, the reduction of freshwater input to the estuary resulted in carbon flows to the ocean lower than expected in tropical regions. The estuarine mixing zone behave as a carbon retainer during the drought and as an exporter in the rainy season. These results may be a prognostic of the environmental changes in the estuaries under semiarid tropical climate regions due to the decrease of the riverine inflow and high marine intrusion in a scenario of global climate change.

Keywords: carbon, stable isotopes, ultrafiltration, aromaticity.

LISTA DE FIGURAS

LISTA DE TABELAS

SUMÁRIO

1. INTRODUÇÃO

A zona costeira (ZC) representa apenas 8% da superfície terrestre (CROSSLAND et al., 2005), porém é um importante contribuinte no balanço global de carbono devido aos seus fortes gradientes e fluxos de matéria e energia, tanto em direções latitudinal como longitudinal, que promovem elevada produtividade primária, mineralização e sedimentação da matéria orgânica (BAUER et al., 2013; CAI, 2011). A interação entre os domínios continente e oceano caracteriza a ZC como um conjunto de ecossistemas únicos com elevada concentração de energia, sedimentos e nutrientes.

Na região tropical, o fluxo fluvial de carbono para o oceano é de 0,53 PgC ano^{-1}, sendo 0,21 PgC ano^{-1} (40%) de carbono inorgânico dissolvido (CID), 0,14 PgC ano^{-1} (25%) de carbono orgânico dissolvido (COD), 0,05 PgC ano^{-1} (10%) de carbono inorgânico particulado (CIP) e 0,13 PgC ano^{-1} (25%) de carbono orgânico particulado (COP) (HUANG et al., 2012). É estimado que o fluxo fluvial global de carbono orgânico dissolvido (COD) para o oceano seja de aproximadamente 0,19 PgC ano^{-1} (1 Pg = 10^{15} g) (DAI et al., 2012), levando em consideração a taxa de remoção de 10% de COD pelos estuários, a estimativa é reduzida para 0,17 PgC ano^{-1}. Como o fluxo de COD depende preponderantemente da vazão fluvial, os maiores fluxos de COD correspondem à América do Sul com 0,08 PgC ano^{-1}, que possui as maiores descargas fluviais (DAI et al., 2012).

Entretanto, as incertezas dessas estimativas estão relacionadas às mudanças sazonais e à amostragem desproporcional espacialmente, pois estas abordam majoritariamente rios de grande porte, como o Amazonas, Orinoco, Congo e Niger (HUANG et al., 2012; WU et al., 2013), que são menos vulneráveis aos fatores naturais (sazonalidade) e antrópicos quando comparados a rios de menor porte. Logo, faz-se necessário o aumento de estudos em rios de menor porte, principalmente frente às mudanças climáticas globais que somada ao rápido desenvolvimento da economia e da população têm alterado o fluxo de carbono através desses ambientes (HUNG; HUANG, 2005; MOORE et al., 2013; OURSEL et al., 2013; STANLEY et al., 2012; WORRALL; BURT; ADAMSON, 2004).

Os estuários são ecossistemas da zona costeira de grande relevância para a compreensão do Ciclo Global de Carbono (CGC), pois estabelecem a principal conexão entre os dois maiores reservatórios de carbono da superfície terrestre, o oceano e o continente (ATEKWANA; TEDESCO; JACKSON, 2003; CAI, 2011). Eles atuam como reatores biogeoquímicos, promovendo a remoção do carbono de origem terrestre da coluna d'água através da mineralização microbiana (31%) e de processos de mistura (69%) (HE et al., 2010),

além da fixação do carbono atmosférico em biomassa fitoplanctônica através da fotossíntese (ZHAI; DAI, 2009).

A qualidade da matéria orgânica natural (MON) está intimamente relacionada a sua origem (autóctone ou alóctone) (FINDLAY; SINSABAUGH, 2003) e possui um papel determinante no comportamento do carbono estuarino. Em um estuário tropical de pequeno porte, por exemplo, o COD apresentou comportamento conservativo em períodos de grande fluxo fluvial devido a preponderância de COD de origem terrestre com baixa reatividade. Enquanto que durante a seca, a produtividade biológica e a degradação do COD conferiu a ele comportamento não conservativo (WU *et al*., 2013).

Em estuários do semiárido brasileiro, a estimativa de fluxo de carbono é desafiadora devido à grande variabilidade das vazões fluviais (CAMPOS *et al.*, 2000), causada pela forte influência da sazonalidade e das barragens construídas ao longo do curso do rio para abastecimento humano (DIAS *et al*., 2011). Como exemplo, o estuário do rio Jaguaribe é controlado artificialmente por barragens existentes ao longo do seu percurso, que normalizam o aporte de água doce para o estuário, com vazões na ordem de 20,4 a 350 m^3s^{-1} até a zona da foz do rio. Como consequência, tem sido observada a intrusão salina, mudanças nas características hidrológicas e maior retenção de materiais (MARINS et al., 2003; DIAS; MARINS; MAIA, 2009; LACERDA *et al*., 2013).

O controle artificial dos rios pelas barragens provoca a alteração do fluxo de contaminantes e causa efeitos similares ao congelamento das águas de rios de regiões polares (LACERDA *et al*., 2012). Durante a estação seca, os fluxos de contaminantes são minimizados devido ao Tempo de Residência (TR) das águas estuarinas ser relativamente mais elevado, podendo chegar a vários dias. Enquanto que durante o período de maior descarga fluvial, esses fluxos são mais intensos e o TR das águas estuarinas são menores, gerando maior exportação de contaminantes para a zona costeira adjacente (DIAS *et al*., 2011). Dessa forma, é muito provável que este processo também afete o destino e os fluxos de carbono no estuário do rio Jaguaribe visto que seu comportamento é fortemente controlado pelas marés (LACERDA; MARINS; CAVALCANTE, 2017).

Maiores TR em estuários intensificam o processamento de carbono orgânico, pela atividade autóctone fitoplanctônica (LEBRETON et al., 2016), assim como a interação da MO com metais. No estuário do rio Jaguaribe o aumento do tempo de residência fornece uma condição ideal para o acúmulo de material particulado em suspensão (MPS), nutrientes e carbono que podem contribuir para a ocorrência do processo de eutrofização e floculação no estuário (DIAS et al., 2016). Além disso, atividades antropogênicas são fontes significativas

de metais traço (Cu e Hg) (LACERDA et al., 2011; LACERDA; SANTOS; MADRID, 2006), nutrientes e provavelmente MO (ESCHRIQUE et al., 2010; MARINS et al., 2011) para o estuário do rio Jaguaribe. Mesmo localizad**o** em uma área rural, o inventário de fontes de nitrogênio e fósforo apontam que fontes antropogênicas superam em pelo menos uma ordem de grandeza as fontes naturais, destacando-se entre as antrópicas a aquicultura seguida de águas residuais e a pecuária (LACERDA et al. 2008).

A MON pode controlar a mobilidade e biodisponibilidade de metais através da formação de complexos metálicos (MOUNIER et al., 2011), sejam eles importantes para a produção primária, como o cálcio, ou nocivos à biota, como o mercúrio. A associação entre a matéria orgânica dissolvida (MOD) e metais depende do metal, das características da MO e das condições físico-químicas do ambiente como foção iônica, pH e competição com outros cátions (BRULAND; LOHAN, 2003; LOUIS; PERNET-COUDRIER; VARRAULT, 2014). A matéria orgânica coloidal é conhecida por "blindar" os metais, por estarem mais sujeitos a remoção por floculação e/ou sedimentação durante grandes mudanças nos processos de mistura do que esta fração orgânica (WILKINSON; LEAD, 2007). Entretanto, isso está mais ligado a fatores como a labilidade do metal, que está condicionada a fonte da MON, destino (tamanho) do coloide orgânico, polaridade da MON e às condições do meio (LUAN; VADAS, 2015) do que a fração por si só.

Dessa forma, acredita-se que a qualidade da MOD, e sua associação com o os metais ao longo do gradiente de salinidade, tenha sido responsável pelo aumento das concentrações de Hg nas ostras do estuário do rio Jaguaribe dentro de um curto espaço de tempo (13 anos) (RIOS et al., 2016), mostrando níveis tão alto quanto áreas metropolitanas. E também à maior biodisponibilidade de mercúrio em organismos da região estuarina do que na fluvial do estuário do rio Jaguaribe (MOURA; LACERDA, 2018).

Com períodos de chuvas cada vez menores e mais intermitentes, a ação da onda de maré no estuário do rio Jaguaribe tem causado modificações neste importante ecossistema, como a formação de novas ilhas (GODOY; MEIRELES; LACERDA, 2018) e avanço da colonização de manguezais (GODOY; LACERDA, 2015; MAIA et al., 2006), mostrando que as alterações hidrodinâmicas podem alterar o transporte de materiais na interface continente-oceano. Nesse cenário, as concentrações de carbono orgânico podem reduzir, assim como a fonte (marinha versus terrestre) e a qualidade da MON podem ser modificadas. Tudo isso altera não apenas a reatividade OM, mas também o funcionamento do estuário como um todo, devido ao seu papel fundamental no processo biogeoquímico como produção bacteriana, organização da rede trófica, complexação de metal e ciclagem de carbono (SHIN et al.,

2016a; VAZQUEZ et al., 2011). Logo, este trabalho apresenta-se como um elo entre estudos relacionados à mobilidade dos metais e a presença destes na biota do estuário do rio Jaguaribe, visto que a matéria orgânica natural é um importante carreador geoquímico de metais.

O primeiro capítulo contém a presente introdução da tese. O segundo apresenta o referencial bibliográfico sobre a matéria orgânica natural em estuários. O terceiro capítulo traz a hipótese científica e os objetivos do trabalho. O quarto corresponde a um resumo da metodologia de amostragem ao longo dos anos de 2015 a 2018, nas estações seca e chuvosa. O quinto corresponde aos resultados desta tese em forma de três artigos: o primeiro submetido e aceito com revisões a serem feitas para a revista Frontiers in Earth Science, onde foram avaliados a influência de processos hidrodinâmicos e biológicos sobre o comportamento do carbono no estuário do rio Jaguaribe em três campanhas de amostragem temporal (Capítulo 5.1); o segundo é o artigo submetido para a revista Regional Studies in Marine Science, no qual são identificadas as principais fontes de carbono para o estuário do rio Jaguaribe durante três amostragens espaciais (Capítulo 5.2); o terceiro um manuscrito em processo de submissão, no qual foi avaliada a interação da matéria orgânica com metais traço em diferentes tamanhos moleculares, utilizando a técnica de ultrafiltração seguida de análises de fluorescência da matéria orgânica de metais em ICP-MS (Capítulo 5.3). O sexto capítulo trata das conclusões e considerações finais e o sétimo às referências bibliográficas adicionais.

Estes estudos foram realizados em parceria com o Laboratório de Ciências Ambientais da Universidade Estadual do Norte Fluminense Darcy Ribeiro (UENF) e com o Institut Méditerranéen d'Océanologie (MIO) da Université de Toulon. Na UENF foram realizadas as análises dos fenóis de lignina dissolvidos e da composição elementar e isotópica do carbono orgânico dissolvido, particulado e sedimentar do estuário do rio Jaguaribe. No MIO foram realizadas medidas da fluorescência da matéria orgânica dissolvida e análises em ICP-MS de metais dissolvidos em amostras do estuário do rio Jaguaribe.

2. REFERENCIAL TEÓRICO

2.1. Importância da matéria orgânica natural no meio ambiente

A matéria orgânica (MON) é uma mistura heterogênea de moléculas derivadas da decomposição biológica e da atividade metabólica de organismos (FINDLAY; SINSABAUGH, 2003), apresentando diferentes tamanhos, funcionalidades, idade e origem (alóctone e autóctone). A MON é ubíqua em ambientes marinhos e desempenha papel importante em processos biogeoquímicos e ambientais, como ciclagem de carbono e nutrientes, fornecimento de energia para consumidores e controle da qualidade da água (SANTINELLI; NANNICINI; SERITTI, 2010a; WANG et al., 2007; YANG et al., 2016).

O carbono (C) é o principal constituinte da MON. A capacidade que ele possui de formar uma imensa variedade de compostos, atrelada às suas diversas propriedades, faz dele o principal elemento químico responsável pela manutenção da vida. O carbono está persente em todas as moléculas orgânicas em elevada proporção, sendo um dos átomos mais abundantes da biomassa dos organismos, correspondendo a 50% da massa seca dos seres vivos. O C apresenta-se como moeda energética dos organismos e das células, estando presente em vários processos como a produção primária a transferência de energia e matéria entre os componentes da teia alimentar e os estoques da biomassa nos ecossistemas aquáticos (ESTEVES, 1988; KILLOPS; KILLOPS, 2005).

Atualmente o carbono tem sido reconhecido como peça chave no funcionamento do planeta, pois a sua presença nos principais reservatórios do planeta (oceano, continente e atmosfera) permite a interconexão desse sistema e regulação do clima global. Na atmosfera, o C encontra-se principalmente na forma inorgânica, que é o dióxido de carbono (CO_2) (CHIANG; KOUTAVAS, 2004; FALKOWSKI et al., 2000). Nos últimos anos tem sido observado que as atividades antrópicas têm causado um incremento das concentrações de CO_2 na atmosfera, que por sua vez tem causado o aumento da temperatura média global (IPCC, 2014). Como esse incremento é a causa primária das mudanças climáticas globais, o interesse pelo estudo do ciclo do carbono tem sido crescente.

O ciclo global do carbono consiste na movimentação desse elemento entre os principais compartimentos da terra (Figura 1) (DEGENS; ITTEKKOT, 1987). Essa movimentação pode ser rápida, como através da respiração e fotossíntese, ou lenta, como no caso o carbono oriundo o intemperismo das rochas, transporte e deposição carbonática (escala geológica) (FALKOWSKI, et al., 2000). Mesmo possuindo fluxos com diferentes magnitudes, o estoque de carbono nos reservatórios era constante, pois eles ocorriam de forma equilibrada.

Entretanto, a partir da era industrial, a injeção de CO_2 antropogênico na atmosfera tem perturbado esse equilíbrio. Os oceanos têm atuado como importantes mitigadores dos efeitos das emissões humanas de CO_2, pois os oceanos têm agido como sumidouros de cerca de 26% das emissões humanas de CO_2 (QUÉRÉ et al., 2018).

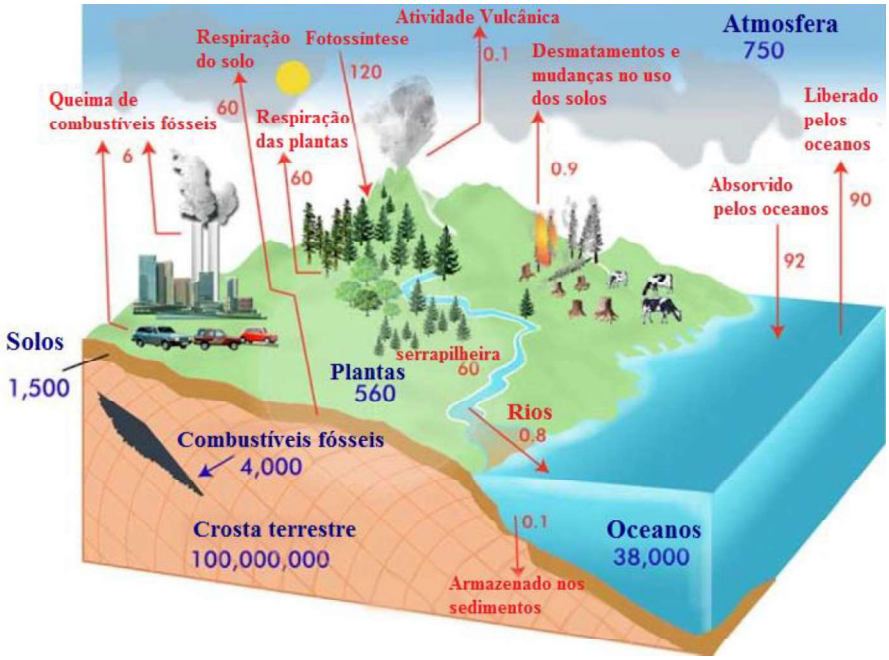

Figura 1 - Ciclo Global do Carbono (Fonte:www.globe.gov/project/carbon). Unidade: Petagramas (Pg) = 10^{-15}g. Estoques: Pg. Fluxos: Pg ano^{-1}

As mudanças no uso dos solos também têm promovido a liberação de CO_2 para atmosfera através do desflorestamento, assim como aumentado o aporte de C para os rios (Figura 2) (BAUER et al., 2013). Contudo, ao mesmo tempo que os seres humanos estão aumentando o transporte fluvial de materiais através da erosão dos solos, eles estão diminuindo este fluxo para a zona costeira através da retenção de sedimentos nos reservatórios (HEDGES et al., 1994) e a retenção os fluxos hídricos na construção e grandes reservatórios. Isso promove déficit sedimentar, redução de aporte de nutrientes e consequentemente redução da produtividade primária na zona costeira (Figura 2).

Os estuários são vias desse transporte, e são ambientes bastante produtivos e dinâmicos. Além disso, são caracterizados por um forte gradiente físico-químico, atrelado às atividades biológicas, que dependendo das condições da maré, descarga fluvial e atmosfera sofrem variações no espaço e no tempo. Logo, o comportamento do carbono introduzido nos estuários depende das propriedades biogeoquímicas do carbono e das características particulares de cada estuário (DAI et al., 2000).

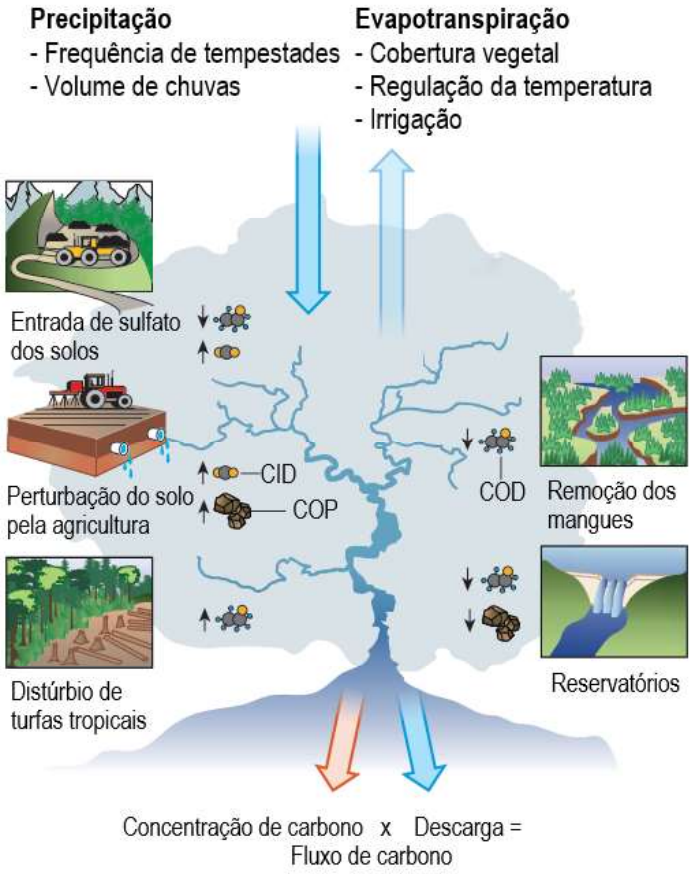

Figura 2 - Processos naturais e antropogênicos que alteram o aporte de carbono fluvial para a plataforma continental.

2.2. Origem e composição da matéria orgânica em estuários

A matéria orgânica natural (MON) estuarina é composta de materiais orgânicos de origem alóctone e autóctone. A MON autóctone corresponde aos detritos originados dos processos de produção primária e decomposição dos organismos aquáticos in sito, enquanto que a MON alóctone origina-se de processos de lixiviação dos solos e dos detritos de origem terrestre (Figura 3) (BAUER; BIANCHI, 2011).

Os compostos de origem autóctones são relativamente mais lábeis por possuírem maiores concentrações de nitrogênio, sendo compostos principalmente por aminoácidos,

proteínas e lipídeos. Já a MO de origem alóctone é mais refratária, contêm baixo teor de nitrogênio e pode representar a maior fonte de matéria orgânica dissolvida para os ecossistemas aquáticos, sendo composta principalmente pelos ácidos húmicos e fúlvicos. Geralmente, possuem baixa relação C:N devido às altas concentrações de substâncias húmicas.

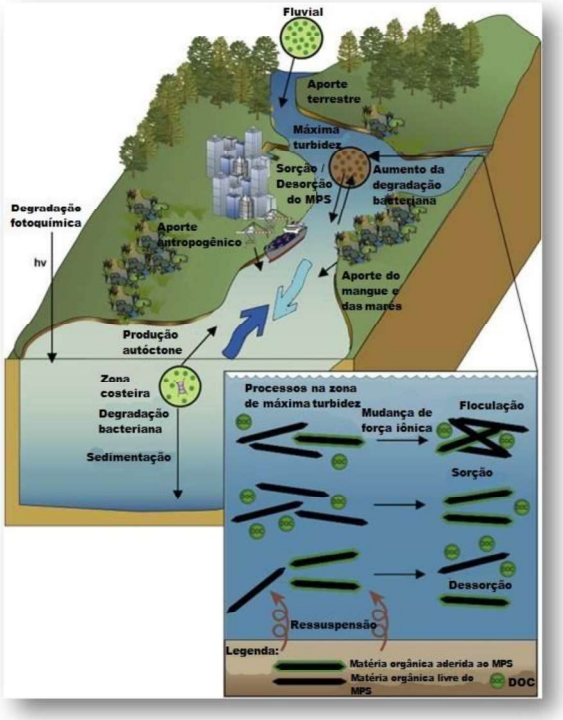

Figura 3 - Fontes e processos biogeoquímicos na zona de mistura estuarina.

Existem, também as fontes antrópicas, que são oriundas da emissão de efluentes orgânicos e disposição inadequada de resíduos sólidos. A MON antrópica é classificada como alóctone, mas geralmente possui propriedades similares às da MON autóctone, como a sua labilidade.

A caracterização da MON estuarina é bastante complexa devido à grande mistura de materiais e às diferentes etapas de degradação. Existem duas classes de MON em ambientes aquáticos: uma com natureza bem definida; como os aminoácidos, os carboidratos, ácidos orgânicos, ligninas, celulose e etc; e o humo, que é de natureza heterogênea poli funcional e com diferentes graus de polimerização. Devido a sua importância no metabolismo dos organismos, os compostos não húmicos encontram-se em baixas concentrações nos estuários (~20% da MON). Já os compostos húmicos, por serem refratários, tendem a acumularem-se nesses ambientes e permanecerem lá por vários anos (mais de 50% da MON)

(FINDLAY; SINSABAUGH, 2003). Os compostos húmicos caracterizam uma etapa intermediária da MON entre os processos de decomposição e mineralização. Como esses processos são relativamente lentos, o humo desempenha um papel importante, pois possui propriedades químicas que o faz interagir com a biota ou com outros parâmetros ambientais.

2.3. Partição geoquímica da MON

A MON em ambientes aquáticos pode ser separada em três domínios: particulado, coloidal e dissolvido. A matéria orgânica particulada (MOP) ou o carbono orgânico particulado (COP) correspondem às partículas retidas em filtros com porosidade entre 0,22 e 0,45 μm. As concentrações de carbono orgânico dissolvido (COD) variam de aproximadamente 40 μmol L^{-1} na água do mar (HANSELL et al., 2009) até de 5000 μmol L^{-1} em pântanos. Nas águas costeiras (estuários, lagoas), os valores típicos de água superficial variam de 100 μmol L^{-1} a 500 μmol L^{-1}. Em rios o COD varia de 250 μmol L^{-1} a 800 μmol L^{-1} (FINDLAY; SINSABAUGH, 2003).

A matéria orgânica coloidal (MOC) ou carbono orgânico coloidal (COC) é definido como macromoléculas ou agregados que têm limites de tamanho entre 1 nm e 1 μm. Enquanto a matéria orgânica verdadeiramente dissolvida ou carbono orgânico verdadeiramente dissolvido corresponde a moléculas menores que 1 kDa (WILKINSON; LEAD, 2007). Historicamente, a separação das fases particulada e dissolvida tem sido feita através da filtração utilizando filtro de 0,22 a 0,45 μm (EATHERALL; NADEN; COOPER, 1998). A etapa de filtração também é utilizada para reduzir a complexidade da amostra e preservar a fase dissolvida através da remoção da maioria dos microrganismos (FINDLAY; SINSABAUGH, 2003). Entretanto, a fração coloidal encontra- se misturada com a dissolvida, pois a separação de ambos não é possível por meio da filtração convencional (Figura 4).

A técnica da ultrafiltração é utilizada para a separação e determinação da composição das frações coloidais e dissolvidas, proporcionando um cenário dos processos de partição geoquímica e mecanismos associados ao transporte de metais nos ecossistemas aquáticos (WILKINSON; LEAD, 2007). Este método permite o processamento de grandes volumes de amostra sem adição de reagentes (EYROLLE; CHARMASSON, 2000), sendo eficiente para isolar e concentrar materiais coloidais e dissolvidos em águas fluviais, estuarinas e marinhas (BABIARZ et al., 2003; DAI et al., 1998; YI et al., 2014). O fracionamento físico ocorre pela diferença de peso molecular em fluxo tangencial mediante da ultrafiltração, possibilitando detecção e concentração compostos orgânicos e inorgânicos em baixas concentrações em ambientes aquáticos (HEDGES et al., 1994).

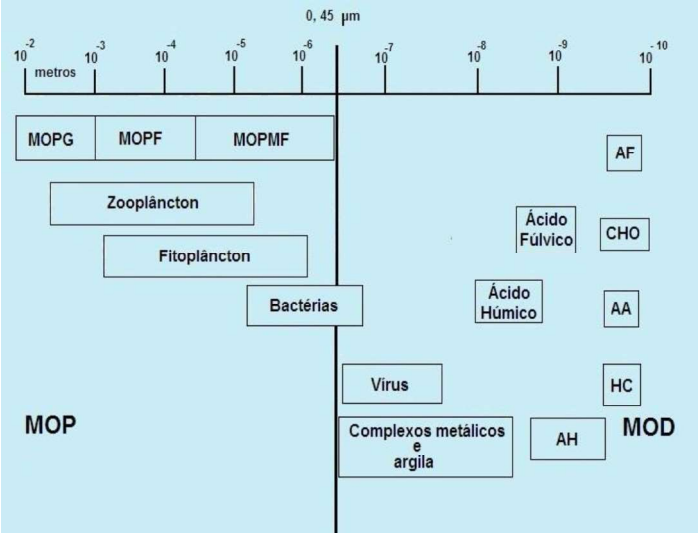

Figura 4 - Variação dos tamanhos da matéria orgânica particulada e dissolvida e dos compostos de carbono em águas naturais. AA, aminoácidos; CHO, carboidratos; AF, ácidos graxos; HC, hidrocarbonetos; AH, ácidos hidrofílicos; MOPF, matéria orgânica particulada fina; MOPMF, matéria orgânica particulada muito fina; MOPG, matéria orgânica particulada grossa. Fonte: (Adaptada de Eatherall, Naden e Cooper (1997)).

A abundância e as características da MON variam entre os diferentes compartimentos ambientais. Os coloides orgânicos representam de 30 a 40% da MOD (<0.22 µm) nos oceanos do mundo, sendo quase metade compostos por carboidratos (WILKINSON; LEAD, 2007). Contudo, a variação do tamanho da partícula está fortemente relacionada às condições ambientais e as fontes. XU; GUO, (2017) observaram que a MON era composta principalmente por partículas de baixo peso molecular (<1kDa) tanto em ambiente fluvial, lacustre como marinho, correspondendo a cerca de 60%, 70% e 76% da MON nesses ambientes respectivamente. Estudos utilizando ultrafiltração observaram que as substâncias húmicas em águas costeiras estão distribuídas principalmente na fração <1 kDa (MOPPER et al., 1996; YI et al., 2014), enquanto que proteínas e carboidratos mostram-se mais relacionados à frações maiores, embora encontradas principalmente na faixa <10 kDa (XU; GUO, 2017)(STOLPE et al., 2014).

2.4. Composição isotópica da matéria orgânica natural

O carbono da matéria orgânica natural é uma mistura de dois isótopos estáveis, ^{12}C e ^{13}C. Na Terra as abundâncias relativas de ^{12}C e ^{13}C são 98,89% e 1,11%, respectivamente. Os compostos de carbono de origem biológica são relativamente

enriquecidos com o isótopo mais leve, enquanto o isótopo mais pesado é retido nas principais formas de carbono inorgânico (carbonato, bicarbonato e dióxido de carbono) (KILLOPS; KILLOPS, 2005).

A razão isotópica de uma amostra é normalmente expressa por valores de δ (com unidades de permil ou ‰) em relação ao padrão, e sua forma geral pode ser representada por:

$$\delta^{13}C\ (‰) = [(^{13}C/^{12}C)_{\text{amostra}} / (^{13}C/^{12}C)_{\text{padrão}} - 1] \times 10^3$$

A aplicação de isótopos estáveis para avaliar as fontes e a ciclagem da matéria orgânica em estuários tem sido amplamente utilizada, principalmente para distinguir entre as contribuições alóctone e autóctone (BAUER; BIANCHI, 2011) (Tabela 1). A composição isotópica do carbono ($\delta^{13}C$) é ideal para a identificação de origem, pois é menos afetada pelos processos diagenéticos e biológicos. Enquanto que a razão C:N e a assinatura isotópica do nitrogênio ($\delta^{15}N$) são modificadas pelos mesmos, sendo mais adequadas para a avaliação do processamento da MON no meio ambiente (MIDDELBURG; HERMAN, 2007).

A composição isotópica tem sido usada para avaliar processos de eutrofização através de pressões antropogênicas (ABREU et al., 2006), consequências da mudança da cobertura vegetal na bacia de drenagem do estuário (REZENDE et al., 2010), dieta alimentar de organismos (ABRANTES et al., 2014; BEZERRA et al., 2015) e despejos de efluentes urbanos (BARROS et al., 2010).

Em estuários dominados por marés, a distribuição e a origem da MOP são governadas primariamente pela dinâmica do material particulado em suspensão (MPS) (MIDDELBURG; HERMAN, 2007). Nos estuários túrbidos, a assinatura isotópica do carbono é constante ao longo do estuário devido à intensa mistura entre as fontes que uniformizaram os valores de $\delta^{13}C$. Já os estuários com MPS baixo ou intermediário, apresentaram valores de $\delta^{13}C$ bastante variáveis: empobrecidos na zona de rio, enriquecidos na zona costeira e intermediários na zona de mistura (MIDDELBURG; HERMAN, 2007). O tempo de residência e a descarga fluvial também são determinantes para o controle da MON nos estuários. Em ambientes com curto tempo de residência, a contribuição autóctone é pequena devido à rápida exportação de carbono dificultar a ciclagem do mesmo no estuário (BIANCHI et al., 1997). Enquanto que em estuários com elevado tempo de residência (~1 ano), o fitoplâncton autóctone é dominante, sendo observada apenas uma pequena influência de MON continental durante o período chuvoso (LEBRETON et al., 2016).

Contudo, a determinação das fontes e a compreensão dos processos biogeoquímicos que controlam a MOD estuarina são bastante difíceis em estuários, porque o MON é proveniente de múltiplas origens e se alteram com o tempo (LEBRETON et al.,

2016). Nos casos onde MOP e/ou MOD exibem comportamento não conservativo, devido a processos biogeoquímicos (produção de fitoplâncton e respiração bacteriana) e dinâmica sedimentar complexa durante a mistura estuarina, a razão isotópica torna-se mais complexa de avaliar. Além disso, a sobreposição das assinaturas isotópicas ocorre frequentemente (LU et al., 2014; YE et al., 2018), como pode ser observado na Tabela 1 a sobreposição da assinatura isotópica das plantas C_3 com o fitoplâncton fluvial, por exemplo. Por isso, muitos estudos combinam outras ferramentas como, medidas de fluorescência (YA; ANDERSON; JAFFÉ, 2015), radiocarbono e biomarcadores (por exemplo, fenóis de lignina e lipídios) para determinar fontes de carbono em sistemas costeiros (RALISON et al., 2008; RAYMOND; BAUER, 2001; SPENCER et al., 2009).

Tabela 1- Composição isotópica do carbono e nitrogênio das principais fontes de MON em estuários.

Fonte	$\delta^{13}C$ (‰)	$\delta^{15}N$	Referência
Plantas C_3	-26 a -30	-2 a +5	BIANCHI; BAUER, 2011
Plantas C_4	-12 a -14	3 a 7	BIANCHI; BAUER, 2011
Fitoplâncton fluvial	-28.4 a -32.6	5 - 8	YE et al., 2017
Fitoplâncton marinho	-18 a -24	6 - 9	BIANCHI; BAUER, 2011
Solos	-23 a -27	2,6 a 6,4	BIANCHI; BAUER, 2011
Esgoto doméstico	-30 a -22,7	-2.5 a -0,9	WANG et al., 2004

2.5. Lignina

A lignina é um composto polifenólico de alto peso molecular proveniente quase que exclusivamente de plantas vasculares. Além disso, a lignina constitui de 20% a 30% de tecido vegetal vascular (KIRK;FARRELL, 1987), ficando atrás apenas da celulose como o biopolímero mais abundante (BROWN, 1969). Dentre os diversos marcadores de matéria orgânica terrestre, a lignina destaca-se por ser um biomacropolímero encontrado exclusivamente em plantas vasculares (GÕNI & HEDGES, 1992). Além disso, a mineralização da lignina é mais lenta do que a de outros biopolímeros (HATCHER et al.,1995), sendo um marcador ideal e específico para plantas vasculares, ou um indicador de

matéria orgânica terrestre em ambientes marinhos (HEDGES; MANN, 1979). Dessa forma, a lignina tem sido uma ferramenta bastante utilizada para avaliar o aporte de MON alóctone para os oceanos e ambientes costeiros (BIANCHI et al., 2009; DITTMAR; KATTNER, 2003) e verificar mudanças nas fontes MOD com variação nas condições hidrológicas (SPENCER et al., 2008).

Através da oxidação alcalina, com óxido de cobre, a molécula de lignina é quebrada em onze principais fenóis, que são separados em quatro grupos: p-hidroxil (p), vanilil (V), siringil (S) e cinamil (C) (HEDGES; ERTEL, 1982). A soma de 6, 8 ou 11 desses fenóis corresponde ao aporte de matéria orgânica terrestre para o meio. Oito fenóis de lignina (dois fenóis de cinamil "C", três fenóis de siringil "S" e três fenóis de vanilil "V") foram medidos para avaliar fontes vegetais de matéria orgânica dissolvida. Estes rendimentos de fenol são convencionalmente representados como lambda ($\Lambda 8$; mg por 100 mg de carbono orgânico) e Σ_8 (a soma dos oito fenóis principais normalizados para o volume da amostra).

Com relação à lignina, as gimnospermas são compostas quase inteiramente por monômeros de vanilil, enquanto as angiospermas possuem siringil e vanilil. As razões S/V e C/V são usadas para distinguir fontes de MON derivadas de vários componentes de plantas terrígenas (BLAIR; ALLER, 2012). A relação S/V diferencia as angiospermas (S/V> 0) das gimnospermas (S/V = 0) e a razão C/V distingue o tipo de tecido, lenhoso (C/V = 0) dos não-lenhosos (C/V > 0) Entretanto, a diagênese pode alterar as proporções, pois os fenóis de cinamil e siringil são mais afetados do que o vanillil (TAREQ; TANAKA; OHTA, 2004). Então, o Índice de Vegetação de Fenol da Lignina (LPVI) (Tareq et al., 2011, 2004) é utilizado para identificar a fonte da vegetação.

$$LPVI = [S\ (S + 1) / (V + 1) + 1] \times [C\ (C + 1) / (V + 1) + 1]$$

onde V, S e C são expressos em% do $\Lambda 8$. O LPVI leva em conta a heterogeneidade da planta e a sequência digenética dos grupos fenólicos.

A razão entre as forma ácidas e aldeídicas dos fenóis do grupo vanilil e siringil (Ac/Al)v,s é um proxy do grau de oxidação da lignina durante a diagênese. Razões abaixo de 0,3 são típicas de tecidos frescos. Enquanto que (Ad/Al)v,s acima de 0,4 indicam MO degradada, e acima de 0,6 são consideradas altamente degradadas. Altas proporções (Ad/Al)v,s (~ 1.2) também são indicativas do processo de lixiviação.

2.6. Fluorescência Molecular da MOD

A matéria orgânica dissolvida (MOD) nas águas naturais apresenta propriedades óticas. Uma subfração da MOD apresenta propriedade da fluorescência quando absorve radiação

ultravioleta e é atribuída à presença da matéria orgânica dissolvida colorida (MODC). Os compostos húmicos são os principais responsáveis por este fenômeno visto que eles representam de 70 a 85% da MOD em ambientes aquáticos. Nos primeiros trabalhos sobre o tema, a fluorescência era frequentemente utilizada para quantificação da MOD (SIERRA et al., 1996). Contudo, com o aprimoramento da técnica, como o uso de correções dos espectros e ferramentas estatísticas (BALCARCZYK et al., 2009; LUCIANI et al., 2009), essa propriedade tem sido utilizada para caracterizar a matéria orgânica dissolvida nos ambientes aquáticos. As substâncias húmicas fluorescem entre 430 e 540 nm por uma excitação de 340 – 360 nm, enquanto que as proteínas fluorescem no domínio 270 - 280 por uma excitação entre 300 – 340 (STEDMON; MARKAGER, 2005). A Tabela 2 resume as propriedades de fluorescência dos fluóforos identificados e citados por Coble (2007).

Tabela 2 - Propriedades de fluorescência dos fluoróforos identificados em ambientes marinhos.

Componente	Nome do pico	Ex/Em	Número do pico	Fonte	Pico
Tirosina, tipo proteína	B	275/305	8	autóctone	γ
Triptofano, tipo proteína	T	275/340	7	autóctone	δ
Desconhecido	N	280/370			
Ácido húmico	A	260/400-460	4	ácido fúlvico, autóctone, húmico terrestre	α'
Ácido húmico	A	260/400-460	1	ácido húmico, alóctone, húmico terrestre	α'
Ácido húmico	A	260/400-460	3	ácido húmico, alóctone, húmico terrestre	α'
Ácido húmico marinho	M	290-310/370-410	6	antropogênico de águas residuais e agricultura	β
Ácido húmico	C	320-360/420-460	5	terrestre, antropogênica, agricultura	α
Pigmento	P	398/660			
Ácido húmico		250 (385)/504	2	ácido fúlvico, terrestre, autóctone	

Esta técnica é altamente sensível e seletiva, fácil de usar e necessita de pequeno volume de amostra (COBLE, 2007; FELLMAN et al., 2009). Em geral, a fluorescência da MOD possui um amplo espectro de excitação entre 250 e 400 nm e amplo espectro de emissão 350 a 500 nm. O mapeamento detalhado das propriedades de fluorescência da MOD produz matrizes de emissão de excitação (MEE) construídas pela junção dos espectros de emissão e excitação, que são adequados para técnicas de análise de dados multivariada, como PARAFAC (LIN et al., 2016; SHIN et al., 2016a; XU; GUO, 2017). Através da decomposição de um conjunto de MEEs, a análise de PARAFAC quantifica o número significativo de componentes fluorescentes independentes.

O PARAFAC modela dados tridimensionais usando a seguinte equação, montada minimizando a soma dos quadrados dos resíduos (εijk).

$$Xijk = \sum_{f=1}^{F} aif\ bjf\ ckf + \varepsilon ijk\ ,\ i = 1,..,I;\ j = 1,..,J;\ k = 1,..,K$$

Xijk é um elemento da matriz tridimensional com dimensões I, J e K. Na análise das MEEs, os números Xijk são a intensidade da fluorescência da amostra i medida em comprimento de onda de emissão j e comprimento de onda de excitação k. O termo final εijk representa os sinais não explicados (resíduos contendo ruídos e outras variações não modeláveis). O resultado do modelo são os parâmetros a, b e c. Idealmente, representam, respectivamente, a concentração, o espectro de emissão e o espectro de excitação dos fluoróforos fundamentais (STEDMON; RASMUS, 2008). A equação é idêntica à da fluorescência de uma mistura de fluoróforos assumindo que eles se comportam de acordo com a lei de Lambert-Beer e que não há interações entre eles. Se existem F fluoróforos na mistura, o sinal mensurado é a soma da contribuição de cada um (LUCIANI et al., 2008).

Como se trata de uma amostra complexa e desconhecida, não se sabe o número significativo de espécies fluorescentes na amostra. Então, previamente à modelagem com o PARAFAC, utiliza-se a análise de variância residual, core consistency diagnostic (CONCORDIA) para determinar o número de componentes apropriados para esse conjunto de dados.

2.7. Interação da MON com metais em estuários

Elementos traço são caracterizados por possuírem concentrações menores que 1 mg L^{-1} em águas naturais (GAILLARDET; VIERS; DUPRE, 2003). A abundância de metais traço em rios depende de sua abundância na crosta continental e da sua mobilidade durante o intemperismo e transporte. A crosta terrestre é a fonte final de elementos traço em corpos

hídricos, que chegam ao estuário, principalmente, carreados pelo material particulado. Elementos traço atingem os estuários principalmente por meio do intemperismo das rochas, deposição atmosférica e atividades antropogênicas.

A contaminação dos corpos hídricos por metais traço desperta grandes preocupações porque eles são importantes poluentes ambientais e possuem longo tempo de residência em sedimentos e organismos. Os estuários funcionam como filtros de metais, no transporte entre o continente e o oceano, promovendo sua precipitação devido ao intenso gradiente físico-químico e à quantidade de partículas (YANG; VAN DEN BERG, 2009). Além disso, nos ecossistemas aquáticos, esses elementos podem sofrer transformações químicas que os tornam ainda mais nocivos ao ambiente. Um exemplo é a complexação do mercúrio (Hg), formando uma neurotoxina (metil mercúrio), que é facilmente incorporada pelos organismos e consequentemente biomagnificada na cadeia trófica (BEZERRA et al., 2015). Embora os estuários estejam sujeitos à contaminação por metais traço através de processos naturais, as atividades antrópicas têm se mostrado a principal forma de entrada de metais em corpos hídricos. Dentre elas, destaca-se: a mineração, atividades industriais, urbanização, agricultura e carcinicultura (LACERDA et al., 2011; OLIVEIRA; MARINS, 2011).

Os metais-traços chegam ao estuário, principalmente, associados ao material particulado em suspensão e/ou dissolvidos na coluna d'água (GAILLARDET; VIERS; DUPRE, 2003). A partição geoquímica dos metais é determinante para o transporte dos mesmos e é modificada pelo intenso gradiente físico-químico, gerado pela mistura entre água doce e marinha. Os principais fatores são: especificidade e concentração do metal, força iônica, pH, oxigênio dissolvido, concentração e características do material em suspensão (WANG et al., 2017). Em estuários, o metal associado a partículas tende a sedimentar através dos processos de adsorção e floculação, diminuindo sua mobilidade no sistema. Entretanto, a remobilização dos sedimentos pelas marés e atividades antrópicas podem causar a remobilização desses metais, que podem ligar-se à MOD aumentando também sua biodisponibilidade (LACERDA; MIGUENS, 2011). Na fração dissolvida, o metal pode adsorver-se na superfície dos coloides por forças eletrostáticas. Tanto os coloides orgânicos como inorgânicos estão envolvidos na adsorção não específica (OLIVEIRA; MARINS, 2011). A matéria orgânica coloidal (MOC) é muito reativa devido à sua alta área de superfície específica e abundância de sítios ativos que podem contribuir para o processo de ligação com o metal (FANG et al., 2015b; LOUIS et al., 2009). Além disso, a MOC intermedia as mudanças entre a fração verdadeiramente dissolvida e a particulada, por meio do processo de mistura, como floculação, agregação e desagregação (GIANI et al., 2005; XU et al., 2018).

Em águas estuarinas metais como o cobre (Cu), mercúrio (Hg) e zinco (Zn), por exemplo, encontram-se principalmente ligados a colóides orgânicos (LUAN; VADAS, 2015; SIMPSON et al., 2014; WANG et al., 2017). Enquanto que, metais como Pb e Zn podem ter alta afinidade por colóides inorgânicos ricos em ferro (LUAN; VADAS, 2015).

A avaliação da variação das concentrações do metal com a variação da salinidade indica a ocorrência de processos biogeoquímicos durante a mistura estuarina. Elementos com baixa reatividade apresentam comportamento conservativo, variando linearmente com a salinidade, ou seja, sofrem apenas diluição ou concentração (dependendo do metal) sem sofrerem alterações em suas formas químicas. Enquanto que, metais mais reativos, sofrem processos de adição ou remoção da coluna d'água de forma não linear através de reações químicas e biológicas, apresentando comportamento não conservativo (OLIVEIRA; MARINS, 2011).

2.8. Estuário do rio Jaguaribe

O estuário do rio Jaguaribe localiza-se no litoral nordestino do Brasil, no Estado do Ceará, com 633 km de extensão e uma bacia de drenagem de 72.043 km^2. O semiárido brasileiro é marcado por um forte regime de chuvas sazonais, controlado pela Zona de Convergência Intertropical (ZCIT). O deslocamento sazonal da ZCIT para o sul promove a ocorrência de chuvas no nordeste brasileiro, enquanto seu retorno ao norte causa uma seca intensa durante o inverno e a primavera austral. Em anos de forte El Niño, o deslocamento para o sul é ainda mais intenso, reduzindo a aridez na região. Na zona costeira, a pluviosidade anual varia de 400 a 2000 mm; com média de 912,7 mm nos últimos 30 anos (FUNCEME, 2017).

O semiárido brasileiro é caracterizado por baixa (<700 mm ano^{-1}) e concentrada (4-5 meses) precipitação com a prevalência de evaporação (1.900 mm ano^{-1}) sobre a entrada de água doce durante a maior parte do ano (SCHETTINI; VALLE-LEVINSON; TRUCCOLO, 2017). A sazonalidade regional é definida por dois períodos diferentes em termos de precipitação: a estação chuvosa (janeiro a maio) e a estação seca (junho a dezembro), geralmente sem qualquer precipitação de agosto a novembro. Esta região tem sido apontada como uma das mais afetadas pelas mudanças climáticas globais (ALMAGRO et al., 2017; KROL; BRONSTERT, 2007; ZHANG et al., 2017) com cerca de 20% de redução na precipitação anual nos últimos 50 anos. anos (GODOY; LACERDA, 2014, 2015).

Durante o período de estudo, a precipitação anual esteve sempre abaixo da média

histórica devido ao efeito do evento El Niño, que promoveu a seca mais severa já registrada no semiárido nordestino entre 2012 e 2016 (Marengo et al., 2017) (Figura 2). Como resultado, o Castanhão, que é o maior reservatório construído na bacia do Rio Jaguaribe com cerca de 6,7 bilhões de m^3 de capacidade de armazenamento de água (SANTOS et al., 2017), testemunhou redução de sua cota de armazenamento de cerca de 85% em novembro de 2011 para cerca de 4% em outubro 2017, devido à ausência de chuvas na bacia do reservatório (DNOCS, 2017; SANTOS et al., 2017).

As descargas de água doce caíram de 60/130 m^3s^{-1} para 20 m^3s^{-1} após a construção das principais represas do rio Jaguaribe (DIAS; MARINS; MAIA, 2013). Como a água é um recurso escasso, várias barragens foram construídas ao longo dos rios para melhorar a disponibilidade de água e regular seu fluxo (KROL e BRONSTERT, 2007), resultando em uma pequeno aporte de água doce e material fluvial para o estuário e o oceano (DIAS; CASTRO; LACERDA, 2013; MOLISANI et al., 2013), como pode ser observado através da formação da pluma estuarina apenas em episódios de chuvas intensas (Dias et al., 2013a). Além disso, o estresse hídrico favorece a intrusão marinha e consequentemente a colonização do estuário por novas áreas de mangue (GODOY; MEIRELES; LACERDA, 2018), bem como a erosão das margens (MARINS et al., 2003).

Outra consequência relevante do balanço hídrico negativo é o aumento do tempo de residência (TR) da água do mar no estuário (DIAS et al., 2016), pois promove uma condição ideal para o acúmulo de material particulado em suspensão (SPM), nutrientes e carbono que podem potencializar o processo de eutrofização e floculação no estuário (DIAS et al., 2016). O maior tempo de permanência na água do mar também pode levar o estuário à condição hipersalina, que pode reduzir a produção de MON pela atividade biológica (PINCKNEY; PAERL; BEBOUT, 1995; SOUZA et al., 2003), alterar as propriedades químicas da matéria orgânica dissolvida (MOD) e seu comportamento (CATALÁN et al., 2013; MENDOZA; ZIKA, 2014).

A foz do rio é cercada por aproximadamente 7,29 km^2 de manguezal (GODOY; LACERDA, 2014; GODOY; MEIRELES; LACERDA, 2018) incluindo novas áreas de colonização que correspondem a 0,29 km^2. Os manguezais são grandes fornecedores de carbono orgânico terrestre para águas costeiras (BIANCHI; BAUER, 2011; PRASAD; RAMANATHAN, 2009; SAKHO et al., 2015), principalmente em regiões, como o NE do Brasil, onde a vegetação dominante (Caatinga, vegetação arbustiva seca) tem baixa produção de biomassa vegetal e os solos são pobres em matéria orgânica (MENEZES et al., 2012). No entanto, em alguns ambientes hipersalinos, a MON derivada dos organismos marinhos possui

maior contribuição do que os derivados de manguezais, devido à alta influência da água do mar (RAY; SHAHRAKI, 2016).

Entre as fontes de atividades antrópicas locais, a carcinicultura é fonte potencial de MON para o estuário do rio Jaguaribe devido a três fatores principais: (1) é a principal atividade econômica desenvolvida nas proximidades do estuário (mais de 3.000 ha de fazendas de camarão); suas emissões de nutrientes superam as naturais e (3) estão próximas das margens, despejando seus resíduos diretamente na água estuarina (LACERDA et al., 2008; MARINS et al., 2011). Além disso, o estuário abriga também áreas urbanas de tamanho médio, com uma população total de aproximadamente 119.000 habitantes. Fortim, Aracati e Itaiçaba possuem baixas taxas de esgotamento sanitário adequado, correspondendo à 2,1%, 4,5% e 3,8% respectivamente (IBGE, 2019).

Em síntese, mudanças ambientais têm ocorrido nesse ambiente como reflexo das pressões antrópicas e condições climáticas (El Niño e mudanças climáticas inclusive), dentre elas destaca-se a eutrofização, supressão do manguezal pela atividade de carcinicultura e simultânea expansão do manguezal devido à forte intrusão salina causada pelo aumento do nível do mar e redução do fluxo fluvial. Visto a importância da matéria orgânica na regulação dos processos biogeoquímicos e as modificações que estão ocorrendo neste estuário, acredita-se que o transporte e a dinâmica da MO esteja sendo continuamente alterada e que isto esteja acontecendo em outros estuários semiáridos também.

3. HIPÓTESE E OBJETIVOS

3.1 HIPÓTESE

Com a intensificação das secas e o aumento das demandas de água doce para atividades humanas, o estuário do Rio Jaguaribe está sob estresse hídrico crescente, resultando na redução dos fluxos de materiais para o oceano, e na variação do tempo de residência das águas estuarinas. Desta forma, é esperada a consequente modificação da qualidade da matéria orgânica estuarina e, que os processos que governam a mistura e o destino do carbono no estuário do rio Jaguaribe sejam diferentes dos estuários clássicos. Além disso, a ampla variabilidade climática da região e a crescente pressão antrópica sobre as vazões da bacia de drenagem podem estar reduzindo os fluxos de carbono para o estuário. Em relação a influência do tempo de residência, espera-se que com seu aumento a associação dos metais com a matéria orgânica seja favorecido, aumentando a biodisponibilidade desses contaminantes.

3.2 OBJETIVO GERAL

Avaliar os fluxos e o comportamento do carbono no estuário do rio Jaguaribe. Investigar as concentrações e caracterizar a matéria orgânica natural, bem como sua interação com os metais ao longo do gradiente de salinidade do estuário do rio Jaguaribe em diferentes condições de maré e estações climáticas.

3.2.1 Objetivos específicos

a. aplicar diferentes técnicas analíticas (fluorescência molecular, absorbância e fenóis de lignina) para caracterização da MON (**Capítulos 5.1, 5.2, 5.3**).

b. quantificar os teores de COD, COP, CID e Clorofila (Chl-*a*) na zona de máximo turbidez no estuário do rio Jaguaribe **(Capítulo 5.1)**;

c. avaliar a influência dos parâmetros hidrodinâmicos e da sazonalidade sobre o comportamento do carbono **(Capítulo 5.1)**;

d. quantificar os teores de COD, CID, COP e Chl-*a* ao longo do gradiente de salinidade do estuário do rio Jaguaribe **(Capítulo 5.2)**;

e. avaliar as diferentes origens de matéria orgânica natural ao longo do gradiente de salinidade estuarino **(Capítulo 5.2)**;

f. estudar a interação da matéria orgânica natural com metais ao longo do gradiente de salinidade estuarino **(Capítulo 5.3)**;

e. avaliar a mobilidade geoquímica do carbono orgânico e dos metais na água do estuário **(Capítulo 5.3)**;

4. ESTRATÉGIA DE AMOSTRAGEM

Foram realizadas um total de sete campanhas de amostragem no estuário do rio Jaguaribe dentro do período de 2012 e 2018 durante os períodos de seca e chuva, somando conhecimento preliminar (Cavalcante, 2015) sobre o carbono na região estuarina às avaliações feitas durante este projeto de doutorado. Na Tabela 2 foi feito um resumo das principais informações referente a cada campanha.

Nas primeiras três campanhas (Tabela 3), foram realizadas amostragens eulerianas na zona de máxima turbidez do estuário, cujos objetivos específicos incluíram medidas dos teores de COD, CID, COP e Chl-*a,* a influência dos parâmetros hidrodinâmicos e da sazonalidade sobre o comportamento do carbono, caracterizando parcialmente a origem do carbono (objetivos específicos a, b, c) que resultaram no capítulo 5.1.

Posteriormente, outras três campanhas lagrangeanas foram realizadas para avaliar a origem e o comportamento da MON ao longo do gradiente de salinidade estuarino, com resultados expressos no capítulo 5.2.

Por fim, na última campanha foi feita uma amostragem lagrangeana para avaliar as características óticas da MOD, partição geoquímica e sua interação com os metais, com resultados expressos no capítulo 5.3.

Tabela 3 - Síntese das campanhas de amostragem.

	DATA	ABORDAGEM	CAPÍTULO	PARÂMETROS AVALIADOS
1*	Set/2012			Salinidade, pH, temperatura, Chl-*a*
2**	Mai/2014	Euleriana	5.1	COP, COD, CID, $\delta^{13}C$
3*	Jul/2015			TR, vazão, percentual de água doce
4*	Mar/2016			Salinidade, pH, temperatura, Chl-*a*. MPS,
5**	Dez/2016	Lagrangeana	5.2	COP, COD, $\delta^{13}C$, $\delta^{15}N$, fenóis de lignina,
6*	Jun/2017			nitrogênio particulado e dissolvido
7**	Abr/2018	Lagrangeana	5.3	Salinidade, pH, temperatura, Chl-*a,*COD, POC, Fluorescência-MOD, ultrafiltração, metais dissolvido (ICP-MS)

*campanhas realizadas na estação seca

**campanhas realizadas na estação chuvosa

5. RESULTADOS E DISCUSSÃO

5.1. CARBON FLUXES IN A TROPICAL SEMIARID ESTUARY DURING SEVERE DROUGHT YEARS

ABSTRACT

This study assesses the seasonal and hydrodynamic factors controlling carbon budgets and fluxes in the maximum turbidity zone (MTZ) in a tropical semiarid estuary under extreme drought, the Jaguaribe River estuary in northeast Brazil. Dissolved organic carbon (DOC) and particulate organic carbon (POC) concentrations increased with residence time and freshwater volume. The Stable Isotope Analysis in R (SIAR) of POC and the absence of correlation between DOC and Chl-*a* indicated that organic matter was predominantly terrestrially derived. Stable isotope ($\delta^{13}C$, $\delta^{15}N$) ratios of POC suggested mangrove as important POC source. Dissolved inorganic carbon concentrations reflected the seasonal variability of the semiarid climate, being higher in the dry season due to the concentrating effect caused by the negative water balance. The reduced freshwater supply to the estuary resulted in carbon fluxes smaller than expected for a tropical region. Therefore, the MTZ behaved as a retainer of carbon during the dry season and as an exporter only in the rainy season. The expected intensification of droughts in NE Brazil by climate changes associated with anthropogenic activities in the watershed will enhance carbon retention and contribute to a continuous degradation of the estuary through eutrophication.

Key Words: Dissolved inorganic carbon, Dissolved organic carbon, Particulate organic carbon, mangrove, Jaguaribe River estuary.

5.1.1. Introduction

Carbon plays an essential role in the function of the planet as the primary source of energy to food chains and as the main regulator of the Earth's climate (HOFMANN et al., 2011). Semiarid ecosystems, somewhat neglected as a major player in the carbon cycle, are being considered important contributors to the global carbon cycle and may even dominate the inter-annual variability in regions strongly controlled by the El Niño–Southern Oscillation (ENSO) (ZHANG et al., 2017). The Brazilian semiarid zone is affected by El Niño, which strengthens further droughts in the region, increasing its vulnerability to climatic changes (MARENGO et al., 2017). This region is considered one of the areas most affected by climate change through the reduction of annual rainfall (CHIANG; KOUTAVAS, 2004; LACERDA; GODOY; MAIA, 2010). In addition, several dams were built in semiarid river basins to mitigate the effects of water scarcity (KROL; BRONSTERT, 2007). This is characteristics of the Jaguaribe River, the largest in Brazil completely inside of the semiarid region where more than 170 water reservoirs were built to assure water supply to agriculture, local human settlements and Fortaleza City (~ 3.6 million of inhabitants) (MARENGO et al., 2017; MARINS et al., 2002).

The result of extended droughts and river damming is the reduction of freshwater input and higher seawater intrusion in the Jaguaribe River estuary (DIAS; MARINS; MAIA, 2009) (Figure 5), mainly during the dry season when the saline intrusion reaches about 34 km inland, which provides ideal conditions for the retention of nutrients and suspended particulate material (SPM) (DIAS et al., 2016), trigging eutrophication and flocculation of organic matter (OM) in this area. Besides, significant changes in this major ecosystem, such as the formation of new islands (GODOY; LACERDA, 2013) and the rapid expansion of mangroves (GODOY; LACERDA, 2015), have been observed. The incoming tide brings suspended particulate material (SPM) to the middle estuary (MARINS; DIAS, [s.d.]) from the erosion of mangrove soils, resuspension of bottom sediments and transport of marine sands (LACERDA; MARINS, 2002). In estuaries without significant influence of river discharges; as for example a mangrove tidal creek in Sepetiba Bay, SE Brazil; DOC and POC concentrations and fluxes are primarily dependent on tidal net water fluxes (REZENDE et al., 2007).

Mangrove ecosystems are major suppliers of terrigenous organic carbon to coastal waters (BIANCHI; BAUER, 2011; PRASAD; RAMANATHAN, 2009; SAKHO et al., 2015), mainly in regions like the NE Brazil, where the dominant vegetation (Caatinga, the dry tropical forests) has low plant biomass and soils are poor in OM (MENEZES et al., 2012).

However, in some hypersaline environments, the marine-derived OM is more important than the mangrove-derived due the high seawater influence (RAY; SHAHRAKI, 2016). Apart from mangroves, local anthropogenic sources, such as shrimp farm, which is the most important economic driver of the estuary, may also contribute to carbon fluxes. Shrimp farms, in particular, is of high environmental relevance due to their high nutrient emission, higher than the natural one; their location surrounding the estuary and their effluents being released directly into tidal creeks (LACERDA et al., 2008; MARINS et al., 2011).

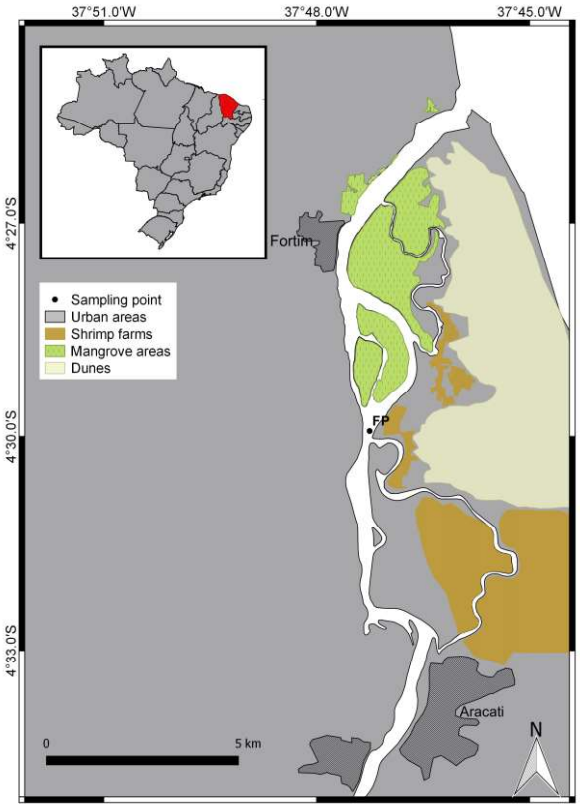

Figure 5 - Location of the study area and the sampling station at the fixed point (FP).

Carbon transport from land to the ocean through estuaries is key to the understanding of the global carbon cycle because these land-ocean boundaries display complex biogeochemical processes and strong physicochemical gradients that can modify the carbon fate in a relatively short time scale (days). The maximum turbidity zone (MTZ) is relevant to the understanding of the carbon dynamic of several estuaries, due to the high freshwater residence time (RT) and the intensification of biogeochemical processes, such as flocculation, sorption/desorption, and organic carbon mineralization (ABRIL et al., 2002; BATTIN et al., 2009; FISHER; HAGY; ROCHELLE-NEWALL, 1998; GU; ZHANG; JIANG,

2009). The MTZ normally acts as a carbon retainer, reducing the transport of materials in the continent-ocean interface due to the mineralization of the labile riverine organic matter, the dilution of riverine organic-rich materials (ABRIL et al., 2002) and the settle down of particles under low discharges conditions (GU; ZHANG; JIANG, 2009).

This characteristic hydrodynamic of the Jaguaribe River estuary have been observed to play a fundamental role over some transported materials such as SPM and mercury (Hg), for example (LACERDA et al., 2013). It has been reported the blocking of the Hg flow to the ocean during the dry season, which increases Hg residence time in the estuary. Contrariwise, river flow is relatively high during the rainy season and Hg is efficiently exported to the coastal zone, reducing its RT in the estuary. The long water RT in the estuary favors Hg complexation with dissolved organic matter (DOM), resulting in higher bioavailability as demonstrated by biomonitors (COSTA; LACERDA, 2014). This interaction attests the importance of organic matter as a geochemical carrier of toxic metals. Thus, understanding the carbon dynamics in semiarid estuaries could also contribute to the assessment of the estuary's environmental quality.

With ongoing intensification of droughts due to climate change and increasing freshwater demands for human activities, the Jaguaribe River estuary is under growing hydric stress that has reduced the fluxes to the ocean. Then, it is expected that the decreased freshwater inflow is reducing the riverine OM contribution to the estuary as well the carbon export to the ocean. On the other hand, the high marine intrusion might favor the input of the marine and mangrove OM in the estuary. Then, the aim of this study is to evaluate seasonal variations of DOC, POC, and dissolved inorganic carbon (DIC) discharge from the drainage basin to the Jaguaribe River estuary and their behavior during three semidiurnal tidal cycles in different years. In addition, the study aims to quantify the relative contribution of marine and non-marine carbon sources to the estuary.

5.1.2. Materials and methods

5.1.2.1. Study area

The Jaguaribe River is in the northeastern equatorial region of Brazil, in the State of Ceará, with 633 km of extension and a drainage basin of 72,043 km^2, being the largest contributor of fluvial waters to the Atlantic Ocean in about 860 km of coastline, between Cabo do Calcanhar and the Parnaíba River Delta (Figure 5). In this region, where the trade winds of both hemispheres join, the Intertropical Convergence Zone (ITCZ) regulates the

climate. The seasonal displacement of the ITCZ southward promotes the occurrence of rains in the Brazilian northeast, while its return to the north causes an intense drought during the austral winter and spring.

The Brazilian semiarid is characterized by low (<700 mm $year^{-1}$) and concentrated (4-5 months) precipitation with the prevalence of evaporation (1,900 mm $year^{-1}$) over rainfall during most of the year (SCHETTINI; VALLE-LEVINSON; TRUCCOLO, 2017). The regional seasonality is defined by a short season from January to May and a large dry season from June to December, usually without any precipitation whatsoever from August to November. This region has been pointed out as one of the most affected by global climate change (ALMAGRO et al., 2017; KROL; BRONSTERT, 2007; ZHANG et al., 2017), with about 20% reduction in annual rainfall in the past 50 years (GODOY; LACERDA, 2014, 2015). During the three years study period, annual rainfall was always below the historical average (Figure 6). As result, the Castanhão, which is the biggest reservoir built in the Jaguaribe River watershed with about 6.7 billion m^3 of water storage capacity (SANTOS et al., 2017), witnessed a volume reduction from about 85% in November 2011 to about 3.9% in October 2017, due to the absence of rain in the reservoir's basin characterizing one of the longest drought periods observed in the region (DNOCS, 2017; SANTOS et al., 2017).

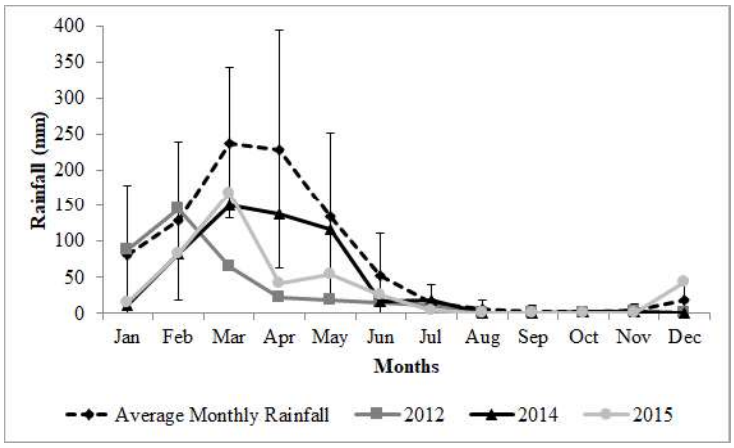

Figure 6- Monthly rainfall averages and standard deviations between 1980 and 2009 and monthly averages in 2012. 2014 and 2015 (FUNCEME, 2015).

The river mouth is surrounded by approximately 7.29 km^2 of mangroves (GODOY; LACERDA, 2014; GODOY; MEIRELES; LACERDA, 2018) including recent areas of mangrove colonization that cover 0.29 km^2. The estuary also harbors over 3,000 ha of shrimp farms, as well as medium-size urban areas with a total population of about 119,000 inhabitants. A previous study (ZOCATELLI et al., 2007) of the isotopic composition of

sediments from the Jaguaribe River estuary pointed to natural and anthropogenic sources of organic matter in the principal channel and the secondary tributaries of river. Such materials include sediments from erosive processes, organic matter leached from mangroves and from shrimp farms discharges.

Tides are semidiurnal, with an average tidal wave period of 12 hours and 50 minutes. The estuary´s wave propagation curve was estimated using daily water level data provided by the Brazilian Hydrography and Navigation Department, for the port of Areia Branca-Termisa (RN), and showed a 2-hour delay relative to that datum (DIAS; MARINS; MAIA, 2009). The mixture of fluvial and coastal water follows a longitudinal gradient of salinity modulated by tides during the dry season and by high fluvial discharges during the rainy season when advection transports this mixture to the inner continental shelf (DIAS; CASTRO; LACERDA, 2013). In the dry season of 2012, longitudinal sampling of the suspended matter showed that the location of estuarine MTZ (Figure 7) was the same in previous years (DIAS et al., 2016; MARINS et al., 2011), being established as fixed sampling station to all campaigns performed in this study (Figure 5). MTZ depth vary from 2.4 m in ebb tide to 5.5 m in flood tide.

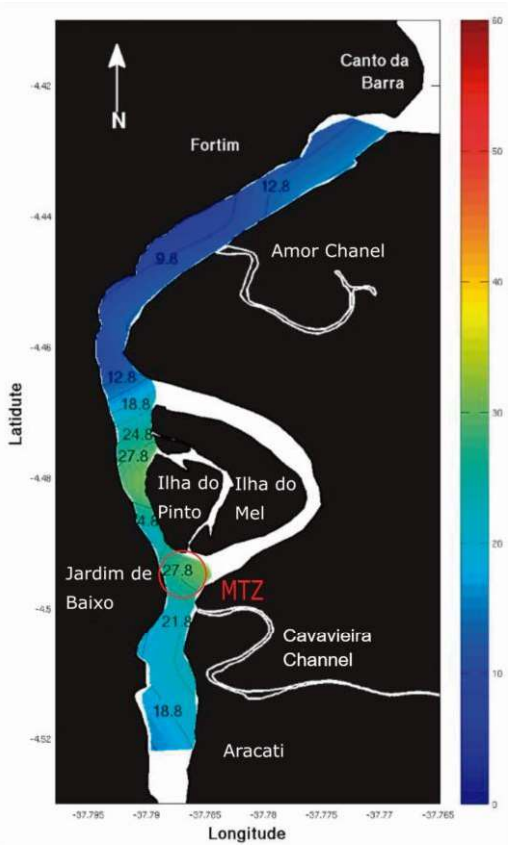

Figure 7 - Location of the maximum turbidity zone (MTZ).

5.1.2.2. Sampling

Given its relevance, three sampling campaigns were conducted at the MTZ of the estuary, two during the dry season (September 2012 and July 2015) and one in the rainy season (May 2014), all at spring tide. The average monthly precipitation of the campaigns was 0, 5 and 116 mm in September 2012, July 2015 and May 2014, respectively. Since July 2015, a strong negative ENSO occurred with increasing intensity in September and October (ALIZADEH-CHOOBARI, 2017; YEOMAN; JIANG; MITSCH, 2017).

Water collection and hydrochemical measurements were collected, every hour, in a fixed point of MTZ (Figure 5), in subsurface depth (0.5 m) during a tidal cycle of 13 hours (in each campaign). In the field, dissolved oxygen and pH were measured with a portable YSI (model 85/100 FT) multiparametric probe, while salinity and temperature were measured with a compact temperature and depth probe (Compact CTD model AST D687; JFE Advantech Co., Ltd. Nishinomiya, Hyogo Japan), with a 15 Hz data acquisition frequency. The CTD was used as a standalone unit, and the data were stored in the device's memory. After the CTD was pulled from the water, the data were downloaded and subjected to an initial quality control procedure. Inconsistent data due to systematic and random errors were deleted, and these data gaps were filled using linear interpolation such that only the profiles with a level of interpolation of ≤ 5% were included in the analysis. During pre-processing of the CTD data, spurious data were detected and excluded based on a maximum rate of change of each variable; values exceeding this limit were excluded. We used a Gaussian filter to fill the gaps left by the removal of inconsistent data. After the pre-processing, we evaluated the profiles at 0.5-m depth intervals from the surface to the bottom, and values that differed from the average by more than 3 times the standard deviation of each block were eliminated (EMERY; THOMSON, 2001).

Hourly water sample were sampled in duplicates, a total of 26 samples in each campaign for the analyses of DOC, DIC, POC and Chl-*a*. Water samples were filtered with pre-combusted (at 450ºC, 12h) GF/F Whatman fiberglass filters with a 0.7 µm mesh for further analysis of DOC, DIC, POC and isotopic composition ($\delta^{13}C$, $\delta^{15}N$) of POM (particulate organic matter). Chlorophyll *a* (Chl-*a*) was quantified in samples retained in AP40 fiberglass filters until saturation. It was not possible to evaluate the POC from the rainy season campaign of May 2014, due to loss during transport to the laboratory. The filtered water samples and the filters were kept under refrigeration according to storage protocols until their testing in the lab (GRASSHOFF; KREMLING; EHRHARDT, 1999). Mangrove leaves (*Rhizophora mangle* and *Avicennia Shaueriana*) were collected to measure its isotopic

composition ($\delta^{13}C$, $\delta^{15}N$). After being washed, frozen and lyophilized, the plant samples were milled using a knife mill.

5.1.2.3. Analytical techniques

DOC and DIC were measured with a Hyper TOC Analyzer (Thermo Fisher Scientific, Delft, Netherlands), according to the manufacturer. For determination of DOC, samples were acidified with HNO_3 (10%) and purged with an inert gas (O_2) to remove inorganic carbon. Next, the organic carbon remaining in the acidified sample (HNO_3) was oxidized by the UV- persulphate (UV_NPOC) photo-oxidation method. The oxidation product (CO_2) of DOC was carried by ultrapure O_2 gas to the non-dispersive infrared analysis detector (NDIR) and then quantified. DIC was measured by the 18% nitric acid oxidation (UV_ DIC) methodology that employs acidification of the sample to convert dissolved inorganic carbon in CO_2 before sending it to infrared non-dispersive detectors to measurement. Standards used to prepare mixed calibration curves were potassium hydrogen phthalate, calcium carbonate and hydrogen calcium carbonate, which were diluted to a concentration series adequate for each analysis. The detection limit was 11.63 and 11.42 μmol L^{-1} for DOC and DIC respectively.

Chl-*a* was extracted from filters in acetone 90% overnight and quantified using a spectrophotometer (JEFFREY; HUMPHREY, 1975). The DOC, DIC and Chl-*a* results were represented by the average of sampling duplicates (Coefficient of Variation <10%) to each hour of the tidal cycle.

The elemental and isotopic compositions C and N in the suspended particulate material and leaves were determined using a Flash 2000 elemental analyzer, with a Conflo IV combined to a Delta V Advantage mass spectrometer (Thermo Scientific IRMS). The analytical control was performed by sampling replicates (Coefficient of Variation <10%) and certified standards (Elemental Microanalysis Protein Standard) resulting in a 95% precision. The SIAR model (*Stable Isotope Analysis in R*) was used to calculate the mixture of carbon sources.

5.1.2.4. Assessment of the carbon discharge

Hourly instant current velocities were measured every hour with an ADCP (Sontek/YSI) with a 1500 MHz frequency, towed on a boat moving across the estuarine MTZ, perpendicularly to the water flow, to integrate the entire river section. The equipment was programmed for a 5-second burst interval with 0.25 m cells each, at depths between 6 and 7

meters in the rainy season and 3 to 4 meters in the dry season. The transported volume (Tv) or discharge (Q_f) in the mean area of the transversal section (A=A(x, Z)) was calculated:

$$T_V = \frac{1}{T}\int_0^T \left[\frac{1}{A}\iint_A \vec{v}.\vec{n}dA\right]dt$$

Where $\vec{v} = \vec{v}(x,Z,t)$ is the velocity vector, $\vec{n}$ is the vector normal to section A; T is the time interval of a full tidal cycle; x is the horizontal distance of the section; and Z is the depth (MIRANDA; CASTRO; KJERFVE, 2002). Freshwater percentage in the transported volume and water residence time were calculated according to MIRANDA, CASTRO AND KJERFVE (2002) and JONGE, (1992), based on the flows measured in the transversal section.

The salinity average of the estuarine system was calculated assuming a mixing of marine (V_P) and continental (V_f) water volumes in a semidiurnal tidal cycle, when the entire volume is removed from the system during the ebb tide. Therefore, for the purpose of conservation of mass (volume) we used:

$$S = \frac{V_P}{(V_P+V_f)}S_0$$

Where S is the estuary´s mean salinity ($g.kg^{-1}$) during flood and ebb tides, assuming that it is well mixed, and S_0 is the seawater salinity of the adjacent oceanic region (FEISTEL, 2003; LUKETINA, 1998; MIRANDA; CASTRO; KJERFVE, 2002).

The freshwater fraction (V_{fw}) was calculated:

$$V_{fw} = \frac{V_f}{(V_P+V_f)}$$

The flushing time (T_D) and the Residence Time (RT) represent the time in which one water particle remains within the estuarine system during the flood and ebb tides. According to Ketchum (1950), the T_D for liquid volumes and the RT of the water in an estuarine system are the ratio between the volume of freshwater (V_{fw}, m^3) and the discharge (Q_f, $m^3.s^{-1}$) in the MTZ:

$$RT = \frac{V_f}{Q_f}$$

The DOC, DIC and POC flows were obtained according to the following equation:

$$T_{XC} = \iint_A \varphi\vec{v}.\vec{n}dA = \iint_A \varphi.udA = \overline{\varphi u}A$$

where T_{XC} is the discharge of carbon fractions [$kg.s^{-1}$], u is the integrated average velocity in the water column ($m.s^{-1}$), φ is the average concentration of carbon geochemical fractions to each hour, DOC, POC and DIC ($mg.L^{-1}$), and A is the average area of the section transversal to the direction of the flow (m^2). This methodology has been successfully applied

to this estuary (DIAS et al., 2016; DIAS; MARINS; MAIA, 2013b).

5.1.2.5. Statistical analysis

Spearman correlation coefficients were calculated using a raw data matrix to explore possible correlations among variables for each campaign separately. Principal component analysis (PCA) was performed for the rainy and dry seasons separately to describe the relationships between salinity, pH, FWP, RT, DIC, DOC, POC and Chl-*a*. The hourly samples were taken as cases, and the parameters as variables. A correlation matrix was created (data were normalized by z scores) for extracting the eigenvalues and eigenvectors. Thereafter, the principal components were obtained by multiplying an eigenvector by the original correlated variables. A t-test was applied to evaluate differences of DOC and DIC averages between the sampling campaigns.

5.1.3. Results

5.1.3.1. Hydrology and water chemistry and Chl-a

Salinity varied between 5.5 and 36.3 $g.kg^{-1}$ (Figure 8A). Salinity exhibited strong seasonal variations, with higher salinity during the dry season relative to the wet season. The thermohaline indexes proposed by Dias et al. (2013a) for the Jaguaribe River estuary and the adjacent continental shelf were applied to this salinity range to characterize the water masses occurring in the estuary. The measured salinities were typical of coastal waters (34.5 - 36) in the dry season and typical of estuarine waters in the rainy season (Table 4).

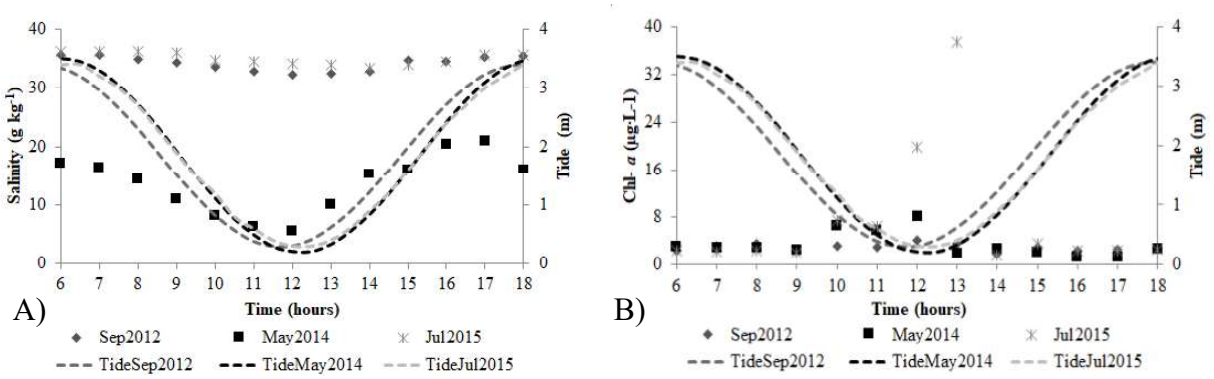

Figure 8 - Temporal variation of (A) salinity and (B) Chl-*a* concentrations in the dry and rainy seasons.

Instantaneous water discharges measured in the Jaguaribe River estuary ranged from 7 to 877 $m^3.s^{-1}$ (Table 4) similar to previous studies (DIAS et al., 2011; DIAS;

MARINS; MAIA, 2009). A bidirectional flux in the MTZ was observed during both seasons demonstrating a relevant influence of tides in the system, mainly in the dry period. Flood tide flows were greater than ebb tide ones in the dry season, but very similar in the rainy season, indicating greater saline intrusion into the estuary during dry seasons (Table 4).

The total water volume (TV) in the Jaguaribe River estuary varied between 1.6 x 10^5 and 2 x 10^7 m³. The average volume was very similar between tides, except in September 2012, when the average TV was one order of magnitude greater during the flood period (Table 4) indicating a net entrance of marine water. Freshwater RT and the freshwater fraction of the total volume (FWP) in the estuary were extremely low in the dry season due to extensive drought conditions, ranging from 8 to 44 min and from 0.5 to 11.8%, respectively (Table 4). During the 2014 rainy season, there was a 10-fold increase of RT and FWP (158 to 316 min and 42.5 to 84.9% respectively). In both seasons, the higher RT and FWP for each tidal cycle occurred at low tide, when discharge and marine influence were lower.

Chl-*a* concentrations varied from 1.2 to 37.5 $\mu g.L^{-1}$, displaying a constant pattern most of the time, but showed a peak when solar irradiation was most intense (around midday) in May 2014 and July 2015 campaigns and this matched with the tidal change from ebb to flood tide (Figure 8B). Mean Chl-*a* concentrations were 2.8 ± 0.6 (1.7 to 4.1), 3.0 ± 2.1 (1.2 to 8.0) and 7.0 ± 10.0 (1.6 to 37.5) $\mu g.L^{-1}$ in September 2012, May 2014 and July 2015 respectively. The highest Chl-*a* concentration was observed at midday in July 2015.

5.1.3.2. Hydrochemistry and biogeochemical controls of OM and DIC concentrations

POC concentrations varied from 41.2 to 261.4 $\mu mol.L^{-1}$ (Figure 9A), with mean values of 57.6 ± 8.1 $\mu mol.L^{-1}$ and 84.1 ± 62.2 $\mu mol.L^{-1}$ for the 2012 and 2015 campaigns, respectively. Although POC was not determined in the rainy season, a previous sampling in the MTZ in the rainy season of 2016 (unpublished results of author) showed similar concentrations (68.5 $\mu mol.L^{-1}$) to these observed in the earlier two campaigns, suggesting no significant seasonal difference. The similarity between seasons results from the extended drought period from 2012 to 2016. The POC concentrations were practically constant during the tidal cycle in September 2012. In July 2015, at the change of the tide, about four times increase in POC (261.6 µM) happened as observed to Chl-*a*.

Table 4 - Minimum, maximum and mean values of salinity (S), temperature (T), water flow (Qf), total water volume (TV), freshwater percentage (FWP), residence time (RT).

	S (g.kg^{-1})	T (°C)	Qf (m^{3}s^{-1})		TV (10^5 m^3)		FWP (%)		RT (min)	
			Ebb	Flood	Ebb	Flood	Ebb	Flood	Ebb	Flood
September 2012	32.2 - 35.7	27.3 - 29.5	7 – 48	27 – 267	1.6 – 11	6.1 – 60	2.2 – 11.8	2.7 – 11.2	8 – 44	10 – 42
	(34.2±1.3)	**(28.3±0.6)**	**(31±18.1)**	**(160±79.5)**	**(6.8±4.0)**	**(36±17.7)**	**(6.4±3.7)**	**(6.2±3.5)**	**(24±13.8)**	**(23±13.1)**
			Ebb	Flood	Ebb	Flood	Ebb	Flood	Ebb	Flood
May 2014	5.5 - 21	29.7 - 30.6	92 – 335	73 – 389	21 – 75	16 – 87	52 – 83	42.5 – 84.9	197 – 309	158 – 316
	(13.7±5.1)	**(30.3±0.3)**	**(232±80)**	**(244±125)**	**(50±17.9)**	**(55±27.9)**	**(64.8±12.0)**	**(59.4±16.5)**	**(241±44.6)**	**(222±61.4)**
			Ebb	Flood	Ebb	Flood	Ebb	Flood	Ebb	Flood
July 2015	33.1 - 36.3	27.1 – 29.1	70 – 552	181 – 877	16 – 120	40 – 200	0.5 – 6.3	2.2 – 8.2	2 – 23	8 – 31
	(34.5±1.0)	**(28.1±0.8)**	**(316±195.5)**	**(411±257.0)**	**(71±43.6)**	**(92±57.4)**	**(2.9±2.5)**	**(5.3±2.5)**	**(11±9.3)**	**(20±9.4)**

DOC concentrations varied from 34.6 to 614.9 µmol.L^{-1}, with mean values of 429.7 ± 125.2 µmol.L^{-1}, 419.1 ± 96.6 µmol.L^{-1} and 130.9 ± 60.3 µmol.L^{-1} for the 2012, 2014 and 2015 campaigns, respectively. DOC concentrations did not show a clear seasonal pattern. There were no differences between DOC concentrations in the first two campaigns ($p > 0.01$), but DOC concentrations in July 2015 were more than three times lower than those observed in May 2014 ($p < 0.01$) and Set 2012 ($p < 0.01$). The temporal variability of DOC increased in the ebb tide and a decreased in the flood tide. As well as POC, DOC concentrations were higher during the change of tide (Figure 9A and 9B). DOC was the dominant fraction of TOC concentrations during the dry season, ranging from 46 to 91%, with mean values of 87 and 61% of TOC in the 2012 and 2015 campaigns, respectively.

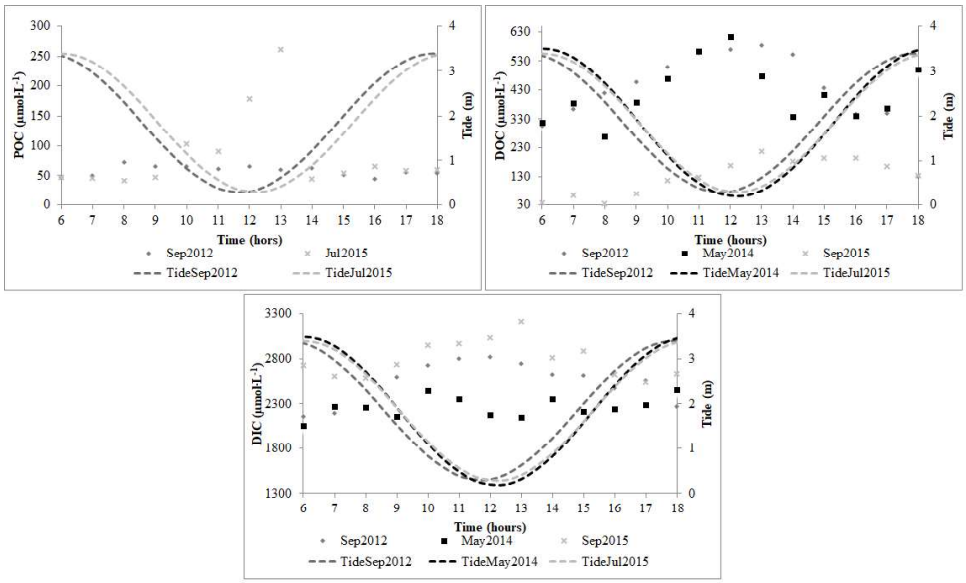

Figure 9 - Temporal variation of (A) POC, (B) DOC and (C) DIC concentrations in the dry and rainy seasons.

DIC concentrations varied from 2,057 to 3,217 µmol.L^{-1}, and mean values of 2,558 ± 212 µmol.L^{-1}, 2,264 ± 113 µmol.L^{-1}and 2,796 ± 197 µmol.L^{-1} for the 2012, 2014 and 2015 campaigns, respectively. DIC concentrations were very variable, being statistically different among the three campaigns ($p < 0.01$ for the three t-test for DIC variability), with higher concentrations in 2015. Tides notably influenced DIC concentrations in 2012 and 2015 (dry season), but not in the 2014 rainy season, showing a seasonal dependence (Figure 9C).

Results of PCA to dry and rainy seasons were represented in Figures 6A and 6B. The factors 1 and 2 explain about 80 % of the data variance to both seasons. The PCA revealed that estuarine hydrodynamic and biological component control OM dynamics in the Jaguaribe River estuary during the rainy season (Figure 10A). Factor 1 explains 61.77% of the data variance. It is dominated by S, FWP, TR, Chl-*a* and DOC, revealing that DOC covaried inversely with salinity and positively with FWP, RT, and Chl a. DIC was related only to pH, and they dominated the factor 2 of the PCA, which explains about 18.18% of the variance. During the dry season, Factor 1 explained 49.09% of the data variance. It is dominated by S, FWP, TR and DOC, revealing that DOC covaried inversely with salinity and positively with FWP, RT. POC, Chl-*a* and DIC

dominated factor 2, explaining 30.71% of data variability.

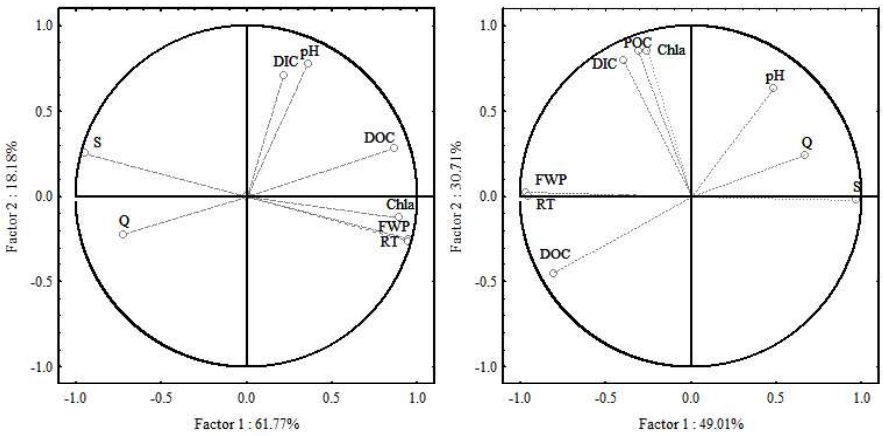

Figure 10 - Principal Components Analysis (PCA) for (A) rainy and (B) dry seasons of the salinity, pH, Chl-a, RT, FWP, DOC, DIC and POC.

The results of the PCA and the Spearman correlation analysis (Table 5) were consistent in most part of the relations. DOC concentrations were shown to be positively correlation with the FWP and RT, whereas the DOC concentrations were strongly and inversely correlated with salinity in both seasons. POC presented significant positive correlation with Chl-*a*. However, in Table 5 no significant correlations were found between Chl-*a* and DOC in rainy season and POC correlated positively with FWP and RT and negatively with salinity. Besides, DIC shown negative correlation with salinity.

Table 5 - Spearman correlation of salinity (S), water flow (Q_f), freshwater percentage (FWP) and residence time (RT) with particulate organic carbon (POC), dissolved organic carbon (DOC), dissolved inorganic carbon (DIC), chlorophyll a (Chl-*a*) concentrations and POC, DOC and DIC fluxes (T_{POC}, T_{DOC} and T_{DIC}) in the Jaguaribe River estuary (α = 0.01). Bold values are significant correlation at p<0.01.

		S	Q_f	FWP	RT	Chl *a*	DOC	DIC	POC
Rainy season (n=13;p<0.01)	**Chl *a***	**-0,670**	-0,434	**0,670**	**0,670**	1,000			-
	DOC	**-0,621**	-0,456	**0,621**	**0,621**	0,335	1,000		-
	DIC	-0,016	-0,247	0,016	0,016	0,137	0,192	1,000	-
	T_{DOC}	0,313	**0,857**	-0,313	-0,313	-0,390	-0,033	-0,192	-
	T_{DIC}	**0,566**	**0,984**	**-0,566**	**-0,566**	-0,495	-0,440	-0,170	-
Dry season (n =26; p<0.01)	**Chl *a***	-0,385	-0,345	0,387	0,375	1,000			
	DOC	**-0,713**	**-0,641**	**0,708**	**0,716**	0,252	1,000		
	DIC	**-0,522**	0,059	**0,523**	**0,515**	**0,543**	-0,026	1,000	
	POC	**-0,503**	-0,354	**0,506**	**0,498**	**0,686**	0,312	**0,565**	1,000
	PN	**-0,601**	**-0,454**	**0,606**	**0,597**	**0,780**	**0,420**	**0,570**	**0,938**
	T_{DOC}	-0,135	**0,638**	0,128	0,153	-0,093	0,073	0,068	-0,078
	T_{DIC}	**0,446**	**0,994**	**-0,448**	**-0,437**	-0,325	**-0,646**	0,095	-0,326
	T_{POC}	0,340	**0,911**	-0,341	-0,331	-0,086	**-0,617**	0,240	-0,074

5.1.3.3. C:N ratios, $\delta^{13}C$ and $\delta^{15}N$ values

The C:N ratio of the SPM was between 5.9 and 12.5, with similar mean values of 10.5 and 10.2 for the 2012, and 2015 campaigns, respectively. There was no clear trend in C:N ratios during tide variation. The $\delta^{13}C$ signature ranged from -28.9 to -25‰ (-27.0‰ ± 1.1), $\delta^{13}C$ values seem to be directly correlated to the tidal cycle (Figure 11A and 11B). The $\delta^{15}N$ isotopic composition of the SPM ranged from 2.2 to 6‰ (4‰ ± 1.0) but seems to be independent from the ebb and flow tides (Figure 11B). The POC:Chl-*a* ratio varied from 83.6 to 447.6, with similar averages of 254.6 and 232.9 for the 2012, and 2015 campaigns, respectively. Low values (<200) occurred mainly in low tide in July2015 (Figure 11C).

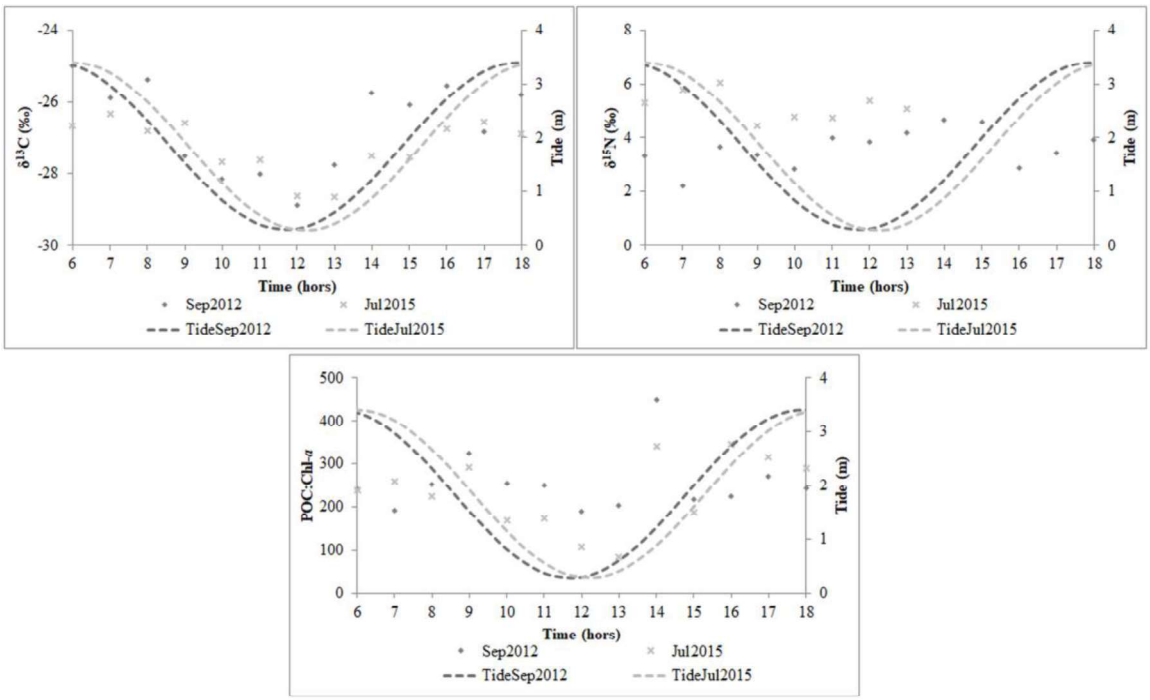

Figure 11 - Temporal variation of (A) $\delta^{13}C$, (B) $\delta^{15}N$ and (C) POC:Chl-*a* in the dry season.

In relation to tides, carbon concentrations normalized by weight, in the SPM were similar between flood and ebb tide (0.64 ± 0.34% and 0.67 ± 0.34%, respectively) as well as for the carbon isotopic composition and C:N molar ratio (-27.1 ± 1.18‰, 10.1 ± 1.6 and -26.8 ± 0.94‰, 10.5 ± 1.7, respectively). On a volumetric basis, the POC contribution to the total organic carbon (TOC) was higher in the 2015 tidal cycle, representing 39%, while in 2012 it represented 13%. In relation to tides, the POC contribution was similar between ebb and flood during the dry periods (~30%). The

$\delta^{13}C$ and $\delta^{15}N$ values of mangroves leaves were of -28.9‰ and 5.5‰ for *Avicennia shaueriana* and -27.6‰ and 3.3‰ for *Rhizophora mangle* respectively, ranging in an interval set for C_3 plants (REZENDE et al., 1990; VILHENA et al., 2018).

5.1.4. Discussion

The Jaguaribe River estuary experiences a decrease in freshwater input caused by the decrease of the annual rainfall in the region, an effect of climate changes, strengthened by river damming (DIAS; MARINS; MAIA, 2009; GODOY; LACERDA, 2013). Droughts have caused a fragmentation of the longitudinal hydrological continuum in the Jaguaribe River at ~36 km of the estuarine mouth in the dry season, characterizing the system temporarily as a tidal creek. Consequently, the supply of sediments from the watershed to the estuary and the SPM transport to the coastal zone have decreased (DIAS et al., 2016; DIAS; MARINS; MAIA, 2013b). On the other hand, the seawater intrusion has increased in the estuary, favoring the occurrence of marine geochemical processes and salt accumulation in the estuary (DIAS et al., 2016). The sampling period corresponded to a severe drought in the region, it is expected a decrease of carbon fluxes through the estuary and a large input of marine and mangrove-derived OM.

5.1.4.1. Organic matter sources

In the dry and rainy seasons, the strong positive correlations between DOC and RT and FWP showed that DOC variability was strongly related to the estuarine dynamics and associated with continental waters. This is expected for the rainy season when a substantial freshwater input occurred in the estuary, but not so much for the dry season when salinity was typically of coastal waters and varied little. During flood and high tide, the DOC concentrations were lowest. On the other hand, DOC concentrations were highest during the ebb and low tide, showing the strong influence of tides on the estuarine flushing and DOC concentrations, as well as POC, FWP and RT. The maximum DOC concentrations in ebb tide might be a result of the higher supply of OM from tidal creeks in ebb tide (REZENDE et al., 1990, 2007) as well as the release of mangrove-derived DOC to the water column through tidal pumping of pore water (KRISTENSEN et al., 2008). DOM fluorescence observed in the Jaguaribe River estuary, during a campaign also performed in May 2014, supports the predominance of

allochthonous DOM sources composed by humic substances (CAVALCANTE et al., 2016). The non-correlation between DOC and Chl-*a* suggests weak phytoplankton contribution to DOM during the dry and rainy seasons and the dominance of terrestrial sources in both seasons. In the rainy season, the PCA showed that DOC and Chl-*a* were driven by estuarine hydrodynamics.

Overall, the $\delta^{13}C$ signal of OM derived from continent and ocean are distinct, with more enriched $\delta^{13}C$ values in the marine OM (−23‰ to −18‰) than in the terrestrial (−30‰ to −25‰) and freshwater phytoplankton (-28‰ to -32‰) (BAUER, 2002; YE et al., 2017). In the Jaguaribe River estuary, $\delta^{13}C$-POM average was -27±1.1‰ pointing to the predominance of continental sources. $\delta^{13}C$ is an efficient tool to differentiate marine organic matter, but it is weak to distinguish fluvial phytoplankton against continental OM sources due to their close carbon isotopic signature (GUO et al., 2015). Then, POC:Chl-*a* can be used to elucidate doubts between terrestrial and autochthones source (SAVOYE et al., 2012). The majority of POC:Chl-*a* ratios from Jaguaribe River estuary were above 200 (Figure 11C), indicating that POC was predominantly detrital or degraded material (BIANCHI et al., 1997). POC:Chl-*a* ratios below 200 occurred in high tide when marine phytoplankton contribution was higher, and at the turning of tide in Jul 2015. The depleted $\delta^{13}C$ values associated with low POC:Chl-*a* ratios in July 2015 was indicative of freshwater phytoplankton as a POM source.

However, the little freshwater volume (<12%) and high salinity in the estuary, during the dry season, avoids freshwater phytoplankton from upstream regions. Therefore, the phytoplankton contribution to $\delta^{13}C$-POC values is probably originated from the shrimp farm since the dominants phytoplankton species from ponds (diatoms and *Pseudanabaena cf limnetica*) (CASÉ et al., 2008) were also founded in the riverine zone of the Jaguaribe River (LACERDA et al., 2018; MOLISANI et al., 2013). Then, the phytoplankton derived from shrimp pounds might have $\delta^{13}C$ values as depleted as the riverine. Since it was not possible to differentiate fluvial phytoplankton against continental OM sources through isotopic analyses, it was employed a two end-member mixing model to assess the relative contributions of marine and non-marine POM to the Jaguaribe River estuary. The non-marine source corresponds to the continental component (vegetation, soils and sediments) and fluvial phytoplankton. The isotopic composition of carbon and nitrogen in these two sources were: non-marine: $\delta^{13}C$ -27.9 ± 1.4‰; $\delta^{15}N$ 5.9 ± 1.7 ‰ and marine: -21.0 ± 0.8 ‰; $\delta^{15}N$ 6.0 ± 0.8 ‰ (BEZERRA et

al., 2015; REZENDE et al., 1990). The SIAR isotope model emphasizes the contribution of non-marine organic matter (94%; ranging from 87 to 98%) when compared to marine (6%; ranging from 2 to 12%) (Figure 12).

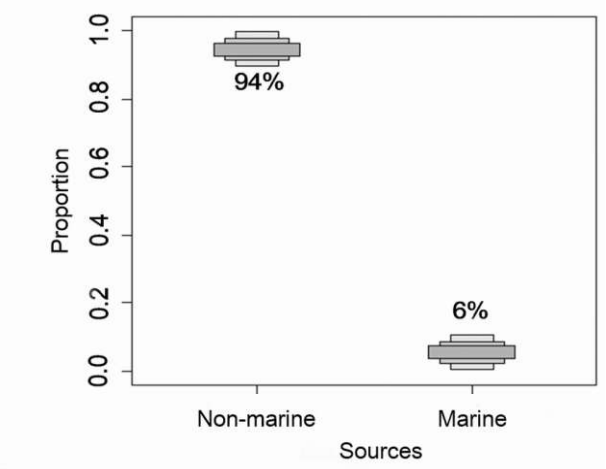

Figure 12 - Model SIAR for Particulate Organic Carbon considering two sources of organic material during the 2012 and 2015 tidal cycles (25%; 75% and 95% represented by different bars).

The SPM generated in the higher portion of the basin are trapped in the Castanhão dam, being liberated only when its floodgates are opened (GODOY; LACERDA, 2014). The reduction of sediment supply is magnified during intense droughts condition because the estuary became disconnected from the fluvial continuum at Itaiçaba city. Then, during the dry season, the SPM originates mainly from the estuary itself and soils of the lower portion of the watershed (GODOY; LACERDA, 2014). As mangroves are the predominant vegetation at the estuary vicinity, they are probably the principal OM source to the estuary. As can be seen through the similarity between the $\delta^{13}C$ and $\delta^{15}N$ values of POC average and mangrove leaves. This significant allochthonous POC source is possibly linked with the rapid expansion of mangrove areas. Rezende *et al.* (1990) showed the mangrove as a significant POC source to the estuary, varying from 16 to 100% of the total organic carbon flux in a mangrove creek, and that this contribution was very dependent on tidal amplitude. Therefore, the results obtained so far in the Jaguaribe River in the current circumstances are very compatible with other regions characterizing the system, at the moment, as a tidal creek.

5.1.4.2. Controls of organic matter and DIC interannual variations

Concentrations of DOC and POC in the Jaguaribe River estuary were typical of estuaries dominated by tides (MIDDELBURG; HERMAN, 2007) and under similar climate and anthropogenic pressures (Table 6). However, these DOC values were more than 50% lower than those reported to the year 2004 to the Jaguaribe River estuary by Mounier et al. (2018). The DOC reduction might be associated to the low terrestrial carbon fluxes as a result of drought and river damming (VAZQUEZ et al., 2011; YU et al., 2011). The lowest DOC concentrations, during the 2015 campaign, had already been measured in the estuary, but only in the estuarine mouth where it is more diluted by seawater (Zocatelli *et al.* 2007). The distinct DOC values in this campaign showed the vulnerability of Jaguaribe River estuary to changes in freshwater supply.

Table 6 - Anthropogenic pressures, water discharges and carbon concentrations in tropical estuaries.

Estuary (County)	Qf ($m^3 s^{-1}$)	Anthropic pressures	DOC ($\mu mol.L^{-1}$)	DIC ($\mu mol.L^{-1}$)	POC ($\mu mol.L^{-1}$)	Reference
Wanquan River (China)	69 - 336	Aquaculture. Urbanization Industry Damming	75 – 203	-	25 – 158	WU et al., (2013)
Yellow River (China)	600 - 693	Agriculture Damming	217 – 258	2.816 – 3.634	-	GU et al. (2009)
Tsengwen River (Taiwan)	0 - 130	Agriculture Damming	100 - 680	-	30 - 660	HUNG; HUANG, (2005)
Betsiboka River (Africa)	271	Aquaculture. Deforestation	41.6 – 125	-	41.6 – 167	RALISON et al., (2008)
Paraíba do Sul River (Brazil)	-	Agriculture. Livestock Farming. Industry. Urbanization	100 – 558	-	-	KRÜGER et al., (2003)
Jaguaribe River (Brazil)	7 - 877	Damming Aquaculture	35 - 615	2.057 - 3.217	41 - 261	**This study**

DIC concentrations in the Jaguaribe River estuary were similar to those observed in estuaries of the largest rivers in the world, as the Pearl River estuary (GUO et al., 2008; JIAO et al., 2008; ZHAI; YAN; QI, 2017) (Table 6). In estuaries, DIC is

controlled mainly by the mineralogy of the drainage basin, freshwater discharge and weathering intensity (GUO et al., 2008). Besides of low weathering rates, the drainage basin mineralogy of the Jaguaribe River is basically composed by silicates (GODOY, 2011; MARINS et al., 2011), that are more resistant to weathering in relation to carbonates minerals, then this two factors were not the cause of the high DIC levels in the estuary. However, the balance of precipitation and evaporation has significant influence in the DIC concentrations in the estuaries under dry climate (CAI et al., 2008). Generally, the high freshwater discharge in the wet season results in a dilution of DIC concentrations (GUO et al., 2008), while high evaporation rates increase DIC concentrations in estuaries (CAI et al., 2008). Therefore, the high DIC concentrations in the Jaguaribe River estuary were probably result of the evaporative process, similarly to a coastal lagoon under Mediterranean climate (DELGADILLO-HINOJOSA et al., 2008). The negative correlation between salinity and DIC (Table 5) occurred due to the DIC dilution by seawaters during the dry season. DIC concentrations reflected the seasonal rainfall variability, being higher during the dry season due to the concentrating effect by the high evaporative water loss and the dilution by higher freshwater discharges in the rainy season, as discussed above.

5.1.4.3. Carbon flux in the estuarine interface

In drought periods, estuarine waters presented higher salinity than the adjacent ocean because of the low freshwater input, the intense evaporation and the stronger influence of the tides. In the two campaigns conducted during the dry season, flood tides prevailed in the estuary and, therefore, the hydraulic push generated by the sea was more intense. Such feature resulted in the retention of POC, DOC and DIC in the MTZ (Figure 13A, 13B and 13C), thus exporting none of them. In this season POC, DOC and DIC fluxes were controlled mainly by estuarine discharges.

During the rainy season, however, the tidal DOC and DIC fluxes were very similar between both tides (Figure 13A, 13B and 13C), with average DIC fluxes one order of magnitude higher than DOC fluxes. The MTZ of the estuary exported 2×10^4 and 1.4×10^5 tons.year^{-1} of DOC and DIC to the downstream region in the rainy season, respectively. DOC and DIC fluxes were also driven by estuarine discharges and not by their concentrations. Probably, POC exportation had happened in the rainy season, since that MPS and elements associated to it, such as Hg, are exported in the rainy season (DIAS; MARINS; MAIA, 2013; LACERDA et al., 2013).

Estuarine water discharges have a central control in DIC, DOC and POC fluxes. Then, it is expected that the gradual reduction of riverine inflow in the Jaguaribe River estuary, by climatological and anthropogenic factors (YU et al., 2011), will further decrease the carbon export capacity by Jaguaribe River. DOC fluxes in the dry season were one order of magnitude greater than in the rainy season, indicating that retention is higher than exportation, suggesting OM accumulation occurs in the estuary during years of low riverine discharge. These factors raise a concern about the environmental quality of the estuarine body because they strengthen the conditions favoring eutrophication processes, which was already been observed in the last campaign of this study.

The DOC, POC and DIC fluxes in the Jaguaribe River estuary were below the average for tropical rivers, as estimated by Huang *et al.*, (2012), because the estuarine environment acts like a geochemical barrier promoting the retention of materials. These low fluxes of DOC through the Jaguaribe River estuary contribute to explain the low DOC levels (mean value of 48.5 μmol L^{-1}) measured in the surface waters of its adjacent continental shelf (CARVALHO et al., 2017). Similarly, the carbon fluxes also decreased after the construction of dams in a semiarid estuary in China (the Yellow River estuary). The Yellow River´s DOC, DIC and POC fluxes were 3.39 x 10^4, 3.38 x 10^5 and 7.0 x 10^4 ton.$year^{-1}$ in the dry season, and 3.04 x 10^4, 3.57 x 10^5 and 1.59 x 10^5 ton.$year^{-1}$ in the rainy season, respectively (GU; ZHANG; JIANG, 2009). The low carbon exportation from the MTZ of the Jaguaribe River estuary can also be related to the decreasing rainfall levels in the Brazilian Northeast region promoted by ENZO event like was observed in the Orinoco River (MORA et al., 2014).

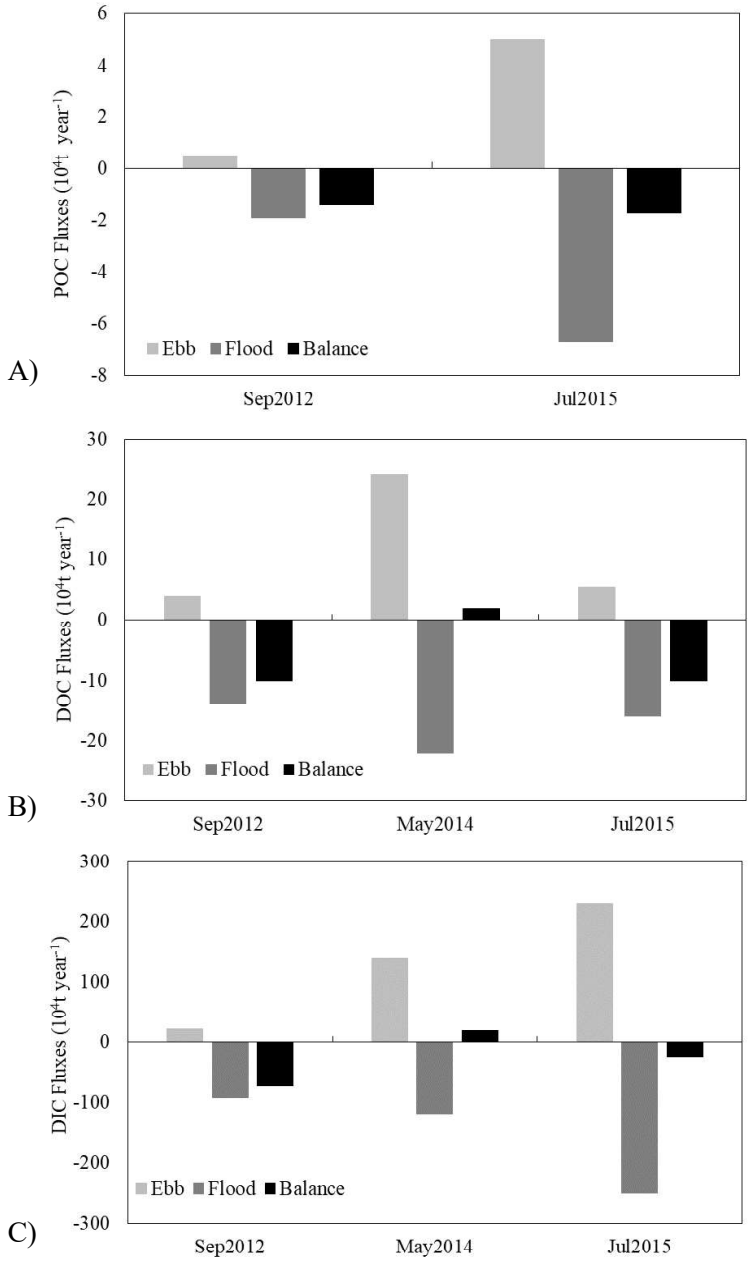

Figure 13 - Fluxes of (A) POC (B) DOC and (C) DIC through cross-section of MTZ of Jaguaribe river estuary for rainy and dry season. Positive values = importation; negative values = exportation.

5.1.5. Conclusions

The carbon behavior and fluxes in the Jaguaribe River estuary was strongly related to the hydrodynamic parameters such as the residence time, discharge and freshwater percentage. The estuarine OM was preponderantly continental-derived and mangroves might be the main OM source to the estuary. However, the phytoplankton activity showed significant influence on the POM dynamic in the dry season that was probably linked to aquiculture activity. DIC concentrations reflected the seasonal

variability of the semiarid climate, being higher in the dry season due the concentrating effect caused by the negative water balance. DOC and DIC concentration were significantly distinct between the sampling campaigns due to the high interannual variability of semiarid region.

The decrease of freshwater discharges by river damming and droughts affected the carbon transport through the Jaguaribe River estuary. In the monitored dry seasons, the Jaguaribe River estuary´s MTZ was a retainer of organic matter and DIC, while during the rainy season it was an exporter. The DIC and DOC flux was lower than expected for a tropical river but like other Chinese and South American rivers suffering the influence of the construction of reservoirs and decreasing precipitation associated with climate change. Projections pointing to intensification of climate change along the northeastern coast of Brazil tend to reduce carbon fluxes in the region's estuaries, as observed in this study, and may strongly influence the functioning of estuarine ecosystem.

Acknowledgments

We acknowledge support from the PRONEX/FUNCAP/CNPq Proc.Nº PR2-0101-00052.01.00/15 and CAPES and CNPq for grants to MC, RM and CR.

Author Contributions

MC and FD performed the sampling campaigns. MC performed Chl-*a*, DOC and DIC experiments under the supervision of RM. CR was responsible for POC and isotopic analyses. FD and MC calculated the hydrodynamics parameters and carbon fluxes. MC produced the graphics. The manuscript was written under the lead of MC, with the contribution of RM, FD, and CR.

Conflict of Interest Statement

The authors declare that the research was conducted in the absence of any commercial or financial relationships that could be construed as a potential conflict of interest.

5.1.6. References

ABRIL, G. et al. Behaviour of organic carbon in nine contrasting european estuaries. **Estuarine, Coastal and Shelf Science**, v. 54, p. 241–262, fev. 2002.

ALIZADEH-CHOOBARI, O. Contrasting global teleconnection features of the eastern Pacific and central Pacific El Niño events. **Dynamics of Atmospheres and Oceans**, v. 80, p. 139–154, 2017.

ALMAGRO, A. et al. Projected climate change impacts in rainfall erosivity over Brazil.

Scientific Reports, v. 7, n. 1, p. 1–12, 2017.

BATTIN, T. J. et al. Biophysical controls on organic carbon fluxes in fluvial networks. **Nature Geoscience**, v. 1, p. 95–100, 2009.

BAUER, J. E. Carbon Isotopic Composition of DOM. In: HANSELL, D. A.; CARLSON, C. A. (Eds.). . **Biogeochemistry of Marine Dissolved Organic Matter**. [s.l.] Elsevier Inc., 2002. p. 405–453.

BEZERRA, M. F. et al. Food preferences and Hg distribution in Chelonia mydas assessed by stable isotopes. **Environmental Pollution**, v. 206, p. 236–246, 2015.

BIANCHI, T. S.; BAUER, J. E. **Particulate Organic Carbon Cycling and Transformation**. [s.l.] Elsevier Inc., 2011. v. 5

CAI, W.-J. et al. A comparative overview of weathering intensity and HCO3− flux in the world's major rivers with emphasis on the Changjiang, Huanghe, Zhujiang (Pearl) and Mississippi Rivers. **Continental Shelf Research**, v. 28, n. 12, p. 1538–1549, 2008.

CARVALHO, A. C. O. et al. Air-sea CO2fluxes for the Brazilian northeast continental shelf in a climatic transition region. **Journal of Marine Systems**, v. 173, p. 70–80, 2017.

CASÉ, M. et al. Plankton community as an indicator of water quality in tropical shrimp culture ponds. **Marine Pollution Bulletin**, v. 56, n. 7, p. 1343–1352, 2008.

CAVALCANTE, M. S. et al. **Caracterização da matéria orgânica dissolvida nas águas do estuário do rio Jaguaribe através da técnica PARAFAC de MEEF**. Congresso Brasileiro de Oceanografia. **Anais**...Salvador: 2016Disponível em: <http://www.cbo2016.org/wp-content/uploads/2017/03/2017-03-6-Anais-CBO2016.pdf>

CHIANG, J. C. H.; KOUTAVAS, A. Tropical flip-flop connections. **Nature**, v. 432, n. 7018, p. 684–685, 2004.

COSTA, B. G. B.; LACERDA, L. D. Mercury (Hg) in fish consumed by the local population of the Jaguaribe River lower basin, Northeast Brazil. **Environmental Science and Pollution Research**, v. 21, p. 13335–13341, 2014.

DELGADILLO-HINOJOSA, F. et al. Dissolved nutrient balance and net ecosystem metabolism in a Mediterranean-climate coastal lagoon: San Diego Bay. **Estuarine, Coastal and Shelf Science**, v. 76, n. 3, p. 594–607, 2008.

DIAS, F. J. D. S. et al. Physical characteristics and discharges of suspended particulate matter at the continent-ocean interface in an estuary located in a semiarid region in northeastern Brazil. **Estuarine, Coastal and Shelf Science**, v. 180, p. 258–274, 2016.

DIAS, F. J. DA S. et al. Comparative analysis of rating curve and ADP estimates of instantaneous water discharge through estuaries in two contrasting Brazilian rivers. **Hydrological Processes**, v. 25, n. 14, p. 2188–2201, 1 jul. 2011.

DIAS, F. J. DA S.; CASTRO, B. M.; LACERDA, L. D. DE. Continental shelf water masses off the Jaguaribe River (4S), northeastern Brazil. **Continental Shelf Research**, v. 66, p. 123–135, set. 2013a.

DIAS, F. J. DA S.; MARINS, R. V.; MAIA, L. P. Hydrology of a well-mixed estuary at the semi-arid Northeastern Brazilian coast. **Acta Limnology Brasiliensia**, v. 21, n. 4, p. 377–385, 2009.

DIAS, F. J. DA S.; MARINS, R. V.; MAIA, L. P. Impact of drainage basin changes on suspended matter and particulate copper and zinc discharges to the ocean from the Jaguaribe River in the semiarid NE brazilian coast. **Journal of Coastal Research**, v. 29, n. 5, p. 1137–1145, 30 set. 2013b.

DNOCS, D. N. DE O. C. AS S. **Açude Castanhão está com apenas 3,9% da capacidade**. Disponível em: <http://www2.dnocs.gov.br/gab-cs/97-noticias-internas/3733-acude-castanhao-esta-com-apenas-3-9-da-capacidade>. Acesso em: 4 dez. 2017.

EMERY, W. J.; THOMSON, R. E. Data analysis methods in physical oceanography. In: **Data Analysis Methods in Physical Oceanography**. Amsterdam: Elsevier Science, 2001. p. xi–xii.

FEISTEL, R. A new extended Gibbs thermodynamic potential of seawater. **Progress in Oceanography**, v. 58, n. 1, p. 43–114, 2003.

FISHER, T. R.; HAGY, J. D.; ROCHELLE-NEWALL, E. Dissolved and particulate organic carbon in Chesapeake bay. **Estuaries**, v. 21, n. 2, p. 215–229, jun. 1998.

GODOY, M. D. P. **Mudanças na sedimentação no estuário do rio Jaguaribe (Ce) devido a mudanças nos usos do solo**. [s.l.] Universidade Federal do Ceará, 2011.

GODOY, M. D. P.; LACERDA, L. D. DE. River-Island Morphological Response to Basin Land-Use Change within the Jaguaribe River Estuary, NE Brazil. **Journal of Coastal Research**, v. 294, n. 2, p. 399–410, 2014.

GODOY, M. D. P.; LACERDA, L. D. DE. Mangroves Response to Climate Change: A Review of Recent Findings on Mangrove Extension and Distribution. **Annals of the Brazilian Academy of Sciences**, v. 87, n. 2, p. 651–667, 2015.

GODOY, M. D. P.; LACERDA, L. D. Changes in estuarine islands and rainfall trends in the Jaguaribe River watershed, Ceará State, Brazil. **Arquivos de Ciências do Mar**, v. 46, n. 2, p. 47–54, 2013.

GODOY, M. D. P.; MEIRELES, A. J. DE A.; LACERDA, L. D. Mangrove Response to Land Use Change in Estuaries along the Semiarid Coast of Ceará, Brazil. **Journal of Coastal Research**, v. 343, n. 3, p. 524–533, 2018.

GRASSHOFF, K.; KREMLING, K.; EHRHARDT, M. **Methods of Seawater Analysis**. 3. ed. Weinheim; New York; Chiester; Brisbane; Singapore; Toronto: Wiley-VCH, 1999.

GU, D.; ZHANG, L.; JIANG, L. The effects of estuarine processes on the fluxes of inorganic and organic carbon in the Yellow River estuary. **Journal of Ocean University of China**, v. 8, n. 4, p. 352–358, 25 out. 2009.

GUO, W. et al. Seasonal variation in sources and processing of particulate organic carbon in the Pearl River estuary, South China. **Estuarine, Coastal and Shelf Science**, v. 167, p. 540–548, 2015.

GUO, X. et al. Seasonal variations in the inorganic carbon system in the Pearl River (Zhujiang) estuary. **Continental Shelf Research**, v. 28, n. 12, p. 1424–1434, jul. 2008.

HOFMANN, E. E. et al. Modeling the Dynamics of Continental Shelf Carbon. **Annual Review of Marine Science**, v. 3, n. 1, p. 93–122, 15 jan. 2011.

HUANG, T.-H. et al. Fluvial carbon fluxes in tropical rivers. **Current Opinion in Environmental Sustainability**, v. 4, n. 2, p. 162–169, maio 2012.

HUNG, J.-J.; HUANG, M.-H. Seasonal variations of organic-carbon and nutrient transport through a tropical estuary (Tsengwen) in southwestern Taiwan. **Environmental geochemistry and health**, v. 27, n. 1, p. 75–95, fev. 2005.

JEFFREY, S. W.; HUMPHREY, G. F. New spectrophotometric equations for determining chlorophylls a, b, c1 and c2 in higher plants, algae and natural phytoplankton. **Biochemical Physiology Pflanzen**, v. 167, p. 191–194, 1975.

JIAO, S. et al. Stable isotopic composition of riverine dissolved inorganic carbon of the Xijiang river inner estuary. **Journal of Geographical Sciences**, v. 18, n. 3, p. 363–372, 2008.

JONGE, V. N. DE. Tidal flow and residual flow in the Ems estuary. **Estuarine, Coastal and Shelf Science**, v. 34, n. 1, p. 1–22, 1992.

KETCHUM, B. (1950). Hydrografic factors involved in the dispersion of pollutants introduced into tidal wateres. **J. Bost. Soc. Civ. Eng**. 37, 296–314.

KRISTENSEN, E. et al. Organic carbon dynamics in mangrove ecosystems: A review. **Aquatic Botany**, v. 89, n. 2, p. 201–219, 2008.

KROL, M. S.; BRONSTERT, A. Regional integrated modelling of climate change impacts on natural resources and resource usage in semi-arid Northeast Brazil. **Environmental Modelling and Software**, v. 22, n. 2, p. 259–268, 2007.

KRÜGER, G. C. T. et al. Dinâmica de carbono orgânico dissolvido no estuário do rio Paraíba do Sul, R. J., sob diferentes condições de maré e descarga fluvial. **Atlântica**, v. 25, n. 1, p. 27–33, 2003.

LACERDA, L. ., GODOY, M. D., AND MAIA, L. P. (2010). Mudanças climáticas globais. **Ciência Hoje**, 46, 32–37.

LACERDA, L. D. et al. Estimating the importance of natural and anthropogenic sources on N and P emission to estuaries along the Ceará State Coast NE Brazil. **Environmental monitoring and assessment**, v. 141, p. 149–64, 2008.

LACERDA, L. D., AND MARINS, R. V. (2002). River damming and changes in mangrove distribution Impacts from Land-based Activities on the Coastal Zone. **ISME/GLOMIS Electron.** J. 2, 1997–2000. Available at: www.glomis.com/ej/pdf/ej03.pdf.

LACERDA, L. D. et al. Pluriannual watershed discharges of Hg into a tropical semi-arid estuary of the Jaguaribe River, NE Brazil. **J. Braz. Chem. Soc.**, v. 24, n. 11, p. 1719–1731, 2013.

LACERDA, L. D., SANTOS, J. A., MARINS, R. V., AND SILVA, F. A. T. F. (2018). Limnology of the largest multi-use artificial reservoir in NE Brazil: The Castanhão Reservoir, Ceará State. **An. Acad. Bras. Cienc**. 90, 2073–2096. doi:10.1590/0001-3765201820180085.

LUKETINA, D. Simple tidal prism models revisited. **Estuarine, Coastal and Shelf Science**, v. 46, p. 77–84, 1998.

MARENGO, J. A. et al. Climatic characteristics of the 2010-2016 drought in the semiarid Northeast Brazil region. **Anais da Academia Brasileira de Ciências**, p. 1–13, 2017.

MARINS, R. V. et al. Impacts of land-based activities on the Ceará coast, north-eastern Brazil. In: **South American Basins: LOICZ Global Change Assessment and Syntesis**

of River Catchment - Coastal Sea Interaction and Human Dimensions. COPYRIGHT ed. Netherlands: LOICZ, 2002. p. 212.

MARINS, R. V et al. Anthropogenic sources and distribution of phosphorus in sediments from the Jaguaribe River estuary, NE, Brazil. **Brazilian Journal of Biology**, v. 71, n. 3, p. 673–678, 2011.

MARINS, R. V; DIAS, F. J. . **ALTERAÇÕES NA HIDROGEOQUÍMICA DO ESTUÁRIO DO RIO JAGUARIBE (CE): DESCARGA OU RETENÇÃO DE MATERIAIS ?**, [s.d.].

MENEZES, R. S. C. et al. Biogeochemical cycling in terrestrial ecosystems of the Caatinga Biome. **Brazilian Journal of Biology**, v. 72, n. 3 suppl, p. 643–653, 2012.

MIDDELBURG, J. J.; HERMAN, P. M. J. Organic matter processing in tidal estuaries. **Marine Chemistry**, v. 106, p. 127–147, 2007.

MIRANDA, L. B.; CASTRO, B. M.; KJERFVE, B. **Princípios em Oceanografia Física de Estuários**. São Paulo: EdUSP, 2002.

MOLISANI, M. M. et al. The influence of Castanhão reservoir on nutrient and suspended matter transport during rainy season in the ephemeral Jaguaribe river (CE, Brazil). **Brazilian journal of biology = Revista brasleira de biologia**, v. 73, n. 1, p. 115–23, 2013.

MORA, A. et al. Temporal variation and fluxes of dissolved and particulate organic carbon in the Apure , Caura and Orinoco rivers , Venezuela. **Journal of South American Earth Sciences**, v. 54, p. 47–56, 2014.

MOUNIER, S.; MARINS, R. V.; LACERDA, L. D. DE. Characterization of the Ceara Costal Zone Organic Matter Inputs. **archives-ouverts**, p. 39, 2018.

PRASAD, M. B. K.; RAMANATHAN, A. L. Organic matter characterization in a tropical estuarine-mangrove ecosystem of India: Preliminary assessment by using stable isotopes and lignin phenols. **Estuarine, Coastal and Shelf Science**, v. 84, n. 4, p. 617–624, 2009.

RALISON, O.H., BORGES, A.V., DEHAIRS, F., MIDDELBURG, J.J., BOUILLON, S., 2008. Carbon biogeochemistry of the Betsiboka estuary (north-western Madagascar). **Org. Geochem**. 39, 1649–1658. https://doi.org/10.1016/j.orggeochem.2008.01.010

RAY, R.; SHAHRAKI, M. Multiple sources driving the organic matter dynamics in two contrasting tropical mangroves. **Science of the Total Environment**, v. 571, p. 218–227, 2016.

REZENDE, C. E. et al. Nature of POC transport in a mangrove ecosystem: A carbon stable isotopic study. **Estuarine, Coastal and Shelf Science**, v. 30, p. 641–645, 1990.

REZENDE, C. E. et al. Dial organic carbon fluctuations in a mangrove tidal creek in Sepetiba bay, Southeast Brazil. **Brazilian Journal of Biology**, v. 67, n. 4, p. 673–680, 2007.

SAKHO, I. et al. A cross-section analysis of sedimentary organic matter in a mangrove ecosystem under dry climate conditions: The Somone estuary, Senegal. **Journal of African Earth Sciences**, v. 101, p. 220–231, 2015.

SANTOS, J. A. et al. Hydrochemistry and trophic state change in a large reservoir in the Brazilian northeast region under intense drought conditions. **Journal of Limnology**, v. 76, n. 1, p. 41–51, 2017.

SAVOYE, N. et al. Origin and composition of particulate organic matter in a macrotidal turbid estuary: The Gironde Estuary, France. **Estuarine, Coastal and Shelf Science**, v. 108, p. 16–28, 2012.

SCHETTINI, C. A. F.; VALLE-LEVINSON, A.; TRUCCOLO, E. C. Circulation and transport in short, low-inflow estuaries under anthropogenic stresses. **Regional Studies in Marine Science**, v. 10, p. 52–64, 2017.

VAZQUEZ, E. et al. Dissolved organic matter composition in a fragmented Mediterranean fluvial system under severe drought conditions. **Biogeochemistry**, v. 102, n. 1, p. 59–72, 2011.

VILHENA, M. P. S. P. et al. The sources and accumulation of sedimentary organic matter in two estuaries in the Brazilian Northern coast. **Regional Studies in Marine Science**, v. 18, p. 188–196, 2018.

WU, Y. et al. Biogeochemical behavior of organic carbon in a small tropical river and estuary, Hainan, China. **Continental Shelf Research**, v. 57, p. 32–43, abr. 2013.

YE, F. et al. Seasonal dynamics of particulate organic matter and its response to flooding in the Pearl River Estuary, China, revealed by stable isotope (δ^{13}C and δ^{15}N) analyses. **Journal of Geophysical Research: Oceans**, v. 122, n. 8, p. 6835–6856, 2017.

YEOMAN, K.; JIANG, B.; MITSCH, W. J. Phosphorus concentrations in a Florida Everglades water conservation area before and after El Niño events in the dry season. **Ecological Engineering**, v. 108, n. July, p. 391–395, 2017.

YU, H. et al. Impact of extreme drought and the Three Gorges Dam on transport of particulate terrestrial organic carbon in the Changjiang (Yangtze) River. **Journal of Geophysical Research: Earth Surface**, v. 116, n. 4, 2011.

ZHAI, W. D.; YAN, X. L.; QI, D. Biogeochemical generation of dissolved inorganic carbon and nitrogen in the North Branch of inner Changjiang Estuary in a dry season. **Estuarine, Coastal and Shelf Science**, v. 197, p. 136–149, 2017.

ZHANG, A. et al. ENSO elicits opposing responses of semi-arid vegetation between Hemispheres. **Scientific Reports**, v. 7, p. 1–9, 2017.

ZOCATELLI, R. . et al. **Distribuição e caracterização da matéria orgânica no gradiente estuarino do r. Jaguaribe, CE, Brasil**. Florianópolis: [s.n.].

5.2. ORGANIC MATTER SOURCES IN A HYPERSALINE ESTUARY FROM THE BRAZILIAN SEMIARID REGION

ABSTRACT

This study evaluated the sources, behavior and quality of organic matter (OM) in a semiarid estuary, NE Brazil, under a sharp decrease of freshwater input due to the rainfall scarcity and river damming. The influence of El Nino brought severe drought to the region, leading to the occurrence of hypersaline conditions in the Jaguaribe River estuary and the absence of seasonal variation on suspended particulate material and OM concentrations. The quantification of carbon sources, using the mixing model Stable Isotope Analysis in R (SIAR), showed that terrigenous OM was the dominant source to the estuary. However, dissolved lignin phenols concentrations diminished when the estuary was under hypersaline conditions due to the relative lower fluvial supply and leaching of soils. The marine sources contribution was also relevant to the OM bulk, principally when the estuary was under hypersaline conditions. Besides, an augment of the marine contribution to the estuarine OM with the permanence of drought was observed when compared with a previous study. With the ongoing increase of the freshwater demands for human consumption and the reduction of rainfall in the semiarid region, it is possible that this modification is intensified not only in this estuary but in other semiarid estuaries.

Key-words: organic matter, drought, hypersaline estuary, stable isotopes, dissolved lignin phenols, Jaguaribe River estuary

Highlights:

- El Niño caused the reduction of freshwater, suspended material and organic matter supply to the northeastern estuary, Brazil.
- Marine intrusion controlled the terrestrial OM delivery to the estuarine waters.
- Observed highest concentrations of organic matter and chlorophyll a in the creek impacted by shrimp farms.
- Lignin phenols showed high degradation of terrestrial organic matter
- The stable carbon isotopic composition reflects the increase of organic matter derived from the sea in the estuary due to the drought intensification.

5.2.1. Introduction

Freshwater flux is crucial in delivering continental organic matter (OM) to estuaries (HEDGES; KEIL; BENNER, 1997; LEE et al., 2017) besides of to balance tidal inputs of saltwater and marine organic matter (LEBRETON et al., 2016). However, estuaries from Brazilian semiarid coast are undergoing shapely decrease of freshwater input due to the effects of climate and anthropogenic pressures (KROL; BRONSTERT, 2007; SCHETTINI; VALLE-LEVINSON; TRUCCOLO, 2017). Droughts are natural phenomena in the semiarid Brazilian because of the insufficiency and unpredictability of precipitation. Beyond that, they are intensified by meteorological events (El Niño and anomalously warm tropical North Atlantic) and climate change (MARENGO et al., 2017). Since water is a scarce resource, several dams were constructed along the rivers to improve water availability and regulate their flow (CAMPOS et al., 2000), resulting in a reduced amount of freshwater reaching the estuary, strong marine intrusion and consequent colonization of the estuary with mangrove (GODOY et al., 2018). This hydric stress reduces the contribution of riverine material to the estuary (DIAS; MARINS; MAIA, 2013; MOLISANI et al., 2013) and consequently to the ocean, as can be observed through the formation of estuarine plume only in episodes of intense rainfall (DIAS; CASTRO; LACERDA, 2013). Besides, this hydric stress favors bank erosion by tides (MARINS et al., 2003).

In the Jaguaribe River estuary, located in NE Brazil, carbon fluxes are low in comparison to other tropical rivers due to its low freshwater discharge and consequently strong choking effect imposed by tides. The drought intensification in this region seems to have caused a decline of DOC concentrations in the estuary (CAVALCANTE, 2015).

Another important output of the negative water balance is the increase of seawater residence time (RT) in the estuary (DIAS et al., 2016). It provides an ideal condition for the accumulation of suspended particulate material (SPM), nutrients and carbon that can enhance eutrophication and flocculation processes in the estuary (DIAS et al., 2016). The longer seawater residence time can also lead a hypersaline condition, that can reduce OM production via biological activity (PINCKNEY; PAERL; BEBOUT, 1995; SOUZA et al., 2003), change chemical properties of dissolved organic matter (DOM) and its behavior (CATALÁ et al., 2013; MENDOZA; ZIKA, 2014).

With ongoing environmental changes, less precipitation and more modifications in the hydrology are expected. In such a scenario, OM concentrations can

be reduced as well as its source (marine vs. terrestrial) and quality can be changed. All this alters not only OM reactivity but also the estuary functioning as a whole due to its key role in the biogeochemical process as bacterial production, trophic web organization, metal complexation and carbon cycling (SHIN et al., 2016b; VAZQUEZ et al., 2011).

The identification of OM sources in estuaries is difficult due to the mixing of several sources and their modifications caused by biogeochemical process. Stable isotope ratios of carbon and nitrogen ($\delta^{13}C$, $\delta^{15}N$) provide information regarding sources and turnover of OM in estuaries (GUO et al., 2015; YE et al., 2018). Although $\delta^{15}N$ is used to trace estuarine organic matter sources, it is not always appropriate. As in cases in which the differences among end-members are small or if isotopic signature alterations during diagenesis and food-chain processing are significant (MIDDELBURG; HERMAN, 2007). Still, $\delta^{15}N$ is a proper tool to identify estuarine organic matter processing. Overall, the $\delta^{13}C$ signal of OM from continent and ocean are distinct, with more enriched $\delta^{13}C$ values for OM derived from marine phytoplankton (−23‰ to −18‰) than for terrestrial-derived OM (−30‰ to −25‰) (BAUER, 2002).

POC/Chl-*a* ratios have been used as an indicator of OM source (LEBRETON et al., 2016; REZENDE et al., 2010). POC/Chl-*a* values above 200 suggest that detrital forms of organic matter are dominant and values below that, it indicates that phytoplankton derived OM dominates (CIFUENTES; SHARP; FOGEL, 1988; SAVOYE et al., 2012). Lignin is a stable phenolic macromolecule restricted to vascular plants and absent in all other living organisms (HEDGES; KEIL; BENNER, 1997), thus lignin oxidation products are being efficiently used to trace and calculate the relative contribution of vascular plant inputs in estuarine systems (HEDGES; KEIL; BENNER, 1997; SPENCER et al., 2009; WARD; RICHEY; KEIL, 2012).

This work contributes to the improvement of the knowledge on the impacts of an intense drought period caused by the El Niño event and the effects of marine intrusion over the estuarine organic matter geochemistry.

5.2.2. Materials and methods

5.2.2.1. Study Area

The study took place in the Jaguaribe River estuary, located within the Northeastern coast of Brazil (Fig. 14), that is marked by a strong seasonal rainfall regime. The annual rainfall coastal zone ranged from 400 to 2000 mm, with an average of 912.7mm, during the past 30 years (FUNCEME, 2017). Rainy events start in January (81mm) and extend to June (52mm), with the highest rainfall in March (238mm). The scarcity of rain extends from July (16mm) to December (19mm), and between August and November frequently no precipitation is observed.

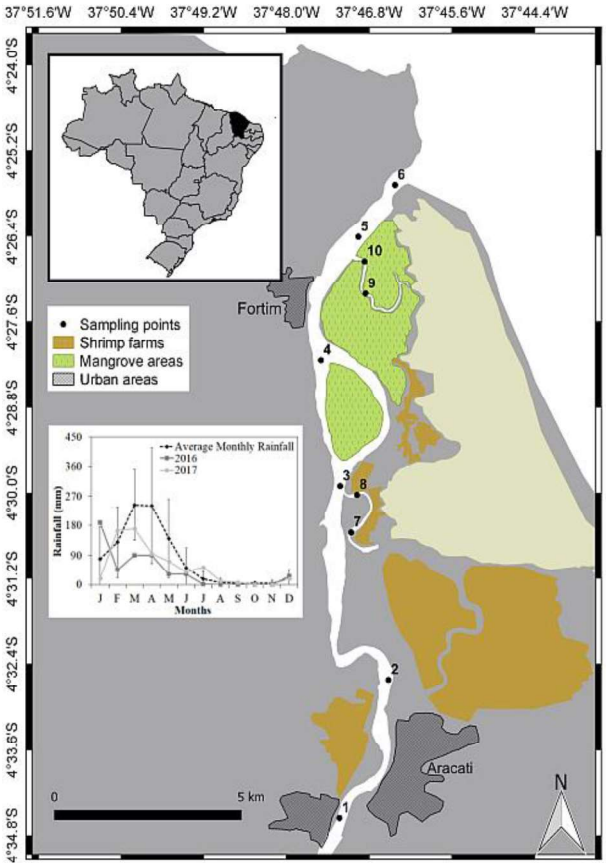

Fig.14. Study area, sampling stations, monthly rainfall averages with standard deviations between 1980 and 2009, and monthly averages in 2016 and 2017

The study years were drier, with a mean annual rainfall of 506.6 in 2016 and 650.2 mm in 2017, due to the effect of the El Nino event that promoted the most severe drought ever recorded in the semiarid region Northeast Brazil between 2012 and 2016 (MARENGO et al., 2017) (Fig. 14). Principally during the year 2016 (ALIZADEH-CHOOBARI, 2017; YEOMAN; JIANG; MITSCH, 2017), occurring a reduction of 62%

of precipitation in March when compared with the historical average for this month (238 mm).

The tidal regime is semidiurnal and meso-tide, with maximum amplitude reaching 3.0 m (DIAS et al., 2011). Freshwater discharges dropped from 60 - 130 m^3s^{-1} to 20 m^3s^{-1} after the built of major dams of the Jaguaribe River (DIAS; MARINS; MAIA, 2013). The temporal variability of the freshwater volume in the estuary reflects in the water RT, that is longer in the dry than the rainy season, reaching extremes values of 0.5 and 13 days respectively.

5.2.2.2. Sampling and sample processing pre-analyses

Sampling campaigns were carried out in the Jaguaribe River estuary at spring tide, two in the rainy season (March 2016 and June 2017) and one in the dry season (December 2016). The composed precipitation 15 days before each campaign were 57.5, 0 and 59.4 mm in March 2016, December 2016 and June 2017, respectively. Six sampling stations were distributed along the principal channel, two in the tributary tidal creeks Cumbe Chanel (CC) and two in the Amor Chanel (AC) (Fig. 14). The Cumbe Chanel is heavily impacted by shrimp farms because they discharge their effluents directly in it (ESCHRIQUE et al., 2010; LACERDA; SANTOS; MADRID, 2006). Whereas, the Amor Chanel is surrounded by a well-preserved mangrove area.

A portable YSI multiparametric probe (model professional plus) was used to measure salinity, temperature and dissolved oxygen and a portable pH meter (Metrohm) to measure pH in situ. Bottom sediments and subsurface water were sampled during all campaigns in duplicate with a van Veen sampler and an acrylic Van Dorn bottle, respectively. The fraction of freshwater (f) in each station was calculated from salinity (S), where 35.5 corresponded to the salinity in the oceanic end-member (FRY, 2002):

$$f = (35.5 - \text{measured salinity})/35.5$$

In addition, end-members samples from soil fluvial plains and mangrove, fluvial bank tree leaves (*Copernicia prunifera*) and mangrove leaves (*Rhizophora mangle* and *Avicennia shaueriana*), grasses (*Paspalum sp*), herbs (*Sesuvium portulacastrum*) and algae (*Ulva fasciata*), were also collected and characterized to investigate their influence as a carbon source to the estuary.

Immediately after sampling, water samples were filtered through pre-combusted (at 450ºC, 12h) Whatman GF/F filters with a 0.7 µm mesh to collect suspended particles for further analysis of particulate organic carbon and particulate

nitrogen (POC, TPN) and its isotopic composition ($\delta^{13}C$, $\delta^{15}N$) besides suspended particulate material (MPS). After filtration, between 1 and 2 L of samples were acidified, to pH 2 (HCl 32%, p.a.), and DOM was isolated from the water according to the solid-phase extraction (SPE) (DITTMAR et al., 2008). After DOM extraction, the cartridges were desalted (0.01 mol L^{-1} HCl), dried with N_2, and immediately eluted with 40 mL of methanol. The elutes were stored at –16°C in the glass ampoules until further analyses of isotopic composition ($\delta^{13}C$ and $\delta^{15}N$) and dissolved lignin phenols. Chlorophyll *a* (Chl-*a*) was quantified in samples retained in AP40 fiberglass filters until saturation, extracted in acetone, and quantified using a spectrophotometer, according to ISO 10260 (1992) protocol.

5.2.2.3. Analitical techniques

DOC concentrations from March 2016 campaign were measured, at the Coastal Biogeochemistry Laboratory (Ceará), by UV-persulphate oxidation method with a HiperTOC Analyzer, according to the manufacturer (THERMO). The DOC results of December 2016 and June 2017 were acquired, at Environmental Science Laboratory (Rio de Janeiro), by the high-temperature catalytic oxidation method on an automated TOC analyzer (Shimadzu TOC 5000). The detection limit was 11 µmol L^{-1} and 4 µmol L^{-1} respectively. DOC data reported the mean of three replicate injections, for which the coefficient of variance was <7%. DOC analyses from December 2016 were performed in the both laboratories to evaluate if the results were statistically different between them. The t-test showed no statistical difference in DOC results between them ($p>0.05$).

Prior to elemental and isotopic organic carbon and nitrogen analysis, the filters were treated in silver plates with HCl vapor to remove carbonates, sediments were weight (~10mg) and acidified with 1 mol L^{-1} HCl in silver capsules to remove carbonates. Plants samples were weight (~1.0 mg) in tin combustion capsules. The stable carbon isotopic composition of SPE-DOM was determined following the Seidel et al. (2015) protocol.

All elemental and isotopic analyses were made using a Flash 2000 elemental analyzer, with an interface Conflo IV, combined to a Delta V Advantage mass spectrometer (Thermo Scientific IRMS). The $\delta^{13}C$ and $\delta^{15}N$ values were expressed in per mil (‰) relative to the PDB standard and atmospheric N_2 respectively. The analytical control was performed by sampling reproductions (Coefficient of Variation <10%) and certified standards resulting above 98% recovering.

The mixing model SIAR (Stable Isotope Analysis in R) with three end-members was used to quantify the relative proportions of different sources in POM, DOM and sedimentary OM from the Jaguaribe River estuary based on their $\delta^{13}C$, $\delta^{15}N$. This is a Bayesian mixing model developed by Parnell et al., (2010), that provides the probability density distributions, mean proportion and credibility intervals (25%, 75% and 95%) for each source added to the model, incorporating uncertainty linked to elemental concentrations, isotopic signatures and fractionation. The $\delta^{13}C$ marine corresponded to a published isotopic value for marine DOM from the Fortaleza shelf (-22.03‰; CARVALHO et al., 2017) and the $\delta^{15}N$ to an average POM samples from the plume of the Jaguaribe River (6.3‰). $\delta^{13}C$ and $\delta^{15}N$ from C_3 plant detritus were the average isotopic composition of C_3 plants measured in this study (Table 7) (-28.5‰ and 4.9‰). $\delta^{13}C$ and $\delta^{15}N$ of OM sediment-derived were the average isotopic composition of C_3 plants measured in this study (Table 7) (-24.2‰ and 5.4‰)

Dissolved lignin phenols were analyzed using the cupric oxide oxidation, and trimethylsilyl derivatives were quantified by capillary gas chromatography (GOÑI; HEDGES, 1990; HEDGES; MANN, 1979). Eight lignin phenols (two cinnamyl phenols "C", three syringyl phenols "S" and three vanillyl phenols "V") were measured to evaluate vascular plant sources of dissolved organic matter. These phenol yields are conventionally represented as lambda (Λ_8; mg per 100 mg of organic carbon) and Σ_8 (the sum of the eight major phenols normalized to the sample volume). Beyond calculation of S/V, C/V and acid/aldehyde ratios, the Lignin Phenol Vegetation Index (LPVI) (TAREQ; KITAGAWA; OHTA, 2011; TAREQ; TANAKA; OHTA, 2004) was used to identify vegetation source. The LPVI considers the plant heterogeneity and the digenetic sequence of the phenolic groups.

5.2.3. Results

5.2.3.1. Hydochemical variables

The salinity along the main channel of the Jaguaribe River estuary varied between 25.1 and 40.2 gkg^{-1}, with mean of 38.2 gkg^{-1} in March 2016, 36.9 gkg^{-1} in December 2016 and 26.4 gkg^{-1} in June 2017. The estuary presented hypersalinity in both campaigns performed in 2016, with salinity higher than from adjacent coastal water, which varies between 34.5 and 36 gkg^{-1} (CARVALHO et al., 2017). Besides, the estuary presented an inverted salinity gradient during these campaigns, with the salinity increasing landward (Fig. 15a, 15b and 15c). However, the reduction of the salinity,

mean of 26.4 gkg^{-1}, and reestablishment of the estuary positive salinity gradient in June 2017 showed that these characteristics are not permanent.

The freshwater percentage was very low, varying between 0 and 29% with an average of 0% in March 2016 and December 2016, and 26% in June 2017. The secondary channels showed salinity higher than the principal channel in the campaigns performed in 2016. While in June 2017, the salinity averages of the secondary channels were lower (Fig. 15c).

The temperature ranged between 27.6°C and 30.8°C, with mean values of 30.7°C, 29.7°C and 29.3°C in March 2016, December 2016 and June 2017 respectively. The dissolved oxygen varied from 2.4 to 6.7 mgL^{-1}, showing mean concentrations of 4.0, 5.3 and 5.5 mgL^{-1} in March 2016, December 2016 and June 2017 respectively. The pH ranged from 7.4 to 8.0, with averages of 7.7, 7.8 and 7.6 in March 2016, December 2016 and June 2017 respectively.

SPM concentrations generally varied between 3.3 and 14.3 mgL^{-1} in the estuary (Fig. 15d, 15e and 15f) main channel with an average of 7.6 mgL^{-1}. They were similar to those observed by Dias et al. (2013a) in the dry season, without exhibit seasonal variability ($p>0.05$). However, the spatial MPS distribution showed significantly higher concentrations in the Cumbe channel (mean value of 29.6 mgL^{-1}) and Amor channel (mean value of 13.9 mgL^{-1}), than in the main channel (mean value of 7.6 mgL^{-1}) ($p<0.05$).

Chl-*a* concentrations were relatively low in the estuary proper (0.4 – 8.4 μgL^{-1}), but high in the Cumbe Channel where values like 35.8 and 58.8 μgL^{-1} were measured. Chl-*a* showed a positive correlation with SPM in December 2016 and March 2016 ($r=0.53$, $p<0.05$), but in June 2017 there was no correlation between them ($p>0.05$).

Similarities among the campaigns were analyzed using multivariate cluster analysis (Fig. S1), considering the parameters evaluated in all of them (hydrochemical parameters, Chl-*a*, and SPM). Two groups were identified: The Group 1 included the March 2016 and December 2016 campaigns, when the estuarine waters presented hypersalinity; and the Group 2 corresponded to June 2017. The groups differed from the others by relative low salinity values in the campaign performed in June 2017 ($p<0.05$, Wilcoxon test). Then, Spearman correlation coefficients were calculated using a raw data matrix to explore possible correlations among variables for each group separately.

1

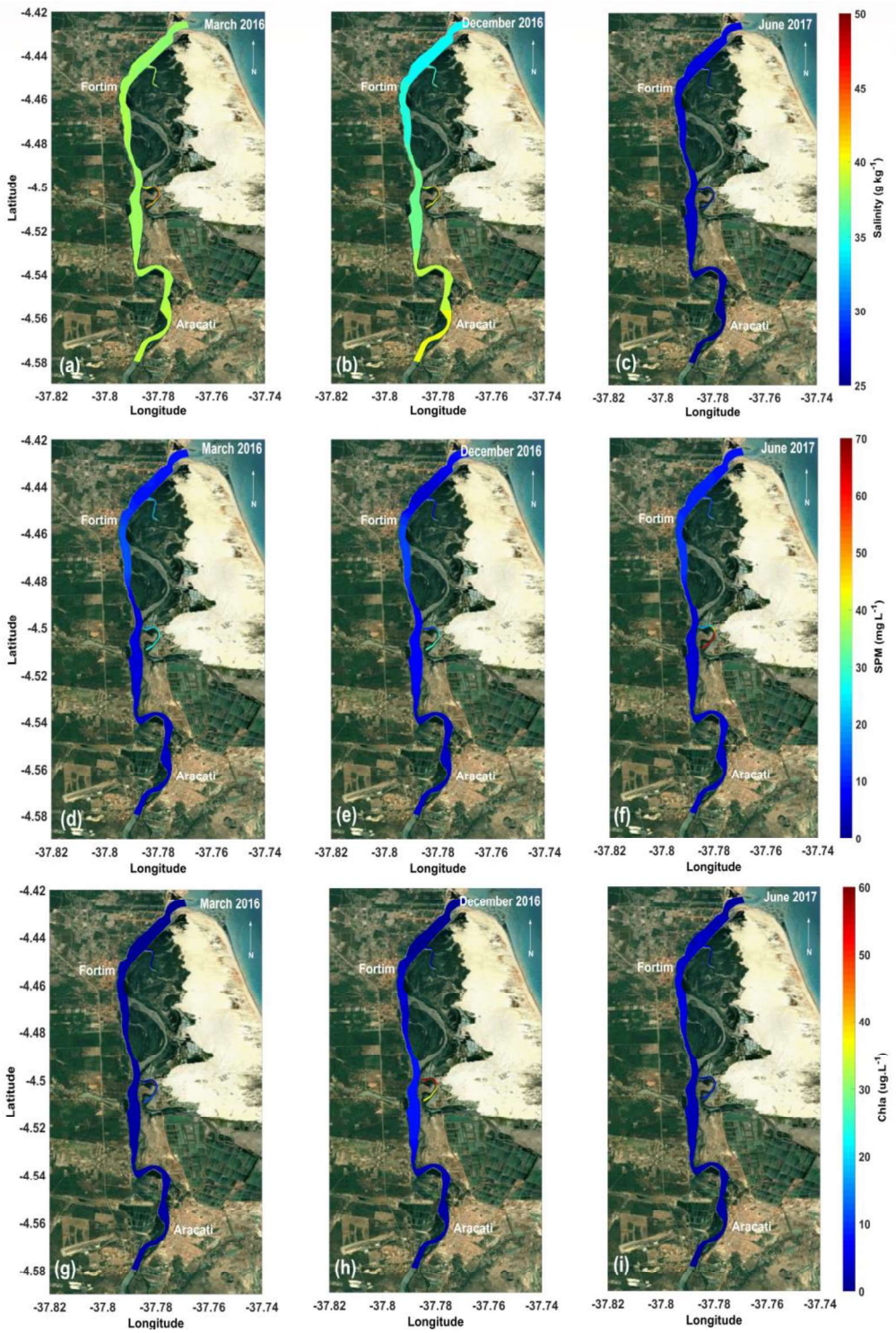

Fig. 15. Distribuition of (a-c) salinity, (d-f) SPM and (g-i) Chl-*a* in the Jaguaribe River estuary.

2

3

5.2.3.2. Behavior of organic matter

POC concentrations varied between 27.4 and 80.9 µmol L^{-1} and the TPN from 2.3 to 8.5 µmol L^{-1} in the main estuary. The POC (Fig. 16a and 16b) and TPN trends along the salinity gradient were practically constant, but with distinctly higher levels at Cumbe Channel in December 2016 and June 2017. POC did not correlate with Chl-*a* in any campaign ($p>0.05$). POC/Chl-*a* suggested a predominantly detritus origin (values above 200) (Guo et al., 2015; Lebreton et al., 2016), ranging from 83.8 to 990.1 with mean values of 217.1 ± 112.2 and 399.7 ± 244.3 in December 2016 and June 2017 respectively. The POC/Chl-*a* values below 200 corresponded to samples with enriched $\delta^{13}C$ values, suggesting a higher contribution from marine phytoplankton.

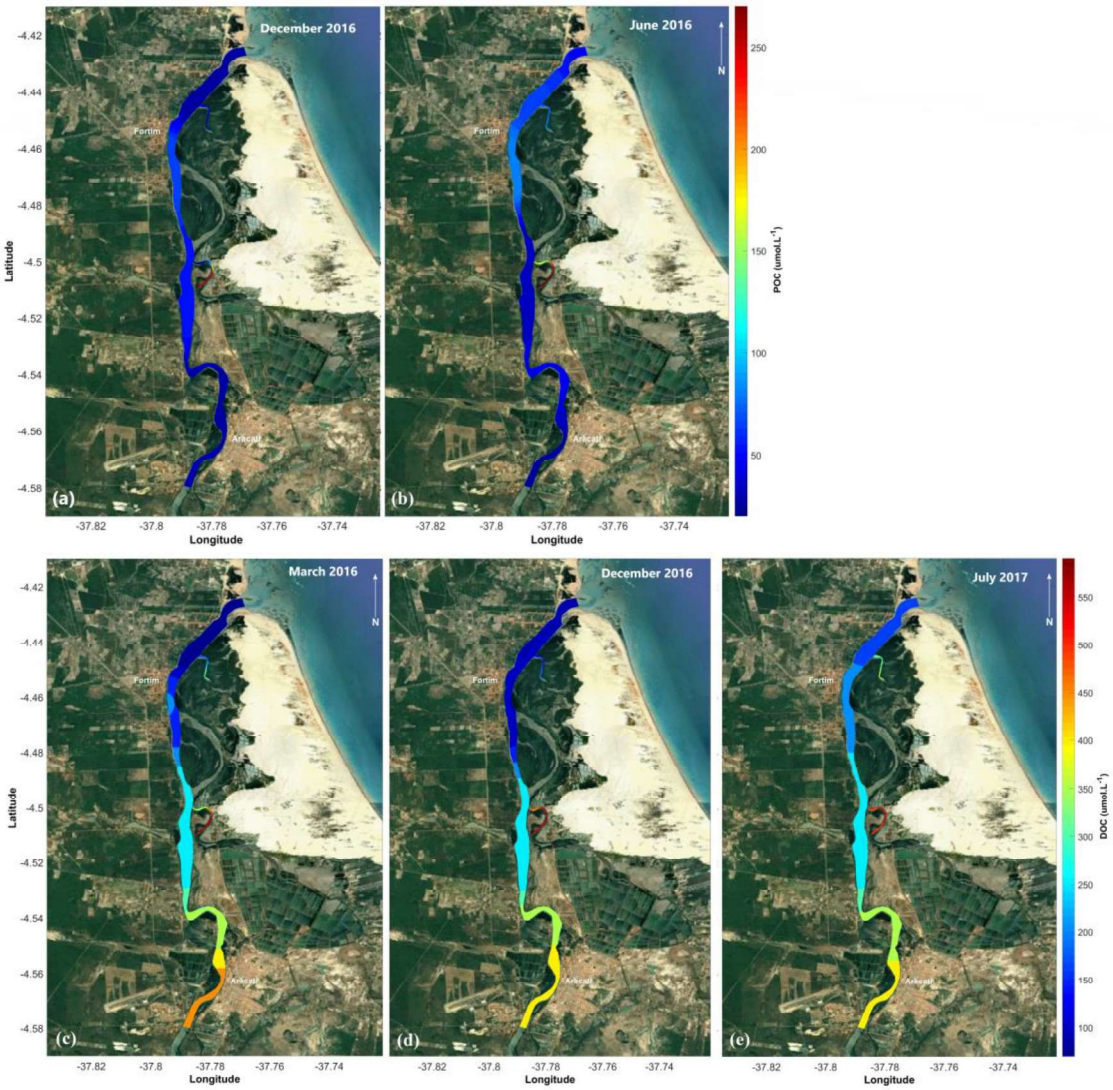

Fig.16. Spatial distribution of (a - b) POC and (c - e) DOC in different seasons in the Jaguaribe River estuary.

Concentrations of DOC ranged from 70.8 to 589.9 µmol L^{-1} and of TDN from 9.4 to 57.1 µmol L^{-1} in the estuary. There was no significant temporal difference in DOC (Fig. 16c – 16e) and TDN levels ($p>0.05$), but spatially, with higher concentrations in the Cumbe channel ($p<0.05$)).

DOC and TDN levels displayed a linear trend with salinity despite the hypersaline conditions, but always decreasing seaward (Fig. 17a – 17e). DOC was the dominant form of organic carbon pool in the water column, representing between 63 and 95 % of the total organic carbon (TOC) in column water. DOC presented a slight correlation with Chl-*a* ($r = 0.55$; $p<0.05$) during the hypersaline period.

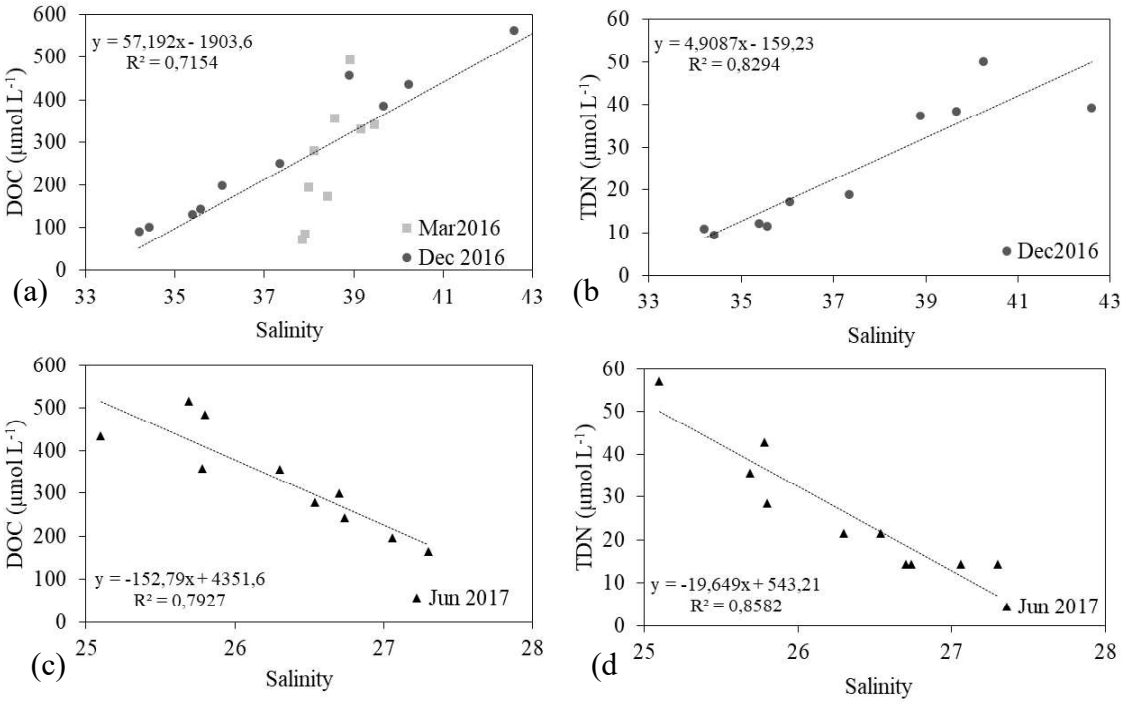

Fig. 17. Linear trend between salinity and (a) DOC in March and December 2016, (b) TDN in December 2016 (c) DOC in June 2017 and (d) TDN in Jun2017 in the Jaguaribe River estuary.

Bottom sediments from the estuary showed relatively low organic carbon (OC) (0.1 – 1.9%) and total nitrogen (TN) (0.02 – 0.26%) contents, and did not vary temporally ($p>0.05$) (Fig. S2). The (C:N)a ratios ranged from 4.7 to 18.8, with averages of 8.4±1.6, 9.3±2.1 and 8.8±2.8 in March 2016, December 2016 and June 2017, respectively.

5.2.3.3. Discrimination of end-members

The $\delta^{13}C$ values of C_3 plants leaves were the most depleted among the end-members and ranged in the interval set for the C_3 vegetation (REZENDE et al., 1990; VILHENA et al., 2018) (Table 7). $\delta^{15}N$ values in mangrove leaves are between 4 and 6‰ (RAY et al., 2015; VILHENA et al., 2018) as observed to *A. shaueriana*, but *R. mangle* presented a more depleted signal (Table 7). Grasses and herbs showed more enriched $\delta^{13}C$ values among the end members (Table 7).

The macroalga *Ulva fasciata*, collected in June 2017, showed enriched $\delta^{13}C$ and $\delta^{15}N$ values (Table 7). For marine end member, it was used literature data of $\delta^{13}C$-DOM (-22.0‰) from the adjacent continental shelf (isobaths of 70 m) of the Jaguaribe river estuary (CARVALHO et al., 2017).

Table 7 - Isotopic carbon and nitrogen composition of end-members of the Jaguaribe River estuary.

	Type	$\delta^{13}C$ (‰)	$\delta^{15}N$ (‰)	(C:N)a
Avicennia shaueriana	C_3 plant	-28.9	5.5	20.7
Rhizophora mangle	C_3 plant	-27.6	3.3	34.8
Copernicia prunifera	C_3 plant	-29.7	5.7	26.8
Leguminous	C_3 plant	-27.6	5.2	23.5
Ulva fasciata	Macroalga	-18.5	5.9	35.4
Fluvial-marine sediment		-24.4	4.8	11.0
Mangrove sedimentl		-24.0	6.0	9.5
Paspalum sp	C_4 grass	-12.9	--	--
Paspalum sp	C_4 grass	-13.4	--	--
Sesuvium portulacastrum	Aizoaceae	-14.0	--	--

The $\delta^{13}C$ values from fluvial plains and mangrove sediments were more enriched than C_3 vegetation (Table 7), probably due to the grass contribution to OM with less depleted $\delta^{13}C$ organic carbon (AITKENHEAD; MCDOWELL, 2000), as well, the advanced stage of OM decomposition (EHLERINGER; BUCHMANN; FLANAGAN, 2000; KRISTENSEN et al., 2008). Besides, they showed C:N ratios below from the expected for terrestrial sources (C:N>12) that suggest intense mineralization. In contrast, $\delta^{15}N$ values reflected well the contribution from C_3 vegetation (Table 7).

5.2.3.4. Isotopic composition of organic matter

The values of POC-δ^{13}C ranged from -25.3‰ to - 22.1‰ for samples collected in December 2016 and -27.3 to -21.5‰ in June 2017. δ^{13}C-POC during hypersaline conditions had more enriched values (-23.5±1.1‰) than POC collected in June 2017 (-24.7±2.0‰), showing statistical differences between the December 2016 and the June 2017 campaigns ($p<0.05$). δ^{13}C-POC was more variable in this last campaign. The δ^{15}N-TPN values varied from 4.7 to 6.2‰ (5.6±0.5‰) and of 5.2 to 6.6‰ (5.8±0.4‰) in December 2016 and June 2017, respectively. The (C:N)a ratios ranged from 8.1 to 13.2 (10.4±1.9) and 7.9 to 13.1 (10.4±1.5).

The distribution of δ^{13}C-DOC showed a similar pattern as δ^{13}C-POC, ranging from -24.1 to -22.4‰ (-23.3±0.6‰) and from -24.9 to -23.1‰ (-24.2±0.5‰) in December 2016 and June 2017 respectively. δ^{13}C- DOC was more enriched in December 2016 campaign than in June 2017. The δ^{15}N-TDN values were of 2.1 to 4.3‰ (2.7±0.6‰) of 3.6 to 5.6‰ (4.6±0.6‰) in December 2016 and June 2017, respectively. The (C:N)a ratios ranged from 11.8 to 19.2 (14.6±2.3) and 17.9 to 22.0 (19.9±1.6). The isotopic composition of DOC and DTN were statistically different between the campaigns ($p<0.05$).

In June 2017, the stable carbon isotopic signature of DOM and POM increased linearly with salinity, along the principal channel, due to the marine contribution with enriched δ^{13}C-OM. While in December 2016, they decreased non-linearly with salinity (Fig. 18a and 18b). In other words, the more enriched values were observed at the sampling stations closest to the sea, indicating inputs of marine OM (−22.0‰) by the tides, which dominate the estuarine circulation.

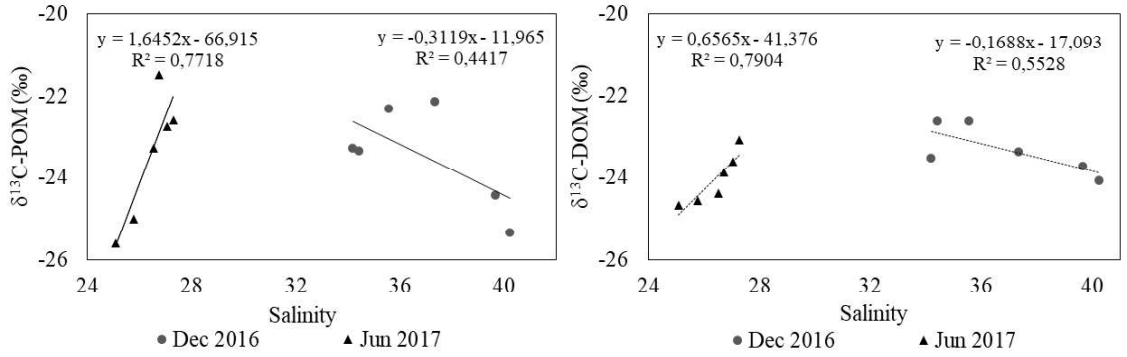

Fig. 18. (a) δ^{13}C-POC and (b) δ^{13}C-DOC variation with salinity in the principal Chanel of the Jaguaribe River estuary in December 2016 and June 2017.

$\delta^{13}C$ signatures of sedimentary organic carbon varied from -26 to -21.2‰, with averages of -24.5±0.8, -25.0±0.8 and -23.9±1.4 ‰ and the $\delta^{15}N$ ranged from 1.8 to 6.2‰, with averages of 4.1±1.6‰, 4.0±1.5‰ and 3.4±1.4‰ in March 2016, December 2016 and June 2017, respectively. Sediments displayed $\delta^{13}C$ values increasing seaward until station 5, and depletion of $\delta^{15}N$.

5.2.3.5. Lignin phenols

Lignin concentrations (Σ_8) and carbon-normalized yields (Λ_8) are presented as the sum of three vanillyl phenols (V), three syringyl phenols (S), and two cinnamyl phenols (C). In the dissolved form, Σ_8 ranged from 2.1 to 50.4 µg L^{-1} (mean = 22.5 ± 16.3 µg L^{-1}) (Table S1) and Λ_8 ranged from 0.6 to 2.1 (mg (100 mg OC)$^{-1}$) (mean = 1.0 ± 0.3 (mg (100 mg OC)$^{-1}$) in the Jaguaribe River estuary. Σ_8 exhibited highest concentrations in June 2017 (mean = 33.7 ± 9.2 µgL^{-1}) than in December 2016 (mean = 11.2 ± 13.9 µgL^{-1}) period (Table S1). While the Λ_8 temporal variation showed higher concentrations in December 2016 than in June 2017, 1.2 ± 0.4 and 0.8 ± 0.1 (mg (100 mg OC)$^{-1}$) respectively. Σ_8 presented a strong positive correlation with DOC (r= 0.718; n=20).

Dissolved syringyl/vanillyl (S/V) phenol ratios in the Jaguaribe River estuary ranged from 0.77 to 1.49 and dissolved cinnamyl/vanillyl (C/V) ratios from 0.56 e 1.91, with averages of 1.1 ± 0.2 and 1.1 ±0.3 respectively. The ratios of vanillic acid to vanillin (Ad/Al)v ranged from 0.54 e 4.36 and the syringic acid to syringaldehyde ratios (Ad/Al)s from 0.73 to 1.85, with averages of 2.3 ± 0.7 and 1.2 ±0.3 respectively (Table S1). The C/V, S/V, (Ad/Al)v, and (Ad/Al)s ratios did not show any significant temporal trends. LPVI values were between 483 and 3004, with average of 1,586 ± 629.

The relative contribution of vascular plant-derived material to organic matter pools can be assessed by the Λ_8 of lignin mg 100 $mgOC^{-1}$. Λ_8 for sediment were of 1.26 and 1.38 and Σ_8 0.18 and 0.17 µg L^{-1} respectively (Table S1). Syringyl and principally cinnamyl phenols more susceptible to diagenetic processes than vanillyl (WARD; RICHEY; KEIL, 2012). The S/V and C/V ratios were lower in sediments when compared with vegetation. As LPVI takes into account the digenetic sequence of phenolic groups (TAREQ; KITAGAWA; OHTA, 2011), it was used to differentiate the types of plants that are contributing to OC. The LPVI values were 1,500 and 4,700 for

fluvial-marine and mangrove sediment respectively, suggesting an angiosperm leaf source (TAREQ; KITAGAWA; OHTA, 2011).

5.2.4. Discussion

5.2.4.1. Effects of drought and dams on the estuarine hydrochemistry of the Jaguaribe River

The salinity distribution observed in June 2017 was characteristic of a positive estuary (fluvial waters spread seaward), even with a weak salinity gradient (Fig. 15a). Whereas in the campaigns performed in 2016, the reduction of freshwater supply and the stronger marine influence led the Jaguaribe River estuary to hypersaline conditions (SANTOS et al., 2017). Besides, the higher seawater RT in the estuary during the dry season favors the concentration of salts in estuarine waters (DIAS et al., 2016). Lacerda et al. (2013) paradoxically compared it with water freezing in rivers draining into the Arctic. During the dry season, the river flows at estuary mouth are blocked and the residence time of continental runoff is longer. Whereas during the periods of higher river discharges, this residence time is shorter.

Hypersaline conditions are a frequent feature in estuaries from this and other semiarid regions (Delgadillo-Hinojosa et al., 2008; Schettini et al., 2017). At the same time, this result was unexpected for the rainy season campaign (March 2016), thus revealing the unpredictability of rainfall in the region and, consequently, the vulnerability of the environmental quality of the estuary. Based on the cluster analysis, it was considered two scenarios: positive (June 2017) and hypersaline (March 2016 and December 2016) estuary.

Schettini et al. (2017) related the anthropogenic stress in three estuaries from the semiarid Brazilian region. They were: the Cocó estuary that receives a large discharge of sewage; the Pacoti estuary that is the more conserved among them; and the Pirangi estuary that presents hypersalinity produced by the negative water balance and by river damming. The average concentration of SPM in the Jaguaribe river estuary (this work) was similar to the Pirangi estuary (~ 15 mg L^{-1}) and three times higher than the Cocó and Pacoti. The high concentrations of SPM in the Pirangi estuary were associated with tidal erosion and its retention capacity (SCHETTINI; VALLE-LEVINSON; TRUCCOLO, 2017).

During the dry season or periods of low freshwater discharge, tides are the main controller of the SPM supply through the resuspension of bottom sediments and

erosion of estuarine margins in the Jaguaribe River estuary. While in periods of high fluvial flow, the SPM comes predominantly from the drainage basin through the leaching of the soils (DIAS et al., 2016). In this work, the absence of correlation between SPM concentration and phytoplankton biomass in the rainy season suggests that terrestrial sources were predominant over in situ algal production. However, a slight correlation between SPM and Chl-*a* showed phytoplankton contribution to SPM during the dry season.

In years of regular rainfall, it is possible to observe seasonal variability of SPM and nutrient concentrations in the Jaguaribe River estuary. Higher SPM concentrations (79% higher) during the rainy than in the dry season already were observed in the Jaguaribe River estuary previously (DIAS; MARINS; MAIA, 2013). Therefore, the low temporal variability of SPM observed in this work seems to be an integrated result to the scarcity of rain and retention of reservoirs (MARENGO et al., 2017; MOLISANI et al., 2013).

5.2.4.2. Behavior of dissolved and particulate organic matter

SPM, DOC, POC, TDN and TPN did not show temporal variability, probably due to the reduced transport of terrestrial material in the estuary during drought conditions. This effect of drought and dams over carbon amount has been noticed in other rivers and estuaries (MORA et al., 2014; VAZQUEZ et al., 2011; YU et al., 2011). DOC and POC concentrations measured in this work were similar to those found in others tropical estuaries affected by river damming (GUO et al., 2015; SCHILLER et al., 2015; VAZQUEZ et al., 2011) and hypersaline estuaries and coastal lagoons (CATALÁ et al., 2013; DELGADILLO-HINOJOSA et al., 2008; YA; ANDERSON; JAFFÉ, 2015).

Lacerda et al. (2008) estimated that anthropogenic nitrogen emissions were more than one order of magnitude higher than natural sources in the Jaguaribe River estuary, being the aquaculture the main responsible for this. This activity releases part of its effluent directly at the Cumbe Channel (stations 7 and 8) (Fig.14), which can be the reason of the high carbon, nitrogen, SPM and Chl-*a* levels in this channel. Besides, high concentration of N-ammonium in the estuarine region next to Aracati city (Fig.14) is related to OM decomposition probably derived from the input of domestic and shrimp farming effluents (ESCHRIQUE et al., 2010).

In the Jaguaribe River estuary, changes in the salinity did not result from the mixing of fresh and marine waters in campaigns performed in 2016, but of a negative water balance and inverse circulation. Besides, the sampling at salinity zero was not possible in any campaign because the estuary became disconnected from the fluvial continuum due to the complete diversion of the river at Trabalhador dike (~36 km of estuarine mouth). All this makes the use of traditional mixing classification inappropriate for this system. Nevertheless, the linear positive relationship between DOC with salinity (Fig. 18) indicates that the oceanic dilution of hypersaline waters caused a positive trend between salinity and DOC and salinity in 2016, similar to the observed in June 2017, but with the opposite sign.

DOC/POC ratios presented a wide range between 1.7 and 15.9 demonstrating the DOC importance in organic carbon balance studies in the Jaguaribe River estuary. The DOC/POC ratios exhibited a decrease with SPM augmentation ($y = 74.49x^{1.389}$; $R^2 = 0.881$) (Fig. S3), as observed by Abril et al. (2002) in estuarine systems. The exponential drop of the DOC/POC ratio with SMP augmentation reflected the occurrence of repartitioning reactions of OM in the estuary, which reduce DOC concentration and consequently its geochemical mobility. He et al. (2010) attributed the microbial degradation (31%) as the principal process controlling the DOC removal, but that other processes, such as flocculation, aggregation and adsorption on to the SPM (69%) were also relevant, especially in the mixing zone.

The OC concentrations in surface sediments at the Jaguaribe River estuary were low. Similar to mangrove sediments from estuaries under dry climate conditions like Somone (0.30-3.90%), Senegal, and Betsiboka estuaries (0.5–1.1%) (RALISON et al., 2008; SAKHO et al., 2015), and from southeastern Brazil (FRAGOSO et al., 2018).

The enriched δ^{13}C-DOC values at the continental shelf under influence of Jaguaribe River (CARVALHO et al., 2017) indicates low exportation of terrestrial OM. Then, the low storage of OM in sediments and the low OM exportation during dry periods, points to a significant OM processing in the Jaguaribe River estuary. Silva, (2016) showed that the Jaguaribe River estuary acts as a CO_2 source to the atmosphere and that it is linked to the trophic state in the estuary, revealing the OM mineralization is an important process in the CO_2 flux in semiarid estuaries.

5.2.4.3. Sources of organic matter in the Jaguaribe River estuary

The dissolved lignin concentrations (Σ_8) in the Jaguaribe River estuary were similar to those from a pristine tropical river, the Epulu (SPENCER et al., 2010), during its hydrological regime of intermediary and post-flush and to the Congo River (Spencer et al., 2009). The highest Σ_8 occurred in June 2017, the period of higher inputs of freshwater in the Jaguaribe River estuary (Fig. 19a), as it was observed in other tropical rivers (Spencer et al., 2010, 2009). The Σ_8 were higher at stations from the upstream region (1, 2 and 3) and secondary channels (Fig. 19a). The strong correlation between DOC and Σ_8 showed the relevance of terrestrial sources to DOM.

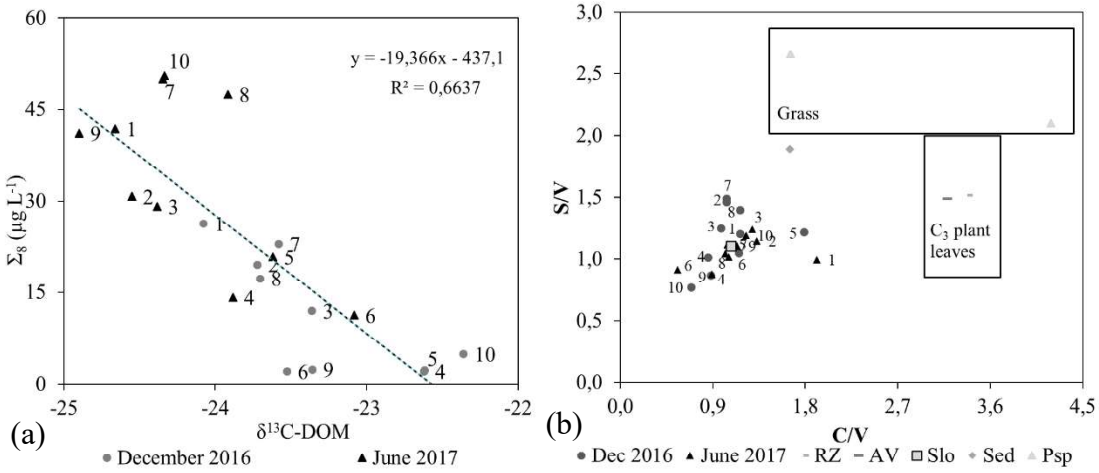

Fig. 19. (a) Linear trend between Σ_8 and $\delta^{13}C$ in December 2016 and Jun2017 and (b) S/V vs. C/V scatter plot. Numbers refer to the sampling site labels

The S/V and C/V ratios are used to distinguish sources of OM derived from several terrigenous plant components. The S/V ratio differentiates angiosperms (S/V>0) from gymnosperms (S/V=0) and the C/V ratio distinguishes the tissue type, woody (C/V=0) from non-woody (C/V>0) (HEDGES; MANN, 1979; JEX et al., 2014). The S/V and C/V ratios of dissolved lignin phenols, from the Jaguaribe River estuary, corresponded to intervals of angiosperm leaves (JEX et al., 2014).

Besides, the S/V ratios in the dissolved fraction were like those of C_3 plant leaves sampled next to the estuary (Fig. 19). However, the C/V ratios were lower in the DOM possibly due to the loss of cinnamyl phenols, since it is the most affected group by diagenetic degradation (Fig. 19a) (TAREQ; TANAKA; OHTA, 2004). The LPVI values of the dissolved lignin phenols were also inserted in the interval for non-woody angiosperms (378 – 2,782) (TAREQ; TANAKA; OHTA, 2004). Since the $\delta^{13}C$ of

grasses and C_3 trees are very distinct from each other (Table 7), $\delta^{13}C$ can be used to distinguish between lignin sources. The stable carbon isotope signature of DOM ranged between -24.9 and -22.4‰ and presented a positive linear relation with Σ_8, suggesting a non-significant contribution of grasses compared with C_3 plants (REZENDE et al., 2010).

In order to define the sources of organic matter in the Jaguaribe River estuary, it was plotted $\delta^{13}C$ against (C:N)a and $\delta^{15}N$ (Fig. 20a and 20b). Fig. 20a indicates the C_3 plant detritus, sediments and marine OM as the main sources of OM in the estuary. The intermediate $\delta^{13}C$-POC values (between -26 and -24 ‰) are common in tidal estuaries with intermediate turbidity due to the extensive mixing of sources (MIDDELBURG; HERMAN, 2007), being the dominance of terrestrial organic matter. It was not possible to clearly observe anthropogenic inputs through Cumbe Channel in this work, probably due to the similarity of the isotopic signal between anthropogenic, as shrimp farm effluents (YOKOYAMA et al., 2002) and sewage (BARROS et al., 2010), and natural sources. The isotopic composition of freshwater phytoplankton is very similar with the terrestrial OM (YE et al., 2017), but the POC/Chl-*a* ratios were above 200 in the depleted $\delta^{13}C$ samples indicating the predominance of non-living OM. POC/Chl-*a* ratios below 200 were found only in samples with enriched $\delta^{13}C$ values, which corresponds to marine phytoplankton.

The low (C:N) ratios of the estuarine OM, compared with C_3 plant leaves, reinforces the occurrence of the diagenetic process (Fig. 20b). The (C:N)a ratio followed this growing order: sediments < particulate < dissolved. It means that the dissolved material is more reworked than the particulate and sediment (BAUER; BIANCHI, 2011), in other words, more degraded and refractory material, clarifying the strong hydrological control over the DOC behavior (CAVALCANTE, 2015). (Ad/Al)v ratio is a proxy of oxidation of terrigenous OM. (Ad/Al)v ratios below 0.3 are typical of fresh tissues. While (Ad/Al)v ratios above 0.4 indicate degraded OM, as humic substances, and higher than 0.6 is considered highly degraded. High (Ad/Al)v ratios (~1.2) are also indicative of the leaching process. The (Ad/Al)v and (Ad/Al)s ratios showed that the dissolved lignin, and consequently terrigenous DOM from the Jaguaribe River estuary, was derived from intense microbial degradation and leaching process (JEX et al., 2014).

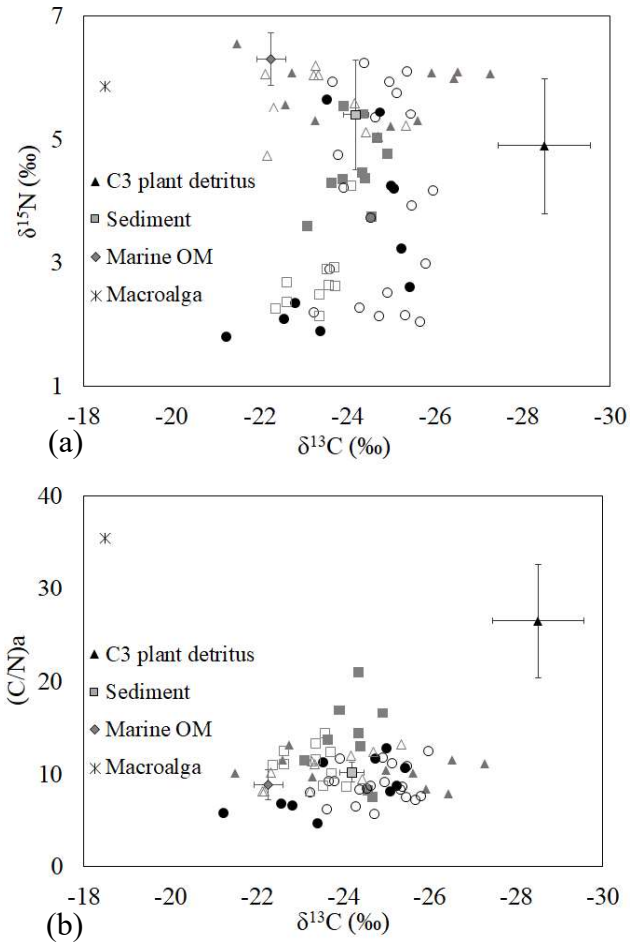

Fig. 20. Relation (a) $\delta^{15}N$ vs $\delta^{13}C$ and (b) C:N ratio vs $\delta^{13}C$ of POM (triangles), DOM (squares), sedimentary OM (circles) of the Jaguaribe River estuary during hypersaline (opened markers) and positive (filled markers) conditions.

The presence of freshwater in the estuarine body in June 2017 did not alter nitrogen and carbon concentrations in the column water, but it shifted $\delta^{13}C$-DOC and $\delta^{13}C$-POC values, indicating temporal variability of in OM sources. In December 2016, the $\delta^{13}C$-DOM and $\delta^{13}C$-POM values were more enriched than in June 2017 and the correlations between Chl-*a* and SPM, TPN and DOC reveal the higher influence of the marine source to the estuarine organic matter in this period. The highest Σ_8 and more depleted $\delta^{13}C$ of POM, DOM and sedimentary OM in June 2017 than in December 2016 indicated the higher contribution of continental sources, mainly sediments and C_3 plants. Besides, the high positive correlation of POC and TPN with SPM in June 2017 suggests that particulate OM was primarily governed by SPM dynamic and consequently by continental runoff and tidal erosion. $\delta^{13}C$-DOC and $\delta^{13}C$-POC average

values in June 2017 were around -24‰ that is suggestive of the soils and sediments contribution to the OM pool (WANG; CHEN; GARDNER, 2004; YE et al., 2018).

The quantitative evaluation of marine and terrigenous components of OM is required for a better understanding of estuarine OM cycling. The SIAR model suggested that the contribution of terrestrial inputs to POM, DOM and sedimentary OM varied from 67 – 79%; 62 – 72% and 69 – 31%, respectively. Marine DOM varied from 21 – 33%; 28 – 38% and 19 – 31% to POM, DOM and sedimentary OM, respectively (Fig. S4). Based on this, the terrestrial-derived OM acted as the dominant source in the Jaguaribe River estuary in both seasons (Fig. S4). Marine DOM contribution to the column water increased when the estuary was under hypersaline conditions due to the prominent seawater intrusion. The marine-derived POM inputs calculated in this study were significantly higher than those founded previously (6%) for the Jaguaribe River estuary (author's unpublished data), probably due to the increase of marine intrusion as an effect of droughts intensification through the years. These results showed the impact of the reduction of freshwater over carbon nature, improving its reactivity and bioavailability.

Organic matter is an effective metal carrier and its quality influences metal complexation capacity (LOUIS et al., 2009; LOUIS; PERNET-COUDRIER; VARRAULT, 2014). The present study supports the "Arctic Paradox" (LACERDA et al., 2013) because it shows the higher OM lability in the estuary during the dry season that may improve mercury reactivity during this season. Besides, the high bioavailability of OM in the dry season helps to explain why Moura and Lacerda (2018) measured higher Hg concentrations in organisms captured in estuarine than in the fluvial zone of the Jaguaribe River.

The organic matter from the Jaguaribe River estuary was mainly derived from C_3 plant debris and sediments. As the low storage of water in the reservoirs keeps their gates closed, trapping the material supply from upper stream regions (DNOCS, 2017; MOLISANI et al., 2013), the terrestrial OM inputs to the estuary come preponderantly from estuarine region that is dominated by mangroves (DIAS et al., 2016; GODOY; LACERDA, 2014). Decreased flow from reservoirs can also trigger erosive processes in mangroves from the Jaguaribe River estuary (GODOY; MEIRELES; LACERDA, 2018) that is an ecological and socioeconomic concern because its degradation can result in a huge release of carbon into the atmosphere in the form of greenhouse gases (PENDLETON et al., 2012).

5.2.5. Conclusion

The severe droughts caused a dramatic reduction of freshwater inputs in the Jaguaribe River estuary, leading the system to hypersaline conditions and reducing the supply of SPM and OM to the estuary.

Overall, terrestrial OM acted as the dominant source to the OM pool in the estuary during rainy and dry seasons. As the rainfall rates were low and consequently the continental runoff, the tides were the chief controller of terrestrial OM delivery to the estuarine waters. The influence of marine sources was also relevant to OM bulk principally during the periods when the estuary was under hypersaline conditions. Besides, high concentrations of OC and nutrients in the Cumbe channel were probably linked to shrimp farm activity.

The δ^{13}C-POC values founded in this work were significantly more enriched than those from 2014 and 2015, indicating the improvement of marine contribution to the estuarine OM with the permanence of drought. The SIAR model showed an increase from 6% to 38% of marine-derived OM in the Jaguaribe River estuary due to the augmentation of seawater influence because of the drought intensification in the last six years.

With the ongoing increase of the freshwater demands for human consumption and the reduction of rainfall in the semiarid region, it is possible that this modification is intensified not only in the Jaguaribe River estuary but in other semiarid estuaries. Besides, these results observed in the Jaguaribe estuary may serve as a prognostic of the effects on the increase the sea level in the geochemistry of the estuarine OM of other world rivers.

Acknowledgments

This study was financed by the FUNCAP (**PRONEX PR2 - 0101 - 00052.01.00/15**). MS Cavalcante was fonded by the Coordenação de Aperfeiçoamento de Pessoal de Nível Superior - Brasil (CAPES) - Finance Code 001. CE Rezende was funded by Conselho Nacional de Desenvolvimento Científico e Tecnológico - CNPq (**305.217/2017-8**) and Fundação Carlos Chagas Filho de Amparo à Pesquisa do Estado do Rio de Janeiro - FAPERJ (**E-6/202.916/2017**).

5.2.6. Reference

Abril, G., Nogueira, M., Etcheber, H., Cabeçadas, G., Lemaire, E., Brogueira, M.., 2002. Behaviour of organic carbon in nine contrasting european estuaries. Estuar. Coast. Shelf Sci. 54, 241–262. https://doi.org/10.1006/ecss.2001.0844

Aitkenhead, J.A., McDowell, W.H., 2000. Soil C:N ratio as a predictor of annual riverine DOC flux at local and global scales. Global Biogeochem. Cycles 14, 127–138. https://doi.org/10.1029/1999GB900083

Alizadeh-Choobari, O., 2017. Contrasting global teleconnection features of the eastern Pacific and central Pacific El Niño events. Dyn. Atmos. Ocean. 80, 139–154. https://doi.org/10.1016/j.dynatmoce.2017.10.004

Barros, G.V., Martinelli, L.A., Oliveira Novais, T.M., Ometto, J.P.H.B., Zuppi, G.M., 2010. Stable isotopes of bulk organic matter to trace carbon and nitrogen dynamics in an estuarine ecosystem in Babitonga Bay (Santa Catarina, Brazil). Sci. Total Environ. 408, 2226–2232. https://doi.org/10.1016/j.scitotenv.2010.01.060

Bauer, J.E., 2002. Carbon Isotopic Composition of DOM, in: Hansell, D.A., Carlson, C.A. (Eds.), Biogeochemistry of Marine Dissolved Organic Matter. Elsevier Inc., pp. 405–453. https://doi.org/10.1016/B978-012323841-2/50010-5

Bauer, J.E., Bianchi, T.S., 2011. Dissolved Organic Carbon Cycling and Transformation. Treatise Estuar. Coast. Sci. 5, 7–67. https://doi.org/10.1016/B978-0-12-374711-2.00502-7

Campos, N., Studart, T., Franco, S., Luna, R., 2000. Hydrological Transformations in Jaguaribe River Basin during 20th Century, in: Proceedings of the 20th Annual American Geophysical Union. Hydrology Days Publications, Fort Collins, pp. 221–227.

Carvalho, A.C.O., Marins, R. V., Dias, F.J.S., Rezende, C.E., Lefèvre, N., Cavalcante, M.S., Eschrique, S.A., 2017. Air-sea CO2fluxes for the Brazilian northeast continental shelf in a climatic transition region. J. Mar. Syst. 173, 70–80. https://doi.org/10.1016/j.jmarsys.2017.04.009

Catalá, T.S., Mladenov, N., Echevarría, F., Reche, I., 2013. Positive trends between salinity and chromophoric and fluorescent dissolved organic matter in a seasonally inverse estuary. Estuar. Coast. Shelf Sci. 133, 206–216. https://doi.org/10.1016/j.ecss.2013.08.030

Cavalcante, M.S., 2015. Transporte de carbono orgânico dissolvido no estuário do rio Jaguaribe sob clima semiárido. Universidade Federal do Ceará.

Cifuentes, L.A., Sharp, J.H., Fogel, M.L., 1988. Stable carbon and nitrogen isotope biogeochemistry in the Delaware estuary Differences exist among natural abundances of stable carbon isotopes (813C) and stable nitrogen isotopes (615N) in organic matter from terrestrial and anthropogenic. Limnol. Ocean. 33, 1102–115.

Delgadillo-Hinojosa, F., Zirino, A., Holm-Hansen, O., Hernández-Ayón, J.M., Boyd, T.J., Chadwick, B., Rivera-Duarte, I., 2008. Dissolved nutrient balance and net ecosystem metabolism in a Mediterranean-climate coastal lagoon: San Diego Bay. Estuar. Coast. Shelf Sci. 76, 594–607. https://doi.org/10.1016/j.ecss.2007.07.032

Dias, F.J. da S., Castro, B.M., Lacerda, L.D. de, 2013a. Continental shelf water masses off the Jaguaribe River (4S), northeastern Brazil. Cont. Shelf Res. 66, 123–135. https://doi.org/10.1016/j.csr.2013.06.005

Dias, F.J. da S., Lacerda, L.D., Marins, R.V., de Paula, F.C.F., 2011. Comparative analysis of rating curve and ADP estimates of instantaneous water discharge through estuaries in two contrasting Brazilian rivers. Hydrol. Process. 25, 2188–2201. https://doi.org/10.1002/hyp.7972

Dias, F.J. da S., Marins, R.V., Maia, L.P., 2013b. Impact of drainage basin changes on

suspended matter and particulate copper and zinc discharges to the ocean from the Jaguaribe River in the semiarid NE brazilian coast. J. Coast. Res. 29, 1137–1145. https://doi.org/10.2112/JCOASTRES-D-12-00115.1

Dias, F.J.D.S., Castro, B.M., Lacerda, L.D., Miranda, L.B., Marins, R.V., 2016. Physical characteristics and discharges of suspended particulate matter at the continent-ocean interface in an estuary located in a semiarid region in northeastern Brazil. Estuar. Coast. Shelf Sci. 180, 258–274. https://doi.org/10.1016/j.ecss.2016.08.006

Dittmar, T., Koch, B., Hertkorn, N., Kattner, G., 2008. A simple and efficient method for the solid-phase extraction of dissolved organic matter (SPE-DOM) from seawater. Limnol. Oceanogr. Methods 6, 230–235. https://doi.org/10.4319/lom.2008.6.230

DNOCS, D.N. de O.C. as S., 2017. Açude Castanhão está com apenas 3,9% da capacidade [WWW Document]. Diário do Nord. URL http://www2.dnocs.gov.br/gab-cs/97-noticias-internas/3733-acude-castanhao-esta-com-apenas-3-9-da-capacidade (accessed 12.4.17).

Ehleringer, J.R., Buchmann, N., Flanagan, L.B., 2000. Carbon Isotope Ratios in Belowground Carbon Cycle Processes. Ecol. Appl. 10, 412–422.

Eschrique, S.A., Braga, E.D.S., Marins, R.V., Gonsalez, V., 2010. Nutrients as indicators of environmental changes in two Brazilian estuarine systems. Safety, Heal. Environ. World Congr. 71–75.

Fragoso, C.P., Bernini, E., Araújo, B.F., Almeida, M.G. de, Rezende, C.E. de, 2018. Mercury in litterfall and sediment using elemental and isotopic composition of carbon and nitrogen in the mangrove of Southeastern Brazil. Estuar. Coast. Shelf Sci. 202, 30–39. https://doi.org/10.1016/j.ecss.2017.12.005

Fry, B., 2002. Conservative mixing of stable isotopes across estuarine salinity gradients: A conceptual framework for monitoring watershed influences on downstream fisheries production. Estuaries 25, 264–271. https://doi.org/10.1007/BF02691313

Godoy, M.D.P., Lacerda, L.D. de, 2014. River-Island Morphological Response to Basin Land-Use Change within the Jaguaribe River Estuary, NE Brazil. J. Coast. Res. 294, 399–410. https://doi.org/10.2112/jcoastres-d-13-00059.1

Godoy, M.D.P., Meireles, A.J. de A., Lacerda, L.D., 2018. Mangrove Response to Land Use Change in Estuaries along the Semiarid Coast of Ceará, Brazil. J. Coast. Res. 343, 524–533. https://doi.org/10.2112/jcoastres-d-16-00138.1

Goñi, M.A., Hedges, J.I., 1990. Potential applications of cutin-derived CuO reaction products for discriminating vascular plant sources in natural environments. Geochim. Cosmochim. Acta 54, 3073–3081.

Guo, W., Ye, F., Xu, S., Jia, G., 2015. Seasonal variation in sources and processing of particulate organic carbon in the Pearl River estuary, South China. Estuar. Coast. Shelf Sci. 167, 540–548. https://doi.org/10.1016/j.ecss.2015.11.004

He, B., Dai, M., Zhai, W., Wang, L., Wang, K., Chen, J., Lin, J., Han, A., Xu, Y., 2010. Distribution, degradation and dynamics of dissolved organic carbon and its major compound classes in the Pearl River estuary, China. Mar. Chem. 119, 52–64. https://doi.org/10.1016/j.marchem.2009.12.006

Hedges, J.I., Keil, R.G., Benner, R., 1997. What happens to terrestrial organic matter in the ocean? Org. Geochem. 27, 195–212. https://doi.org/10.1016/S0146-6380(97)00066-1

Hedges, J.I., Mann, D.C., 1979. The characterization of plant tissues by their lignin oxidation products. Geochim. Cosmochim. Acta 43, 1803–1807.

Howarth, R.W., Swaney, D.P., Butler, T.J., Marino, R., 2000. Climatic Control on Eutrophication of the Hudson River Estuary. Ecosystems 3, 210–215. https://doi.org/10.1007/s100210000020

ISO, 1992. Water quality measurement of biochemical parameters spectrophotometric determination of chlorophyll-a concentration, ISO Norm 10260. International Organization for Standardization, Geneva.

Jex, C.N., Pate, G.H., Blyth, A.J., Spencer, R.G.M., Hernes, P.J., Khan, S.J., Baker, A., 2014. Lignin biogeochemistry: From modern processes to Quaternary archives. Quat. Sci. Rev. 87, 46–59. https://doi.org/10.1016/j.quascirev.2013.12.028

Kristensen, E., Bouillon, S., Dittmar, T., Marchand, C., 2008. Organic carbon dynamics in mangrove ecosystems: A review. Aquat. Bot. 89, 201–219. https://doi.org/10.1016/j.aquabot.2007.12.005

Krol, M.S., Bronstert, A., 2007. Regional integrated modelling of climate change impacts on natural resources and resource usage in semi-arid Northeast Brazil. Environ. Model. Softw. 22, 259–268. https://doi.org/10.1016/j.envsoft.2005.07.022

Lacerda, L.D., Dias, F.J.S., Marins, R. V, Soares, T.M., Godoy, J.M.O., Godoy, M.L.D.P., 2013. Pluriannual watershed discharges of Hg into a tropical semi-arid estuary of the Jaguaribe River, NE Brazil. J. Braz. Chem. Soc. 24, 1719–1731. https://doi.org/10.5935/0103-5053.20130216

Lacerda, L.D., Molisani, M.M., Sena, D., Maia, L.P., 2008. Estimating the importance of natural and anthropogenic sources on N and P emission to estuaries along the Ceará State Coast NE Brazil. Environ. Monit. Assess. 141, 149–64. https://doi.org/10.1007/s10661-007-9884-y

Lacerda, L.D., Santos, J.A., Madrid, R.M., 2006. Copper emission factors from intensive shrimp aquaculture. Mar. Pollut. Bull. 52, 1823–1826. https://doi.org/10.1016/j.marpolbul.2006.09.012

Lebreton, B., Pollack, J.B., Blomberg, B., Palmer, T.A., Adams, L., Guillou, G., Montagna, P.A., 2016. Origin, composition and quality of suspended particulate organic matter in relation to freshwater inflow in a South Texas estuary. Estuar. Coast. Shelf Sci. 170, 70–82. https://doi.org/10.1016/j.ecss.2015.12.024

Lee, Y., Hong, S., Kim, M.S., Kim, D., Choi, B.H., Hur, J., Khim, J.S., Shin, K.H., 2017. Identification of sources and seasonal variability of organic matter in Lake Sihwa and surrounding inland creeks, South Korea. Chemosphere 177, 109–119. https://doi.org/10.1016/j.chemosphere.2017.02.148

Louis, Y., Garnier, C., Lenoble, V., Omanović, D., Mounier, S., Pizeta, I., 2009. Characterisation and modelling of marine dissolved organic matter interactions with major and trace cations. Mar. Environ. Res. 67, 100–7. https://doi.org/10.1016/j.marenvres.2008.12.002

Louis, Y., Pernet-Coudrier, B., Varrault, G., 2014. Implications of effluent organic matter and its hydrophilic fraction on zinc(II) complexation in rivers under strong urban pressure: Aromaticity as an inaccurate indicator of DOM-metal binding. Sci. Total Environ. 490, 830–837. https://doi.org/10.1016/j.scitotenv.2014.04.123

Marengo, J.A., Alves, L.M., Alvala, R.C., Cunha, A.P., Brito, S., Moraes, O.L., 2017. Climatic characteristics of the 2010-2016 drought in the semiarid Northeast Brazil region. An. Acad. Bras. Cienc. 1–13. https://doi.org/10.1590/0001-3765201720170206

Marins, R.V., Lacerda, L.D. De, Abreu, I.M., Dias, F.J.D.S., 2003. Efeitos da açudagem no rio Jaguaribe. Ciência Hoje 33, 66–70.

Mendoza, W.G., Zika, R.G., 2014. On the temporal variation of DOM fluorescence on the southwest Florida continental shelf. Prog. Oceanogr. 120, 189–204. https://doi.org/10.1016/j.pocean.2013.08.010

Middelburg, J.J., Herman, P.M.J., 2007. Organic matter processing in tidal estuaries. Mar. Chem. 106, 127–147. https://doi.org/10.1016/j.marchem.2006.02.007

Molisani, M.M., Becker, H., Barroso, H.S., Hijo, C. a G., Monte, T.M., Vasconcellos, G.H., Lacerda, L.D., 2013. The influence of Castanhão reservoir on nutrient and suspended matter transport during rainy season in the ephemeral Jaguaribe river (CE, Brazil). Braz. J. Biol. 73, 115–23. https://doi.org/10.1590/S1519-69842013000100013

Mora, A., Laraque, A., Moreira-Turcq, P., Alfonso, J.A., 2014. Temporal variation and fluxes of dissolved and particulate organic carbon in the Apure , Caura and Orinoco rivers , Venezuela. J. South Am. Earth Sci. 54, 47–56. https://doi.org/10.1016/j.jsames.2014.04.010

Moura, V.L., Lacerda, L.D. de, 2018. Contrasting Mercury Bioavailability in the Marine and Fluvial Dominated Areas of the Jaguaribe River Basin, Ceará, Brazil. Bull. Environ. Contam. Toxicol. 101, 49–54. https://doi.org/10.1007/s00128-018-2368-7

Parnell, A.C., Inger, R., Bearhop, S., Jackson, A.L., 2010. Source partitioning using stable isotopes: Coping with too much variation. PLoS One 5, 1–5. https://doi.org/10.1371/journal.pone.0009672

Pendleton, L., Donato, D.C., Murray, B.C., Crooks, S., Jenkins, W.A., Sifleet, S., Craft, C., Fourqurean, J.W., Kauffman, J.B., Marbà, N., Megonigal, P., Pidgeon, E., Herr, D., Gordon, D., Baldera, A., 2012. Estimating Global "Blue Carbon" Emissions from Conversion and Degradation of Vegetated Coastal Ecosystems. PLoS One 7. https://doi.org/10.1371/journal.pone.0043542

Pinckney, J., Paerl, H.W., Bebout, B.M., 1995. Salinity control of benthic microbial mat community production in a Bahamian hypersaline lagoon. J. Exp. Mar. Bio. Ecol. 187, 223–237. https://doi.org/10.1016/0022-0981(94)00185-G

Ralison, O.H., Borges, A.V., Dehairs, F., Middelburg, J.J., Bouillon, S., 2008. Carbon biogeochemistry of the Betsiboka estuary (north-western Madagascar). Org. Geochem. 39, 1649–1658. https://doi.org/10.1016/j.orggeochem.2008.01.010

Ray, R., Rixen, T., Baum, A., Malik, A., Gleixner, G., Jana, T.K., 2015. Distribution, sources and biogeochemistry of organic matter in a mangrove dominated estuarine system (Indian Sundarbans) during the pre-monsoon. Estuar. Coast. Shelf Sci. 167, 404–413. https://doi.org/10.1016/j.ecss.2015.10.017

Rezende, C.E., Lacerda, L.D., Ovall, A.R.C., Silva, C.A.R., Martinelli, L.A., 1990. Nature of POC transport in a mangrove ecosystem: A carbon stable isotopic study. Estuar. Coast. Shelf Sci. 30, 641–645. https://doi.org/10.1016/0272-7714(90)90099-D

Rezende, C.E., Pfeiffer, W.C., Martinelli, L.A., Tsamakis, E., Hedges, J.I., Keil, R.G., 2010. Lignin phenols used to infer organic matter sources to Sepetiba Bay - RJ, Brasil. Estuar. Coast. Shelf Sci. 87, 479–486. https://doi.org/10.1016/j.ecss.2010.02.008

Sakho, I., Mesnage, V., Copard, Y., Deloffre, J., Faye, G., Lafite, R., Niang, I., 2015. A cross-section analysis of sedimentary organic matter in a mangrove ecosystem under dry climate conditions: The Somone estuary, Senegal. J. African Earth Sci. 101, 220–231. https://doi.org/10.1016/j.jafrearsci.2014.09.010

Santos, J.A., Marins, R. V., Aguiar, J.E., Chalar, G., Silva, F.A.T.F., Lacerda, L.D., 2017. Hydrochemistry and trophic state change in a large reservoir in the Brazilian northeast region under intense drought conditions. J. Limnol. 76, 41–51. https://doi.org/10.4081/jlimnol.2016.1433

Savoye, N., David, V., Morisseau, F., Etcheber, H., Abril, G., Billy, I., Charlier, K., Oggian, G., Derriennic, H., Sautour, B., 2012. Origin and composition of particulate organic matter in a macrotidal turbid estuary: The Gironde Estuary, France. Estuar. Coast. Shelf Sci. 108, 16–28.

https://doi.org/10.1016/j.ecss.2011.12.005
Schettini, C.A.F., Valle-levinson, A., Truccolo, E.C., 2017. Circulation and transport in short, low-inflow estuaries under anthropogenic stresses. Reg. Stud. Mar. Sci. 10, 52–64. https://doi.org/10.1016/j.rsma.2017.01.004
Schiller, D., Graeber, D., Ribot, M., Timoner, X., Acuña, V., Martí, E., Sabater, S., Tockner, K., 2015. Hydrological transitions drive dissolved organic matter quantity and composition in a temporary Mediterranean stream. Biogeochemistry 123, 429–446. https://doi.org/10.1007/s10533-015-0077-4
Seidel, M., Yager, P.L., Ward, N.D., Carpenter, E.J., Gomes, H.R., Krusche, A. V, Richey, J.E., Dittmar, T., Medeiros, P.M., 2015. Molecular-level changes of dissolved organic matter along the Amazon River-to-ocean continuum. Mar. Chem. 177, 218–231. https://doi.org/10.1016/j.marchem.2015.06.019
Shin, Y., Lee, E.-J., Jeon, Y.-J., Hur, J., Oh, N.-H., 2016. Hydrological changes of DOM composition and biodegradability of rivers in temperate monsoon climates. J. Hydrol. 540, 538–548. https://doi.org/10.1016/j.jhydrol.2016.06.004
Silva, A.R.F. da, 2016. Fluxos De CO2 Na Interface Ar-Água Do Estuário Do Rio Jaguaribe (Ce). Universidade Federal do Ceará.
Souza, M.F.L., Kjerfve, B., Knoppers, B., Landim De Souza, W.F., Damasceno, R.N., 2003. Nutrient budgets and trophic state in a hypersaline coastal lagoon: Lagoa de Araruama, Brazil. Estuar. Coast. Shelf Sci. 57, 843–858. https://doi.org/10.1016/S0272-7714(02)00415-8
Spencer, R.G.M., Hernes, P.J., Ruf, R., Baker, A., Dyda, R.Y., Stubbins, A., Six, J., 2010. Temporal controls on dissolved organic matter and lignin biogeochemistry in a pristine tropical river, Democratic Republic of Congo. J. Geophys. Res. Biogeosciences 115, 1–12. https://doi.org/10.1029/2009JG001180
Spencer, R.G.M., Stubbins, A., Hernes, P.J., Baker, A., Mopper, K., Aufdenkampe, A.K., Dyda, R.Y., Mwamba, V.L., Mangangu, A.M., Wabakanghanzi, J.N., Six, J., 2009. Photochemical degradation of dissolved organic matter and dissolved lignin phenols from the Congo River. J. Geophys. Res. Biogeosciences 114, 1–12. https://doi.org/10.1029/2009JG000968
Tareq, M., Kitagawa, H., Ohta, K., 2011. Lignin biomarker and isotopic records of paleovegetation and climate changes from Lake Erhai , southwest China , since 18 . 5 ka BP 229, 47–56. https://doi.org/10.1016/j.quaint.2010.04.014
Tareq, S.M., Tanaka, N., Ohta, K., 2004. Biomarker signature in tropical wetland : lignin phenol vegetation index (LPVI) and its implications for reconstructing the paleoenvironment. Sci. Total Environ. 324, 91–103. https://doi.org/10.1016/j.scitotenv.2003.10.020
Uncles, R.J., Stephens, J.A., Smith, R.E., 2002. The dependence of estuarine turbidity on tidal intrusion length , tidal range and residence time. Cont. Shelf Res. 22, 1835–1856.
Vazquez, E., Amalfitano, S., Fazi, S., Butturini, A., 2011. Dissolved organic matter composition in a fragmented Mediterranean fluvial system under severe drought conditions. Biogeochemistry 102, 59–72. https://doi.org/10.1007/s10533-010-9421-x
Vilhena, M.P.S.P., Costa, M.L., Berredo, J.F., Paiva, R.S., Moreira, M.Z., 2018. The sources and accumulation of sedimentary organic matter in two estuaries in the Brazilian Northern coast. Reg. Stud. Mar. Sci. 18, 188–196. https://doi.org/10.1016/j.rsma.2017.10.007
Wang, X.-C., Chen, R.F., Gardner, G.B., 2004. Sources and transport of dissolved and particulate organic carbon in the Mississippi River estuary and adjacent coastal

waters of the northern Gulf of Mexico. Mar. Chem. 89, 241–256. https://doi.org/10.1016/j.marchem.2004.02.014

Ward, N.D., Richey, J.E., Keil, R.G., 2012. Temporal variation in river nutrient and dissolved lignin phenol concentrations and the impact of storm events on nutrient loading to Hood Canal, Washington, USA. Biogeochemistry 111, 629–645. https://doi.org/10.1007/s10533-012-9700-9

Ya, C., Anderson, W., Jaffé, R., 2015. Assessing dissolved organic matter dynamics and source strengths in a subtropical estuary: Application of stable carbon isotopes and optical properties. Cont. Shelf Res. 92, 98–107. https://doi.org/10.1016/j.csr.2014.10.005

Ye, F., Guo, W., Shi, Z., Jia, G., Wei, G., 2017. Seasonal dynamics of particulate organic matter and its response to flooding in the Pearl River Estuary, China, revealed by stable isotope (δ^{13} C and δ^{15} N) analyses. J. Geophys. Res. Ocean. 122, 6835–6856. https://doi.org/10.1002/2017JC012931

Ye, F., Guo, W., Wei, G., Jia, G., 2018. The sources and transformations of dissolved organic matter in the Pearl River Estuary, China, as revealed by stable isotopes. J. Geophys. Res. Ocean. https://doi.org/10.1029/2018JC014004

Yeoman, K., Jiang, B., Mitsch, W.J., 2017. Phosphorus concentrations in a Florida Everglades water conservation area before and after El Niño events in the dry season. Ecol. Eng. 108, 391–395. https://doi.org/10.1016/j.ecoleng.2017.07.028

Yokoyama, H., Higano, J., Adachi, K., Ishihi, Y., Yamada, Y., Pichitkul, P., 2002. Evaluation of shrimp polyculture system in Thailand based on stable carbon and nitrogen isotope ratios. Fish. Sci. 68, 745–750. https://doi.org/10.1046/j.1444-2906.2002.00488.x

Yu, H., Wu, Y., Zhang, J., Deng, B., Zhu, Z., 2011. Impact of extreme drought and the Three Gorges Dam on transport of particulate terrestrial organic carbon in the Changjiang (Yangtze) River. J. Geophys. Res. Earth Surf. 116. https://doi.org/10.1029/2011JF002012

5.2.7. Supplementary material

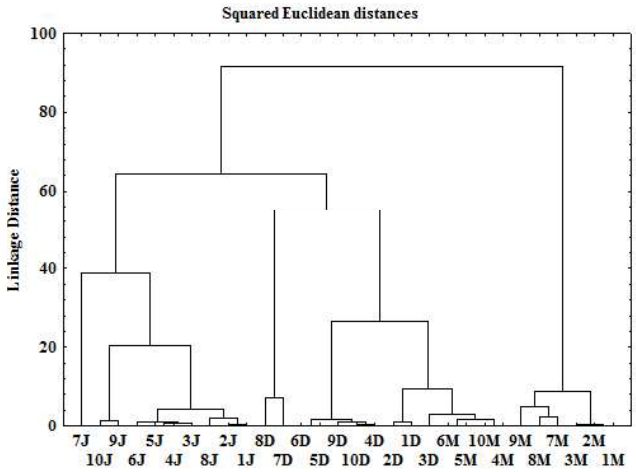

Fig. S1. Cluster analysis of the sampling stations in the Jaguaribe River estuary in March 2016 (M), December 2016 (D) and June 2017 (J).

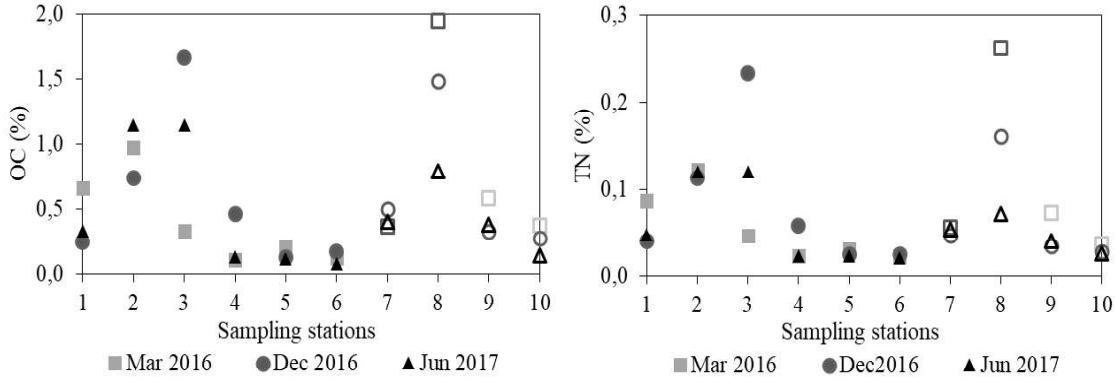

Fig. S2. Spatial variation of (a) OC and (b) TN in the bottom sediment of the Jaguaribe River estuary in different sampling campaings.

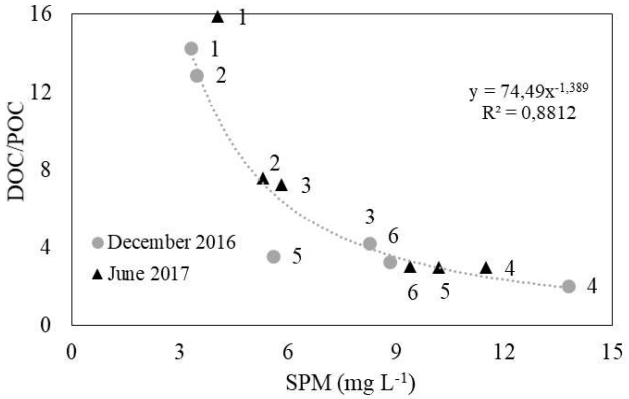

Fig. S3 - Plot of DOC/POC ratios versus suspended matter load (SPM) for the Jaguaribe River estuary. Numbers refer to the sampling site labels

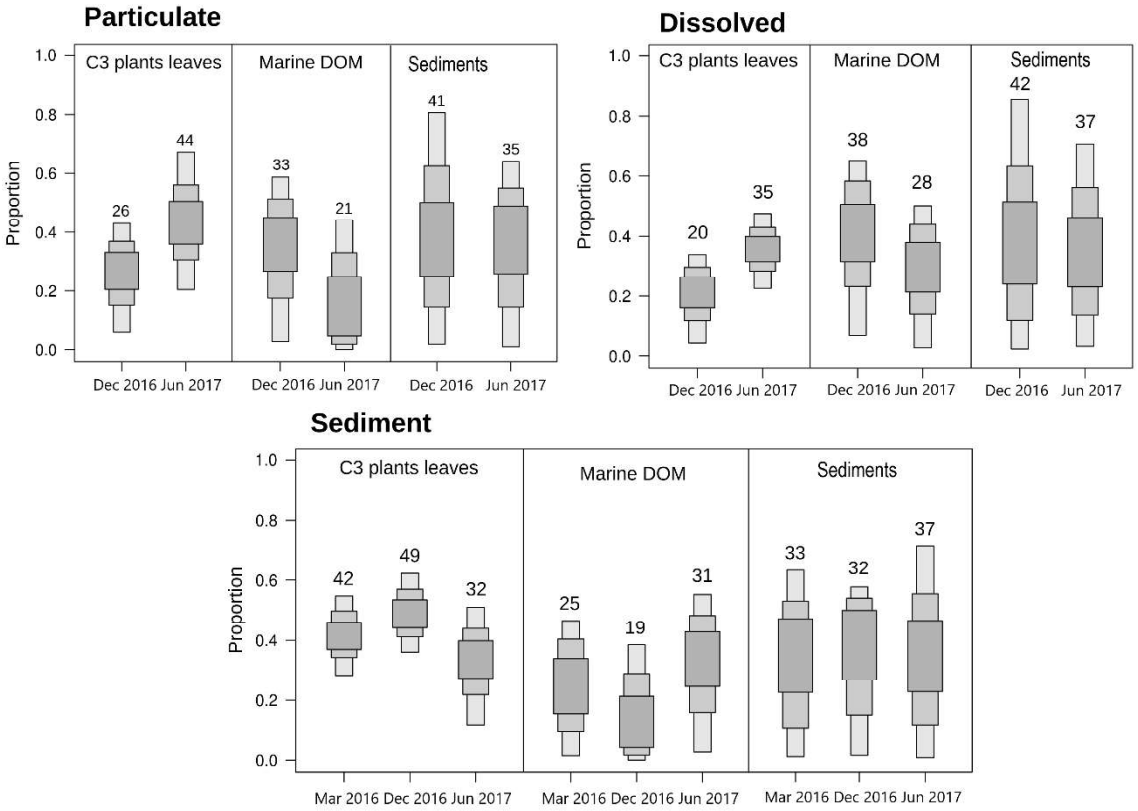

Fig. S4. Model SIAR for particulate dissolved and sedimentary organic matter considering three sources of organic material in three sampling campaigns in the Jaguaribe River estuary (25%; 75% and 95%, represented by different bars).

Table S1. Organic matter composition of DOM and end members from Jaguaribe River estuary.

	$\delta^{13}C$ (‰)	Ac/Al_V	Ac/Al_S	S/V	C/V	λ_8	Σ_8 ($\mu g\ L^{-1}$)	LPVI
D1	-24.08	2.47	1.04	1.20	1.17	0.78	26.38	1,802
D2	-23.72	2.35	1.23	1.46	1.04	0.83	19.62	1,946
D3	-23.36	3.02	1.31	1.25	0.98	0.98	12.03	1,506
D4	-22.62	2.09	0.73	1.01	0.86	1.27	2.13	980
D5	-22.62	2.24	0.83	1.22	1.78	1.34	2.30	3,004
D6	-23.53	0.97	1.00	1.05	1.15	1.02	2.12	1,495
D7	-23.58	2.19	1.39	1.49	1.03	2.14	23.00	1,976
D8	-23.71	2.13	1.23	1.40	1.16	1.14	17.31	2,156
D9	-23.36	0.54	0.84	0.87	0.88	0.92	2.45	835
D10	-22.36	4.36	1.14	0.77	0.69	1.38	4.95	520
J1	-24.66	2.30	1.10	1.00	1.91	0.82	41.87	2,460
J2	-24.55	2.26	1.27	1.15	1.33	0.70	30.77	1,989
J3	-24.39	2.22	1.58	1.24	1.29	0.91	29.18	2,106
J4	-23.88	3.10	1.85	0.88	0.89	0.63	14.20	863
J5	-23.62	2.61	1.57	1.11	1.04	0.77	20.86	1,425
J6	-23.08	2.78	1.82	0.91	0.56	0.91	11.30	483
J7	-24.35	2.26	1.31	1.12	1.05	0.80	49.89	1,438
J8	-23.92	2.47	1.08	1.05	1.03	0.83	47.45	1,288
J9	-24.90	2.09	1.55	1.11	1.14	0.80	41.15	1,571
J10	-24.33	2.10	1.13	1.19	1.22	0.71	50.45	1,890
End-members								
R.mangle	-27.62	2.37	1.50	1.52	3.38	1.68	7.98	7,346
A.Shaueriana	-28.93	2.35	1.80	1.49	3.18	4.40	9.57	6,814
Mangrove sediment	-24.00	1.64	1.05	1.10	1.08	1.26	0.18	1,467
Fluvial-marine sediment	-24.40	1.33	0.74	1.89	1.66	1.38	0.17	4,693
Paspalum sp	-12.90	1.59	0.62	2.66	4.19	18.27	18.27	18,472
Paspalum sp	-13.40	11.93	0.44	2.10	3.87	10.23	10.23	12,729
S. potulacastrum	-14.00	7.81	0.13	0.66	1.99	5.98	5.98	1,423

5.3. ESTUARINE ORGANIC MATTER CHARACTERIZATION AND INTERACTION WITH METALS ISOLATED USING CROSS-FLOW ULTRAFILTRATION

ABSTRACT

Characterization and size distribution of organic matter (OM) in the Jaguaribe River estuary were evaluated using ultrafiltration and fluorescence spectroscopy. Besides, dissolved metals concentrations were obtained by ICP-MS analyses to evaluate the characteristics of dissolved organic matter (DOM) and its interaction with trace metals. The Jaguaribe River is the most important river of Ceará. It is located predominantly in the rural area of Brazil NE, but the Hg concentrations in oysters and sediments reached levels as high as metropolitan sites in this region suggesting that geochemical processes increase Hg bioavailability. The DOC concentrations observed during the rainy season of 2018 were 70% lower than the values of 2004, showing the impact of an extended drought period in the equatorial region of Brazil over the DOC sources to the Jaguaribe river estuary. The three fluorophores, identified by PARAFAC, showed that the estuarine DOM was preponderantly composed by terrestrial-derived humic compounds. DOM had a high degree of aromaticity, but the decrease with salinity suggests that labile aromatic compounds were removed from column water during estuarine mixing. The truly dissolved DOM (< 1 kDa) was the major fraction of DOM (80 ± 2 %), while the colloidal OM (> 1 kDa) comprised 6 ± 1 %. The percentage of truly dissolved and colloidal organic matter concentrations increased with salinity while the percentage of POC decreased, demonstrating a reduction in the OM particle size with increasing salinity. Besides, removal of the OM, during estuarine mixing, occurred more specifically when salinity values were between 3 and 7 g kg-1. Since the chromophoric dissolved organic matter (CDOM) and fluorescent DOM decreased with salinity increase, the photochemical degradation can be a relevant process in organic matter removal and as well as particle reduction. Some metals (Cr, Fe, V, Al, Cu, and Ni) showed significant correlation with DOC and non-conservative reduction with salinity increase, pointing that DOM size and environmental conditions were the main drivers of metal availability in the Jaguaribe River estuary.

Key-words: PARAFAC, partitioning, aromaticity and organic matter

5.3.1. Introduction

Trace metals contamination is a serious concern in the aquatic systems because they are major environmental pollutants and have long-term accumulation in sediments and organisms. Estuaries work as metals filters in the ocean-land transport, promoting their deposition due to the intense physicochemical gradient and quantity of particles (YANG; VAN DEN BERG, 2009). Metal speciation and consequently its fate, transport, bioavailability and toxicity in the estuaries is tightly relate to organic matter dynamic (SIMPSON et al., 2014) and environmental conditions (pH, ionic strength and competition with other cations) (LOUIS et al., 2009). Due to its role in binding and stabilize metals and pollutants in estuaries (WANG et al., 2017), efforts to access information about the composition and partitioning of organic matter, in the dissolved, colloidal and particulate phases, has increased over the last years (STOLPE et al., 2010, 2014; XU; GUO, 2017; ZHOU; GUO, 2015).

The dissolved organic matter (DOM) is a heterogeneous mixture of molecules derived from biological decomposition and metabolic activity of organisms (FINDLAY; SINSABAUGH, 2003), presenting different sizes, functionalities, age and origin (allochthonous and autochthonous). DOM is ubiquitous in marine environments and plays important role in biogeochemical and environmental processes, such as the carbon and nutrients cycling, energy source to consumers and water quality (SANTINELLI; NANNICINI; SERITTI, 2010b; WANG et al., 2007; YANG et al., 2016). The isolation and separation of aquatic colloids are typically preceded by filtration of samples through 1 - 0.2 μm pore-size filters (WILKINSON; LEAD, 2007). Cross-flow ultrafiltration has been widely used to fractionate DOM into different size and molecular weight fractions (WANG et al., 2017; WILKINSON; LEAD, 2007; XU; GUO, 2017), such as reverse osmosis (LOUIS et al., 2009) and flow field–flow fractionation (STOLPE et al., 2014). The high molecular weight (HMW) fraction is usually referred to as colloidal organic matter (COM) and is defined as macromolecules or aggregates that have size between 1 nm to 1 μm, while the low molecular weight (LMW) corresponds to molecules smaller than 1 kDa (WILKINSON; LEAD, 2007). COM is very reactive due to its high specific surface area and abundance of complexing sites that can contribute to the metal binding process (Fang et al., 2015; Louis et al., 2009). In estuarine waters, for example, metals such as copper (Cu), iron (Fe), mercury (Hg) and zinc (Zn) have been shown to be mostly in the colloidal form (LUAN; VADAS, 2015; SIMPSON et al., 2014; WANG et

al., 2017). Besides, COM intermediate partitioning changes between the true dissolved solution and the particulate phase, through mixing processes such as flocculation, aggregation, and disaggregation (GIANI et al., 2005; XU et al., 2018; YI et al., 2014a).

The characterization of DOM forecast the complexation capacity of this geochemical carrier and the metal relation with the DOM different fractions improve the understanding of the carbon effects over the metal cycle. Fluorescence spectroscopy has been widely used to characterize the nature of the part of the chromophoric dissolved organic matter (CDOM), the component of DOM that absorbs light over a wide range of ultraviolet and visible wavelength, by measuring the fluorescent dissolved organic matter (FDOM). This technique is highly sensitive, selective, easy of use, and needs small samples (Coble, 2007; Fellman et al., 2010). The detailed mapping of the FDOM properties produces excitation-emission matrices (EEM) built by the merging excitation and emission wavelength domains, which are suitable for multivariate data analysis techniques such as PARAFAC ("Parallel Factor Analysis") (LIN et al., 2016; SHIN et al., 2016b; XU; GUO, 2017). Through the decomposition of a set of EEMs, the PARAFAC analysis quantifies the significant number of independent fluorescent components.

In 2004, DOC and POC concentrations ranged from 586 to 1.716 and 83 to 273 $\mu mol\ L^{-1}$ respectively along the salinity gradient of the Jaguaribe River estuary, showing marked seasonal variability with relatively high concentrations during the dry season (MOUNIER et al., 2018). Besides, organic carbon concentrations decreased towards the sea and with rising tide due to the dilution process. PARAFAC has identified two components of CDOM in the Jaguaribe River estuary, peaks A and C, which correspond to humic acids. The authors attributed the variation in the intensity ratio of these peaks to the increased contribution of younger organic matter in higher salinity.

The Jaguaribe River estuary is located in the rural area of NE Brazil, without significant sources of metals (OLIVEIRA; MARINS, 2011). However, the Hg concentrations in oysters and sediments increased surprisingly within the post 13 years due to the remobilization from soils and sediments by regional environmental changes (RIOS et al., 2016), showing levels as high as some metropolitan sites. Besides, Moura and Lacerda, (2018) observed that Hg concentrations in tissues of organisms from the estuary marine-influenced portion were higher than those from the fluvial portion, pointing to the importance of hydrodynamic variables (DIAS; MARINS; MAIA, 2013) in controlling the hydrochemistry and Hg bioavailability (LACERDA et al., 2013). It

was hypothesized that the DOM quality and the influence of hydrodynamic parameters determine the association between DOM and metals, being the key parameter of the impact on the biota in the Jaguaribe River estuary. The aim of this study was to evaluate DOM quality and its interaction with trace metals in the Jaguaribe River estuary. It was performed through the quantification of dissolved and particulate organic carbon (DOC, POC), characterization of OM by CDOM determination and the aromaticity index, molecular fluorescence and its correlations with metals (Al, Fe, Cu, Ni, Pb, Cr, Sn, Sr, Rb, Li, Mo, U, V) measured by ICP MS.

5.3.2. Materials and methods

5.3.2.1. Study location and sampling strategy

The Jaguaribe River estuary is located within the Northeastern coast of Brazil (Figure 21). The annual rainfall coastal zone ranged from 400 to 2000 mm, with an average of 912.7mm, during the past 30 years (FUNCEME, 2017). The Brazilian semiarid climate is marked by a strong seasonal rainfall regime. The field campaign was carried during the rainy season, in April 2018. This year, the system was recovering from a severe drought caused by climate events (El Niño and anomalously warm tropical North Atlantic) that lasted 6 years (MARENGO et al., 2017).

Aquaculture, urban, and rural activities are significant sources of nutrients and probably organic matter (Eschrique et al., 2010) to the Jaguaribe River estuary. Emission factors of nitrogen and phosphorus points that anthropogenic sources surpass the natural sources in at least one order of magnitude (LACERDA et al., 2008), being highlighted the aquaculture followed by wastewater and husbandry. Shrimp farming presents high emission factors for Cu and Hg per unit of area to the Jaguaribe River estuary, but contributes with relatively small annual discharges when compared to other sources (LACERDA et al., 2011; LACERDA; SANTOS; MADRID, 2006). However, shrimp farm emissions are directly disposed into estuarine waters and the major part of the Hg present in effluents from shrimp farming occurs as dissolved species (COSTA et al., 2013).

The tidal regime is semidiurnal and meso-tide, with maximum amplitude reaching 3.0 m (DIAS et al., 2011). Freshwater discharges dropped from 60/130 m^3s^{-1} to 20 m^3s^{-1} after the built of major dams of the Jaguaribe River (DIAS; MARINS; MAIA, 2013). As a consequence of low freshwater supply, the tidal intrusion landward in the

Jaguaribe River estuary (DIAS et al., 2016) has caused several impacts as: retention of contaminants (LACERDA et al., 2013), mangrove expansion (GODOY; LACERDA, 2014, 2015), reduction of sediment from watershed (DIAS et al., 2016; DIAS; MARINS; MAIA, 2013b), high saline conditions (DIAS et al., 2016; MARINS et al., 2003).

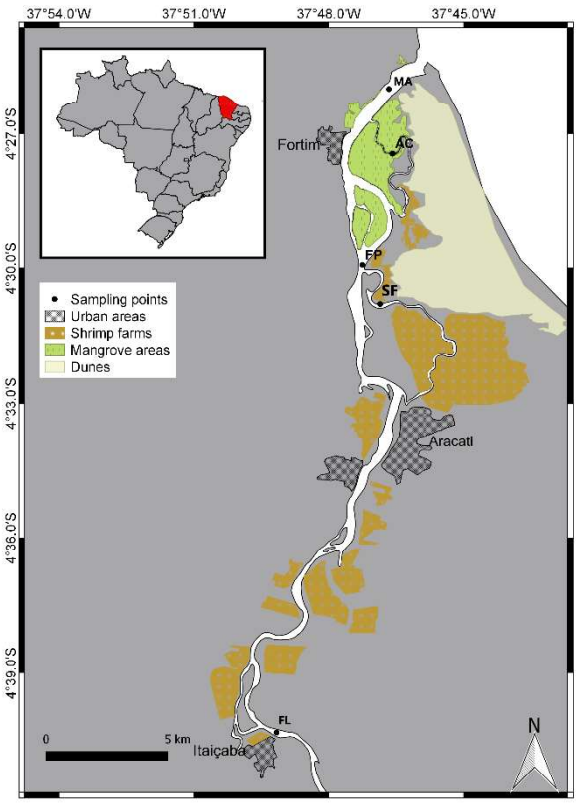

Figure 21 - Study area and sampling stations

Five sampling stations were distributed in the estuary (Figure 21) to collect the water samples and to measure the hydrochemical parameters. The sampling stations corresponded to the fluvial (FL), marine (MA), mangrove (AC) and shrimp farm (SF) end-members and a fixed point (FP) in the estuary's maximum turbidity zone. The SF station was located at the Cumbe Chanel that is heavily impacted by shrimp farms since they discharge their effluents directly into it (COSTA et al., 2013). Whereas, the AC point was in the Amor Chanel that is surrounded by a well-preserved mangrove area. A temporal sampling was performed to evaluate the tidal influence in the organic matter quality and its interaction with trace metals, in a fixed point (FP) at the middle estuary (Figure 21). Every hour and a half, for 9 hours (from 8 am to 5 pm), water samples were taken in a fixed point (FP) at the middle estuary (Figure 21). These samples were

numbered from 1 to 7, following the temporal order of sampling.

A portable YSI multiparametric probe (model professional plus) was used to measure salinity, temperature and dissolved oxygen and a portable pH meter (Metrohm) to measure pH in situ. Subsurface water (0.5 m) was sampled with an acrylic Van Dorn bottle, totaling 11 water samples. Immediately after sampling, water samples were filtered through pre-combusted (at 450ºC, 12h) and acid-washed glass microfiber filters Whatman with a 0.45 μm mesh to collect suspended particles for further analysis of particulate organic carbon and particulate nitrogen (POC, PN) and suspended particulate material (MPS). After filtration, 200 mL samples were conserved by the addition of sodium azide (NaN_3) (1mM fine concentration, so typically 200μL of 1M NaN_3 in 200mL) in the fridge, avoiding biological development and further OM alteration until posterior chemical analyses in the laboratory. Chlorophyll *a* (Chl-*a*) was quantified in samples retained in AP40 fiberglass filters until saturation.

The tidal curve was plotted based on data provided by Diretoria de Hidrografia e Navegação do Brasil for the Areia Branca-Termisa (RN) port. They corresponded to three values of water level for the day of sampling (two at high tide and one at low tide), taking into account the 3-hour delay of the gravity wave between the Areia Branca - Termisa (RN) port and the interior of the Jaguaribe estuary calculated by Dias (2007).

5.3.2.2. Cross-flow ultrafiltration treatment

Three extra subsurface water samples (20 L each sample) with different salinities were pumped from the fixed point (Figure 21) during the high (8 am), slack (9:30 am) and low (11 am) tide that corresponded to points 1, 3 and 5 respectively. The fractionation of colloidal and dissolved phases of these samples was performed by ultrafiltration method. A pre-filtration of samples with a 0.45 μm filter to obtain the bulk samples. The fractionation of the DOM and dissolved metals were achieved sequentially using a tangential flow filtration system (Pellicon 2 - Millipore). The cartridges used had a porosity of 0.1 μm, 10 kDa and 1 kDa molecular weight cut-off.

The material retained in these cartridges were concentrated to a volume of approximately 200 mL, resulting in three COM fractions to each sample (>0.1 μm, >10 kDa and > 1 kDa). At the end of the experiment, seven sub-samples were obtained from each sample: one bulk, three concentrated, and three permeate samples.

The concentration factor of the ultrafiltration (Fc) is the ratio between the

volumes of permeate (Vp) and retentive (Vr) to each membrane (Table S1). Permeate solutions were saved (200 mL) to verification of the efficiency of the ultrafiltration system by a mass balance of DOC (Table 1) and metals. The recoveries (%) in the ultrafiltration process can be calculated as follows:

$$R\ (\%) = [(Cp \times Vp) + (Cr \times Vr)] / [Cb \times Vb] \times 100,$$

where Cb, Cp, and Cr represent DOC and metals concentrations in the bulk, permeate, and retentate respectively. Vb, correspond to the volume of the bulk sample.

Table 8 - DOC, Li, Rb, Sr, Mo, V and Cu recovery (%) in each cartridge to each sample

	DOC			**-**			**-**		
Sample	1	3	5	-	-	-	-	-	-
0.1µm	99.8	96.5	96.8	-	-	-	-	-	-
10kDa	85.5	87.6	92.9	-	-	-	-	-	-
1kDa	108.5	107.2	100.9	-	-	-	-	-	-
	Li			**Rb**			**Sr**		
Sample	1	3	5	1	3	5	1	3	5
0.1µm	93.7	96.7	94.9	96.9	98.0	94.7	97.6	98.4	98.2
10kDa	68.2	94.4	93.8	64.4	95.5	93.8	63.0	96.6	96.6
1kDa	142.0	92.3	92.3	93.9	96.4	93.5	94.1	95.6	95.9
	Mo			**V**			**Cu**		
Sample	1	3	5	1	3	5	1	3	5
0.1µm	97.4	95.6	97.3	83.6	85.9	95.8	128.6	102.7	138.1
10kDa	69.5	95.1	96.9	58.4	96.2	97.3	83.2	78.2	115.7
1kDa	95.3	95.0	95.9	78.1	96.3	99.1	113.5	93.0	123.6

The cartridges were washed with H_3PO_4 (0.1N) solution and 30L of Milli-Q water among the ultrafiltered samples, to remove possible traces of samples and to neutralize the pH of the cartridges. In the concentration step of the fractions, ultrapure water was added continuously until the conductivity was below 100 $\mu S.cm^{-1}$, for the removal of excess salts that could harm the further analyzes.

5.3.2.3. Metal analyses

Metals (Li, Rb, Sr, Mo, U, Sn, Pb, Cu, Ni, Fe, Al, V and Cr) concentrations in the bulk samples were determined by inductively coupled plasma mass spectrometry (ICP-MS, Laboratory MIO-Marseille). Samples were diluted (2 times) with acidified Milli-Q water to avoid the effect of salt concentrations. Indium (In) was used as an internal standard for quality control.

5.3.2.4. Measurements of Chl-a, organic carbon and optical properties

Chlorophyll a (Chl-*a*) and pheophytin was quantified in samples retained in AP40 fiberglass filters until saturation, extracted in acetone, and quantified using a spectrophotometer, according to ISO 10260 (1992) protocol.

DOC was measured using oxidation in a catalytic Pt bed at 650°C with an automated TOC analyzer (Shimadzu TOC 5000). For the determination of DOC, samples were earlier acidified with HNO_3 (10%) and purged with an inert gas (O_2) to remove inorganic carbon. Next, the organic carbon remaining in the acidified sample (HNO_3) was processed. The oxidation product (CO_2) of DOC was carried by ultrapure O_2 gas to the non-dispersive infrared analysis detector (NDIR) and then quantified. The accuracy of analyze was 98% using phthalate calibration. DOC data reported the mean of three replicate injections, for which the coefficient of variance was <2%. Prior to elemental organic carbon and nitrogen analysis in the particulate material, the filters were treated in silver boats with HCl vapor to remove carbonates. POC and PN analyses were made using a Flash 2000 elemental analyzer (Thermo Scientific IRMS). The analytical control was performed by the certified soil reference material (Thermo Scientific, Germany), resulting in above 94% of precision.

The UV absorption spectra were measured from 240–800 nm at medium speed on a double beam UV-1800 (Shimadzu) in 1 cm quartz. Milli-Q water was used as a reference. The absorption coefficient of CDOM, a_{254}, was calculated as $a(\lambda) = 2.303A(\lambda)/L$, where A is the absorbance, λ is the wavelength at 254nm and L is the cell length in meters. The specific ultraviolet absorbance (SUVA) is the aromaticity index of OM, used as a proxy for DOM reactivity and composition. SUVA is defined as the ratio between UV absorbance at $\lambda = 254$ nm and DOC concentration (mg L^{-1}) (Weishaar et al. 2003).

Fluorescence spectra of DOM samples were acquired on a HITACHI F 4500 spectrofluorometer (Triad Scientific) to spatial and temporal bulk samples. Fluorescence excitation–emission matrices (EEM) were constructed by scanning the excitation wavelengths from 250 to 500 nm and emission wavelengths from 250 to 700 nm, both with at 5-nm intervals and a scanning speed of 240 nm min^{-1}. Rayleigh and Raman physical diffusion of light were numerically removed by the method proposed by Zepp et al. (2004). The EEMs were modeled with PARAFAC using MATLAB and the N-way toolbox for MATLAB (Stedmon and Bro, 2008). The analysis of residual variance core

consistency diagnostic (CONCORDIA) was used to determine the number of components before the EEMs decomposition into individual components by PARAFAC analysis. The fluorescence of each component was represented by the maximum fluorescence Fmax (RU, Raman units) (Stedmon and Markager, 2005; Kowalczuk et al., 2009).

5.3.3. Results and discussion

5.3.3.1. Tide variation in the Jaguaribe River estuary

The tide presented minimum and maximum peaks of 0.2 and 3.5 m respectively. The salinity varied from 2.9 to 14.8 g kg^{-1}, reflecting the tidal variation during the temporal sampling (Figure 22). Salinity decreased during the ebb tide, with the minimum value occurring at low tide. The spatial sampling was performed in the ebb tide as well as most of the temporal sampling, except points 6 and 7.

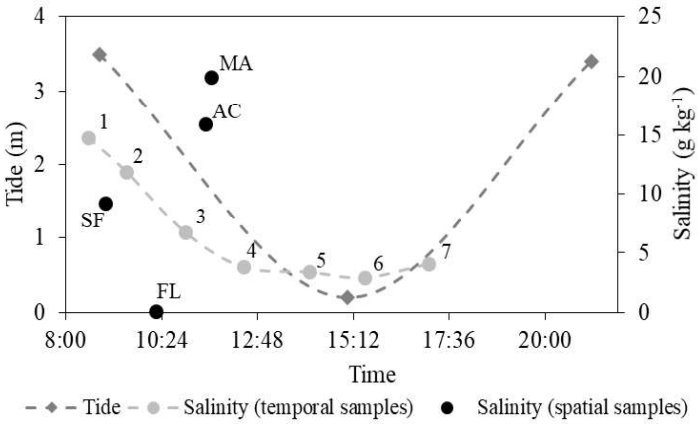

Figure 22 - Tidal and salinity variation in the Jaguaribe River estuary. Numbers and letters refers to the samples from temporal and spatial sampling respectively.

5.3.3.2. Characterization of fluorescent components

Three fluorescent components were identified using the PARAFAC model with CONCORDIA of 84.4%. They were compared to fluorophores from estuarine environments (COBLE, 2007; PARLANTI et al., 2000; STEDMON; MARKAGER, 2005). In these works, it was possible to observe that the differentiation between protein and humic-like DOM is done easier through emission wavelength, which is higher than 370 nm to humic-like DOM and lower than 370 nm to protein-like DOM. The component 1 (C1) presented a fluorescence peak at an excitation/emission wavelength

at 315 nm/420 nm, similar to the marine humic-like Peak M defined by Coble (1996) in seawater. However, with the increased amount of studies it was observed this peak has also been found in terrestrial sources (COBLE, 2007; STEDMON; MARKAGER, 2005) and microbial humic substances (OSBURN et al., 2012; STEDMON; MARKAGER; BRO, 2003). Component 2 (C2) was composed of two separate excitation peaks, the first (265 nm/ 465 nm) and the second (365 nm/465 nm), which were within the range for terrestrial humic compounds analyzed by Stedmon and Markager, (2005) in estuarine waters. The component 3 (C3) was also composed by two separate excitation peaks, the first (285/ 510) and the second (405/510), that resembled a combination of humic-like fluorophores (A and C) derived from terrestrial source (COBLE, 2007) (Figure 23).

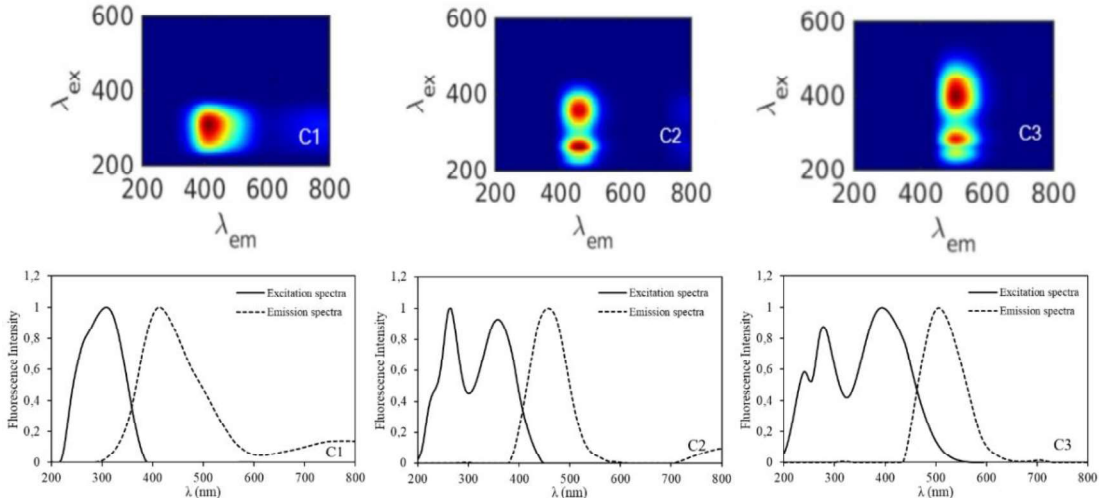

Figure 23 - Contour plots of three components (C1 – C3) of CDOM from the Jaguaribe River estuary identified using the PARAFAC model. Excitation (solid lines), emission loadings (dotted lines) of each contour plot.

5.3.3.3. Variation of the organic matter, optical properties and dissolved metals in the salinity gradient.

In the spatial sampling, the highest POC and DOC concentrations occurred in the fluvial region (Figures 24a and 24b), as observed in 2004 by Mounier et al. (2018), but with DOC concentration 70% lower comparatively. It might have been a result of the intense drought in the region lately (Marengo et al., 2017). However, the DOC and POC concentrations in the estuary mouth were similar to those of the Amor (AC) channel, indicating the influence of this channel in the mouth since the sampling took

place at ebb tide. The Cumbe Channel (SF) presented higher concentrations than AC and similar to the fixed point (1-3) with similar salinity values (Figures 24a and 24b).

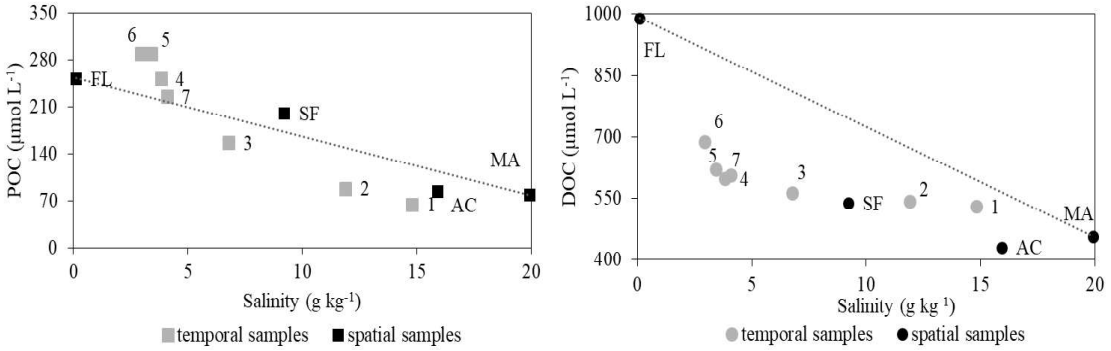

Figure 24 - Concentrations of (a) POC and (b) DOC plotted against salinity with conservative mixing line calculated from fluvial and marine end-members. Numbers and letters refers to the samples from temporal and spatial sampling respectively.

The theoretical conservative mixing lines were plotted using the respective concentrations found between the marine and riverine end-members. POC concentrations were between 56.0 and 289.9 µmol L^{-1}, with an average of 180.4 ± 88.5 µmol L^{-1}. DOC concentrations in bulk samples varied from 430.9 to 990.0 µmol L^{-1}, with an average of 597.0 ± 149.1 µmol L^{-1}. POC and DOC concentrations presented a non-conservative decrease along the estuarine salinity gradient (Figures 24a and 24b). Besides, DOC showed constant concentrations in salinities between 7 and 15 g kg^{-1} during the ebb tide (Figure 22). The behavior of POC and DOC indicates that their dynamics were not controlled only by marine dilution (MOYER et al., 2015), but by biogeochemical processes, as precipitation, adsorption/desorption and microbial and photodegradation.

The temporal variability of DOC did not present significant correlation with Chl-*a* ($r = 0.099$; $p < 0.05$). However, POC showed a significant positive correlation with Chl-*a* ($r = 0.667$; $p < 0.05$), indicating the contribution of phytoplankton to the particulate OM dynamic.

CDOM (a_{254}) varied from 40.1 to 132.9 (m^{-1}), with average of 56.5 ± 26.4 (m^{-1}). The strong relationship between DOC and CDOM ($r = 0.948$, $p<0.01$) showed that CDOM is a representative fraction of the DOM in the Jaguaribe River estuary, as observed in others estuaries (WANG et al., 2004).

$SUVA_{254}$ varied from 6.2 to 7.2 m^{-1}/(mg-C/L), with an average of 7.7 ± 1.4 m^{-1}/(mg-C/L), in the Jaguaribe River estuary. $SUVA_{254}$ values above 3 m^{-1}/(mg-C/L) indicate an high degree of aromaticity and unsaturation of the DOM that reflect environments with high terrestrial inputs. While lower values indicate low aromaticity and higher relative abundances of autochthonous DOM, being 1.8 m^{-1}/(mg-C/L) described as algae and bacterial derived OM (ROSARIO-ORTIZ; SNYDER; SUFFET, 2007) and ocean samples 0.6 m^{-1}/(mg-C/L) (WEISHAAR et al., 2003). The high $SUVA_{254}$ values measured at station 10 was due to the contribution of the mangrove forest to the OM to this channel in the ebb tide (Figure 21).

Normally, CDOM and $SUVA_{254}$ decrease with salinity in estuaries. Some of them present conservative behavior related to the dilution by marine waters (WANG et al., 2014). While others show a non-conservative behavior caused by photodegradation, flocculation and/or precipitation (DIXON et al., 2014; GUO et al., 2007; YAMASHITA et al., 2010). In the Jaguaribe River estuary, CDOM and $SUVA_{254}$ decreased with salinity non-conservatively during the temporal sampling (Figures 25a and 25b), indicating that the DOM suffered changes with the tide dynamics. The decrease of $SUVA_{254}$ indicates a reduction of terrestrial inputs, related to the marine contribution (ROSARIO-ORTIZ; SNYDER; SUFFET, 2007), but also the degradation of labile aromatic compounds by photobleaching and/or flocculation (DIXON et al., 2014). The higher CDOM concentrations in freshwater than in estuarine waters indicates that the DOM is more reactive in freshwater (YI et al., 2014a). Since OM from freshwater was more susceptive to photodegradation, the mixing of fluvial and seawater favors OM degradation due to the less turbidity in the marine waters and consequently higher light penetration (GUO et al., 2012). Then, the non-conservative behavior and reduction of CDOM and $SUVA_{254}$ in the Jaguaribe River estuary show the relevance of tides in the process as photooxidation and flocculation to the DOM cycling in this estuary.

The three components, identified by PARAFAC, were present along all estuary and showed higher concentrations in the freshwater (Figure 25c). The fluorescence intensity of C1 and C2 were similar among them in estuarine waters. C1 had the highest fluorescence intensity in estuarine water, but C2 was the most intense at fluvial end-member. C3 presented the lowest fluorescence values in all salinity gradient.

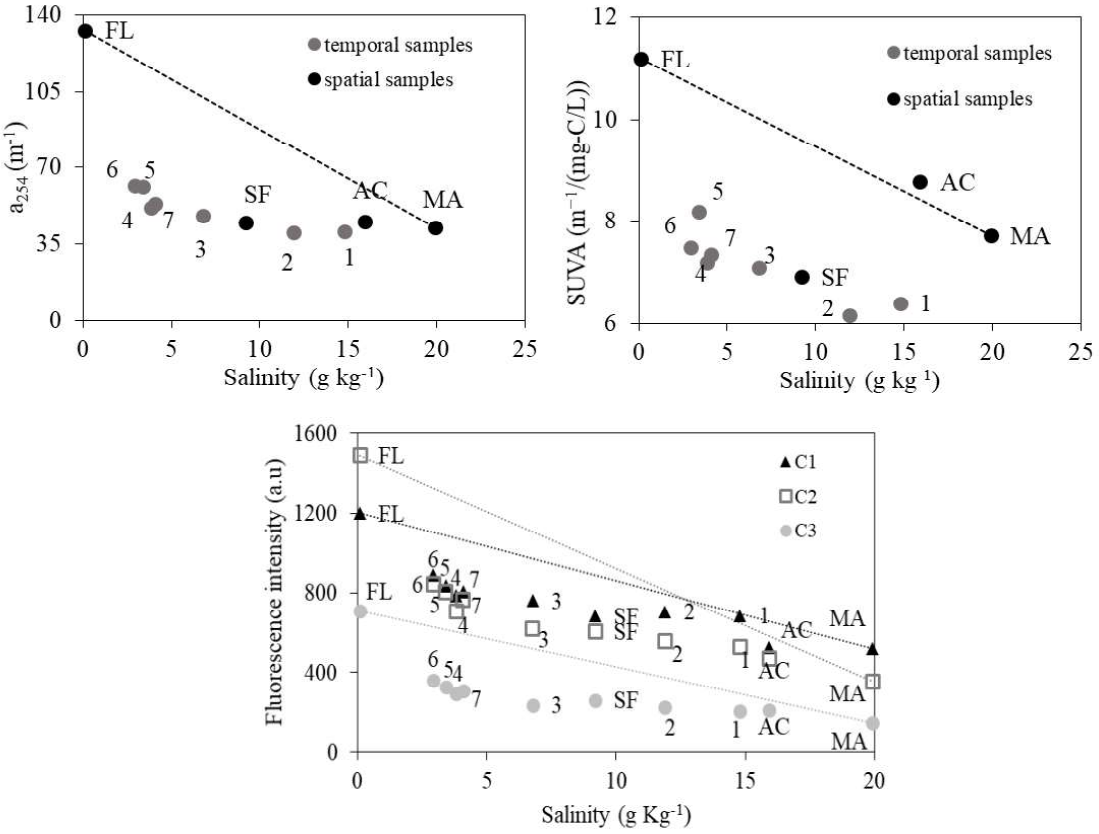

Figure 25 - Variation of the (a) a_{254} (b) SUVA and (c) three components of DOM with salinity. Numbers and letters refers to the samples from temporal and spatial sampling respectively.

A non-conservative decrease was observed in the fluorescence intensity of the components with the increase of salinity (Figure 25c). This behavior was similar to the OM components terrestrial-derived (peaks II, III and IV) from the Piauí River estuary, located at NE Brazil, while the fluorophore marine-derived (peak I) increased (COSTA et al., 2011). The fluorescence intensity of terrestrial OM normally decreases with estuarine mixing (OSBURN et al., 2012; WANG et al., 2017; YI et al., 2014a) as result of the dilution, photobleaching, adsorption and flocculation process (COBLE, 2007; GUO et al., 2007, 2012; WANG et al., 2014). Then, the fluorescence and $SUVA_{254}$ results confirm the terrestrial origin of the OM in the Jaguaribe River estuary during the rainy season. However, the terrestrial inputs are probably reduced during the dry season due to the reduced fluvial supply in this season (DIAS et al., 2016), resulting in a distinct dynamics of the DOM because of its greater lability.

5.3.3.4. Size distributions of OM with estuarine mixing

The POC (> 0.45 μm) ranged from 10.9 to 31.8 % of the OM in the Jaguaribe River estuary and DOC ranged from 89.1 to 68.2 %. The dominant fraction of DOC was the <1 kDa LMW-DOM (Figure 26b), ranging from 474.4 to 544.2 μmol L^{-1} (average of 505.9 ± 35.4 μmol L^{-1}) that corresponds to 57.6 to 77.6 % of the total organic matter (TOM) and between 80.5 and 85.3% of the DOM. The colloidal OM (COM) (>1 kDa) concentrations ranged of 25.8 to 39.3 μmol L^{-1}, with an average of 32.9 ± 4.9 μmolL^{-1} that corresponded to 4.5 ± 1.0 % of the TOM and 5.7 ± 1.0 % of the DOM. Most of the DOM was similar to DOM in the Jiulong River Estuary, where DOM was preponderantly derived from soil leaching (YI et al., 2014a). Mangroves might have been important contributors to the estuarine DOM in the Jaguaribe River, considering that the highest DOC concentrations were observed at low tide (Figure 24b), when the DOM contribution derived from the mangrove through tidal pumping is higher (BOUILLON et al., 2007; REZENDE et al., 2007). However, the percentage of COM in the Jaguaribe River estuary was much lower than observed worldwide (DUAN; BIANCHI, 2006; GUO et al., 2009; STEPHENS; MINOR, 2010; XU; GUO, 2017).

The reduction of POC and the increase of LMW-DOM and COM with salinity increase (Figure 26a) indicate a reduction in OM particle size along the salinity gradient. In a negative freshwater estuary (China), the OM size reduced with salinity. This reduction was caused mainly by physical mixing, followed by photochemical and microbial degradation, disaggregation, and repartitioning. The disaggregation process converts organic aggregates into smaller size fractions as a consequence of the ionic strength increased by the estuarine mixing (XU et al., 2018). Another relevant process was the photodegradation, as discussed previously, that can increase the LMW fraction, remove the CDOM (XU et al., 2018). Another relevant process was the photodegradation, as discussed previously, that can increase the LMW fraction, remove the CDOM (XU et al., 2018) and produce dissolved inorganic carbon (GUO et al., 2012) through the break of COM. The optical properties of the DOM and of its size change suggest photodegradation has an important driver in the OM cycling in the Jaguaribe River estuary.

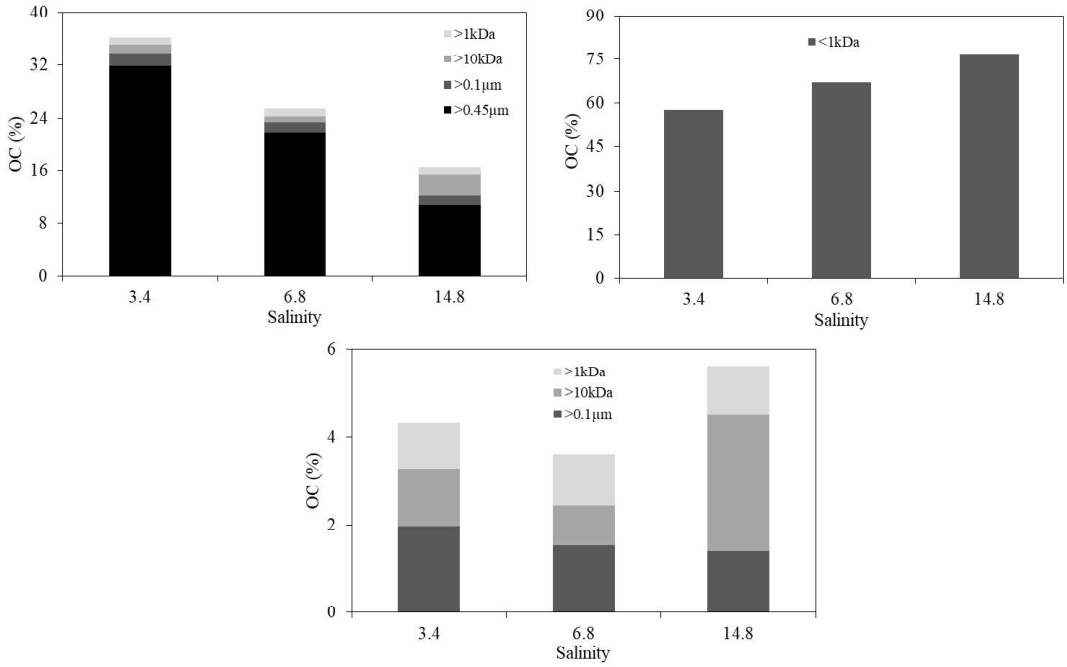

Figure 26 – Size distribution of total organic carbon in the column water of the Jaguaribe River estuary with salinity variation.

The sum of the COM fractions presented an increasing tendency with salinity, but a reduction (~27%) was observed in an intermediary salinity 6.8 g kg^{-1} (Figure 26c), reflecting the behavior of the DOM in bulk samples. Besides, the conversion of COM in LMW with the salinity increasing, as mentioned above, COM removal at salinity 6.8 g kg^{-1} might have been strengthened by flocculation that is commonly reported to salinities below 10 g kg^{-1} (COBLE, 2007).

5.3.3.5. Dissolved metals

Dissolved metals concentrations were presented in Table 9. The concentration order of the metals in the Jaguaribe River estuary was Sr > Al > Rb > Fe > Li > Mo > U > V > Cu > Ni > Pb > Cr > Sn. The concentrations of U, Sn, Pb, V, Cr, Fe, Ni, Al and Cu measured in the Jaguaribe River estuary were within the range for world river waters (GAILLARDET; VIERS; DUPRÉ, 2013). However, the concentrations of Li, Rb, Sr, and Mo were above the range for world river water (GAILLARDET; VIERS; DUPRÉ, 2013), because the estuarine region receives a large contribution of seawater that is rich in these elements (BRULAND; LOHAN, 2003).

Table 10 shows metals relationships with DOC and salinity and inter-element correlation. Besides, similarities among dissolved metals, salinity and DOC were evaluated using multivariate cluster analysis. Two groups were clearly recognized (Figure 27). Group 1 comprising salinity, Li, Rb, Sr, Mo, U, Pb and Sn and Group 2 including DOC, Cr, Fe, V, Al, Cu, and Ni. The Group 1 was arranged in two small groups differed mainly by the similarity with salinity: one group containing salinity, Li, Rb, Sr, Mo and U, and the other Pb and Sn. Table10 shows a positive correlation between Li, Rb, Sr, Mo, and U with salinity. Moreover, they showed conservative mixing behavior (Figure S1). The clustering of Li, Rb, Sr, Mo and U occurred because they present a similar behavior, since they belong to the trace metal groups with high and moderated mobility (GAILLARDET; VIERS; DUPRÉ, 2013). Then these metals are found in high concentrations in seawater (BRULAND; LOHAN, 2003). While Pb and Sn were not significantly correlated with salinity, presenting a non-conservative decline with salinity (Figure S1). Group 2 clustered the variables negatively associated with salinity (Table 10). Besides, in this group, the metals were separated into small groups following their relationship with DOC and their reactivity. The metals with greater association to DOC (Fe, V, and Cr) were separated from the others, as can be seen in Table 10. The groups also reflected their mobility, Cr, Fe, V are classified as metals with low mobility, Ni and Cu as moderate lability and the Al is among the most immobile elements (GAILLARDET; VIERS; DUPRÉ, 2013).

Table 9 - Ranges, averages and standard deviation of dissolved metals concentrations from the Jaguaribe River estuary.

Group 1	Li (µg L^{-1})	Rb (µg L-1)	Sr (µg L^{-1})	Mo (µg L^{-1})	U (µg L^{-1})	Sn (µg L^{-1})	Pb (µg L^{-1})
	1.81 - 73.99	3.20 - 95.39	176.1 - 5578.83	0.70 - 7.12	0.27 - 3.09	0.06 - 0.21	0.01 - 4.55
	34.22 ± 24.87	40.51 ± 31.55	2669.28 ± 1831.87	3.35 ± 2.11	1.18 ± 0.94	0.12 ± 0.06	0.44 ± 1.36
Group 2	Al (µg L^{-1})	V (µg L-1)	Cr (µg L^{-1})	Fe (µg L^{-1})	Ni (µg L^{-1})	Cu (µg L^{-1})	-
	0.97 - 805.54	2.08 - 4.99	0.06 - 0.92	0.68 - 410.97	0.47 - 2.2	0.34 - 2.91	
	75.21 ± 242.23	3.05 ± 0.79	0.16 ± 0.25	39.95 ± 123.06	1.20 ± 0.49	1.24 ± 0.73	

1

Table 10 – Matrix correlation between dissolved metals, salinity and DOC

2

	Li	Rb	Sr	Mo	Sn	Pb	U	Al	V	Cr	Fe	Ni	Cu	DOC	S
Li	1														
Rb	**0.990**	1													
Sr	**0.990**	1	1												
Mo	**1.000**	**0.990**	**0.990**	1											
Sn	-0.072	-0.045	-0.045	-0.073	1										
Pb	-0.363	0.309	0.309	-0.364	**0.664**	1									
U	**0.990**	**0.982**	**0.982**	**0.99**	-0.054	-0.372	1								
Al	**-0.809**	**-0.746**	**-0.746**	**-0.809**	0.464	**0.746**	**-0.8**	1							
V	**-0.909**	**-0.918**	**-0.918**	**-0.909**	-0.027	0.273	**-0.9**	**0.609**	1						
Cr	**-0.881**	**0.927**	**0.927**	**-0.882**	0.027	0.246	**-0.89**	0.554	**0.882**	1					
Fe	**-0.845**	**-0.863**	**-0.863**	**-0.846**	-0.009	0.336	**-0.854**	0.554	**0.973**	**0.9**	1				
Ni	**-0.818**	**-0.863**	**-0.863**	**-0.812**	-0.191	0.109	**-0.854**	0.509	**0.755**	**0.818**	**0.727**	1			
Cu	**-0.772**	**-0.709**	**-0.709**	**-0.773**	0.1	0.5	**-0.8**	**0.8**	0.591	0.509	0.527	**0.682**	1		
DOC	**-0.981**	**-0.973**	**-0.973**	**-0.982**	0.073	0.291	**-0.964**	**0.764**	**0.891**	**0.854**	**0.809**	**0.809**	**0.773**	1	
S	**-0.99**	**1.000**	**1.000**	**0.991**	-0.046	-0.309	**0.982**	**-0.746**	**-0.912**	**-0.927**	**-0.836**	**-0.864**	**-0.709**	**-0.973**	1

The metals clustered with DOC also exhibited a non-conservative behavior, probably being regulated by the OM in the estuary. However, this interaction is worrying, because while DOM-metal association can stabilize toxic metals through their precipitation to bottom sediments, it can also make the contaminants available to the biota (MACHADO et al., 2016).

The metals were distributed mainly in the truly dissolved phase (<1 kDa), as well as the DOM (Figure 28a), corresponding to more than 90% of the bulk sample to each metal. The trace metals in the total colloidal phase (>1 kDa) varied from 3.5 to 7.3 % (Figure 28b-g). Some metals (eg.: Cu, Pb, and Cd) are normally associated with colloids in estuarine environments (WAELES et al., 2008). Metal partitioning depends on the competition between ligands with high and low molecular weight. In the Jaguaribe River estuary, the small concentration of COM may have influenced the low concentration of metals in the colloidal phase.

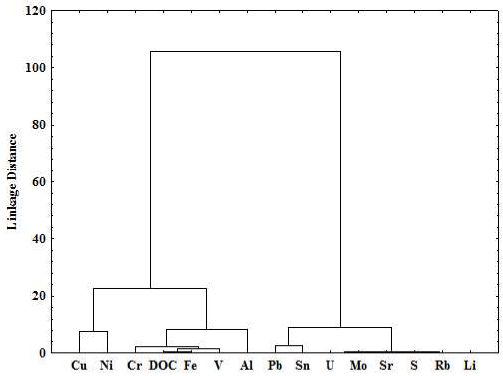

Figure 27 - Cluster analysis of the dissolved metals, salinity and DOC in the Jaguaribe River estuary.

The partitioning of metals concentration between filtration classes were practically constant with salinity variation in the dissolved phase (< 1 kDa), showing a slight increase at salinity 6.8 g kg^{-1} (Figure 28a). Li, Rb, Sr, and Mo were practically constant with salinity variation in the colloidal fraction, showing a slightly decreasing trend in Sn and Mo percentages with salinity. However, the percentage of colloidal V and Cu decrease at salinity 6.8 g kg^{-1} (Figure 28f-g), as observed to the COM, indicating that these metals were regulated by OM. Then, these metals were probably removed from column water by flocculation. The colloidal size distribution of metals varied with salinity, reducing at high tide. The largest colloidal size percentage (>0.1 μm) reduced at salinity 6.8 g kg^{-1}, while the >10 kDa and >1 kDa increased at salinity 6.8 (except the Cu >1 kDa that decreased at salinity 6.8 g kg^{-1}).

In the Jaguaribe River estuary, the DOM was composed predominantly of humic substances that have a strong complexing capacity with metals (Fang et al., 2015; Yang and Van Den Berg, 2009). Besides, the DOM was preponderantly in the truly dissolved phase (<1kDa) that is the OM form with higher mobility. Therefore, metals positively related to DOM (Cu, Ni, Fe, Cr, V) also have high mobility. Different from expected, the DOM sources are the same along the fluvial and estuarine region of the Jaguaribe River estuary, during the rainy season. Then, the OM size and environmental variables that control the reactivity of OM, very probably, were the main drives of metal bioavailability in the Jaguaribe River estuary, since the LMW-DOM

increased in the estuarine region and DOM partitioning was controlled by environmental variables.

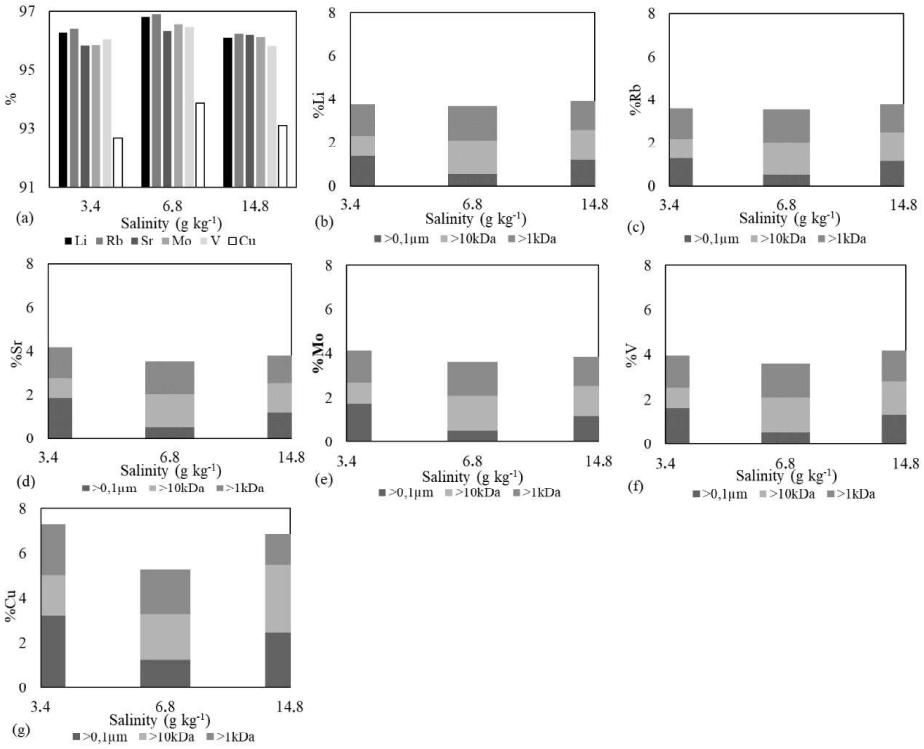

Figure 27 - (a) Distribution of the truly dissolved metals and coloidal size distribution of (b) Li (c) Rb, (d) Sr, (e) Mo, (f) V, (g) Cu with salinity variation in the Jaguaribe River estuary.

5.3.4. Conclusion

The PARAFAC analyses identified three DOM fluorophores derived from terrestrial inputs and composed by humic and fulvic acids, while the correlation between POC and Chl-*a* showed a significant contribution of phytoplankton to the POM. The cluster analysis showed the relationship between DOM and some trace metals (Cu, Fe, Cr, V), indicating that they were associated and that DOM regulated their dynamic. The reduction of metals (Cu and V) associated with colloidal phase and COM at mesohaline salinity pointed to the flocculation and stabilization of these contaminants. However, DOM and trace metals were preponderantly in the truly dissolved fraction (<1 kDa), suggesting their high mobility in the Jaguaribe River estuary. The relationship between DOM and Cu and Cr in this fraction is very worrying due to the high toxicity of these elements to the organisms. Although the source of the OM has not changed along the salinity gradient or with the tide at the fixed point, its reactivity and the relationship between DOM and metals changed. In addition, geochemical processes, such as photo and/or microbial degradation and flocculation of OM, had a great influence on the OM partitioning and consequently on the mobility of trace metals.

5.3.5. Reference

Bouillon, S., Dehairs, F., Velimirov, B., Abril, G., and Borges, A. V. (2007). Dynamics of organic and inorganic carbon across contiguous mangrove and seagrass systems (Gazi Bay, Kenya). *J. Geophys. Res.* 112, 1–14. doi:10.1029/2006JG000325.

Bruland, K. W., and Lohan, M. C. (2003). "Controls of Trace Metals in Seawater," in *Treatise on Geochemistry*, eds. H. D. Holland and K. K. Turekian (Elsevier), 23–47. doi:10.1016/B0-08-

043751-6/06105-3.
Coble, P. G. (1996). Characterization of marine and terrestrial DOM in seawater using excitation-emission matrix spectroscopy. *Mar. Chem.* 51, 325–346.
Coble, P. G. (2007). Marine Optical Biogeochemistry: The Chemistry of Ocean Color. *Chem. Rev.* 107, 402–418. doi:10.1021/cr050350+.
Costa, A. S., Passos, E. D. A., Garcia, C. A., and Alves, J. D. P. H. (2011). A Characterization of Dissolved Organic Matter in the Piauí River Estuary, Northeast Brazil. *J. Braz. Chem. Soc.* 22, 2139–2147. doi:10.1590/S0103-50532011001100017.
Costa, B. G. B., Soares, T. M., Torres, R. F., and Lacerda, L. D. (2013). Mercury distribution in a mangrove tidal creek affected by intensive shrimp farming. *Bull. Environ. Contam. Toxicol.* 90, 537–541. doi:10.1007/s00128-012-0957-4.
Dias, F. J. D. S., Castro, B. M., Lacerda, L. D., Miranda, L. B., and Marins, R. V. (2016). Physical characteristics and discharges of suspended particulate matter at the continent-ocean interface in an estuary located in a semiarid region in northeastern Brazil. *Estuar. Coast. Shelf Sci.* 180, 258–274. doi:10.1016/j.ecss.2016.08.006.
Dias, F. J. da S., Lacerda, L. D., Marins, R. V., and de Paula, F. C. F. (2011). Comparative analysis of rating curve and ADP estimates of instantaneous water discharge through estuaries in two contrasting Brazilian rivers. *Hydrol. Process.* 25, 2188–2201. doi:10.1002/hyp.7972.
Dias, F. J. da S., Marins, R. V., and Maia, L. P. (2013). Impact of drainage basin changes on suspended matter and particulate copper and zinc discharges to the ocean from the Jaguaribe River in the semiarid NE brazilian coast. *J. Coast. Res.* 29, 1137–1145. doi:10.2112/JCOASTRES-D-12-00115.1.
Dixon, J. L., Helms, J. R., Kieber, R. J., and Avery, G. B. (2014). Biogeochemical alteration of dissolved organic material in the Cape Fear River Estuary as a function of freshwater discharge. *Estuar. Coast. Shelf Sci.* 149, 273–282. doi:10.1016/j.ecss.2014.08.026.
Duan, S., and Bianchi, T. S. (2006). Seasonal changes in the abundance and composition of plant pigments in particulate organic carbon in the Lower Mississippi and Pearl Rivers. *Estuaries and Coasts* 29, 427–442. doi:10.1007/BF02784991.
Eschrique, S. A., Braga, E. D. S., Marins, R. V., and Gonsalez, V. (2010). Nutrients as indicators of environmental changes in two Brazilian estuarine systems. *Safety, Heal. Environ. World Congr.*, 71–75.
Fang, K., Yuan, D., Zhang, L., Feng, L., Chen, Y., and Wang, Y. (2015a). Effect of environmental factors on the complexation of iron and humic acid. *J. Environ. Sci. (China)* 27, 188–96. doi:10.1016/j.jes.2014.06.039.
Fang, K., Yuan, D., Zhang, L., Feng, L., Chen, Y., and Wang, Y. (2015b). Effect of environmental factors on the complexation of iron and humic acid. *J. Environ. Sci. (China)* 27, 188–196. doi:10.1016/j.jes.2014.06.039.
Findlay, S. E. G., and Sinsabaugh, R. L. (2003). *Aquatic Ecosystems*. San Diego: Academic Press.
Gaillardet, J., Viers, J., and Dupré, B. (2013). *Trace Elements in River Waters*. doi:10.1016/B978-0-08-095975-7.00507-6.
Giani, M., Savelli, F., Berto, D., Zangrando, V., Cosović, B., and Vojvodić, V. (2005). Temporal dynamics of dissolved and particulate organic carbon in the northern Adriatic Sea in relation to the mucilage events. *Sci. Total Environ.* 353, 126–38. doi:10.1016/j.scitotenv.2005.09.062.
Godoy, M. D. P., and Lacerda, L. D. de (2014). River-Island Morphological Response to Basin Land-Use Change within the Jaguaribe River Estuary, NE Brazil. *J. Coast. Res.* 294, 399–410. doi:10.2112/jcoastres-d-13-00059.1.
Godoy, M. D. P., and Lacerda, L. D. de (2015). Mangroves Response to Climate Change: A Review of Recent Findings on Mangrove Extension and Distribution. *Ann. Brazilian Acad. Sci.* 87, 651–667. doi:10.1590/0001-3765201520150055.
Guo, L., White, D. M., Xu, C., and Santschi, P. H. (2009). Chemical and isotopic composition of high-molecular-weight dissolved organic matter from the Mississippi River plume. *Mar. Chem.* 114, 63–71. doi:10.1016/j.marchem.2009.04.002.
Guo, W., Stedmon, C. A., Han, Y., Wu, F., Yu, X., and Hu, M. (2007). The conservative and non-conservative behavior of chromophoric dissolved organic matter in Chinese estuarine waters. *Mar. Chem.* 107, 357–366. doi:10.1016/j.marchem.2007.03.006.
Guo, W., Yang, L., Yu, X., Zhai, W., and Hong, H. (2012). Photo-production of dissolved inorganic carbon from dissolved organic matter in contrasting coastal waters in the southwestern Taiwan Strait, China. *J. Environ. Sci. (China)* 24, 1181–1188. doi:10.1016/S1001-0742(11)60921-2.
ISO (1992). *Water quality measurement of biochemical parameters spectrophotometric*

determination of chlorophyll-a concentration. Geneva: International Organization for Standardization.

Lacerda, L. D., Dias, F. J. S., Marins, R. V, Soares, T. M., Godoy, J. M. O., and Godoy, M. L. D. P. (2013). Pluriannual watershed discharges of Hg into a tropical semi-arid estuary of the Jaguaribe River, NE Brazil. *J. Braz. Chem. Soc.* 24, 1719–1731. doi:10.5935/0103-5053.20130216.

Lacerda, L. D., Molisani, M. M., Sena, D., and Maia, L. P. (2008). Estimating the importance of natural and anthropogenic sources on N and P emission to estuaries along the Ceará State Coast NE Brazil. *Environ. Monit. Assess.* 141, 149–64. doi:10.1007/s10661-007-9884-y.

Lacerda, L. D., Santos, J. A., and Madrid, R. M. (2006). Copper emission factors from intensive shrimp aquaculture. *Mar. Pollut. Bull.* 52, 1823–1826. doi:10.1016/j.marpolbul.2006.09.012.

Lacerda, L. D., Soares, T. M., Costa, B. G. B., and Godoy, M. D. P. (2011). Mercury emission factors from intensive shrimp aquaculture and their relative importance to the Jaguaribe River Estuary, NE Brazil. *Bull. Environ. Contam. Toxicol.* 87, 657–661. doi:10.1007/s00128-011-0399-4.

Lin, H., Cai, Y., Sun, X., Chen, G., Huang, B., Cheng, H., et al. (2016). Sources and mixing behavior of chromophoric dissolved organic matter in the Taiwan Strait. *Mar. Chem.* 187, 43–56. doi:10.1016/j.marchem.2016.11.001.

Louis, Y., Garnier, C., Lenoble, V., Omanović, D., Mounier, S., and Pizeta, I. (2009). Characterisation and modelling of marine dissolved organic matter interactions with major and trace cations. *Mar. Environ. Res.* 67, 100–7. doi:10.1016/j.marenvres.2008.12.002.

Luan, H., and Vadas, T. M. (2015). Size characterization of dissolved metals and organic matter in source waters to streams in developed landscapes. *Environ. Pollut.* 197, 76–83. doi:10.1016/j.envpol.2014.12.004.

Machado, A. A. de S., Spencer, K., Kloas, W., Toffolon, M., and Zarfl, C. (2016). Metal fate and effects in estuaries: A review and conceptual model for better understanding of toxicity. *Sci. Total Environ.* 541, 268–281. doi:10.1016/j.scitotenv.2015.09.045.

Marengo, J. A., Alves, L. M., Alvala, R. C., Cunha, A. P., Brito, S., and Moraes, O. L. (2017). Climatic characteristics of the 2010-2016 drought in the semiarid Northeast Brazil region. *An. Acad. Bras. Cienc.*, 1–13. doi:10.1590/0001-3765201720170206.

Marins, R. V., Lacerda, L. D. De, Abreu, I. M., and Dias, F. J. D. S. (2003). Efeitos da açudagem no rio Jaguaribe. *Ciência Hoje* 33, 66–70.

Marins, R. V, Paula Filho, F. J., Eschrique, S. A., and Lacerda, L. D. (2011). Anthropogenic sources and distribution of phosphorus in sediments from the Jaguaribe River estuary, NE, Brazil. *Brazilian J. Biol.* 71, 673–678. doi:10.1590/S1519-69842011000400011.

Mounier, S., Marins, R. V., and Lacerda, L. D. de (2018). Characterization of the Ceara Costal Zone Organic Matter Inputs. *archives-ouverts*, 39. Available at: https://hal.archives-ouvertes.fr/hal-01779147.

Moura, V. L., and Lacerda, L. D. de (2018). Contrasting Mercury Bioavailability in the Marine and Fluvial Dominated Areas of the Jaguaribe River Basin, Ceará, Brazil. *Bull. Environ. Contam. Toxicol.* 101, 49–54. doi:10.1007/s00128-018-2368-7.

Moyer, R. P., Powell, C. E., Gordon, D. J., Long, J. S., and Bliss, C. M. (2015). Abundance, distribution, and fluxes of dissolved organic carbon (DOC) in four small sub-tropical rivers of the Tampa Bay Estuary (Florida, USA). *Appl. Geochemistry* 63, 550–562. doi:10.1016/j.apgeochem.2015.05.004.

Oliveira, R. C. B. de, and Marins, R. V. (2011). Trace Metals Dynamics in Soil and Estuarine Sediment as a Major Factor Controlling Contaminants Contribution to the Aquatic Environment: Review. *Rev. Virtual Química* 3. doi:10.5935/1984-6835.20110014.

Osburn, C. L., Handsel, L. T., Mikan, M. P., Paerl, H. W., and Montgomery, M. T. (2012). Fluorescence tracking of dissolved and particulate organic matter quality in a river-dominated estuary. *Environ. Sci. Technol.* 46, 8628–8636. doi:10.1021/es3007723.

Parlanti, E., Wörz, K., Geoffroy, L., and Lamotte, M. (2000). Dissolved organic matter fluorescence spectroscopy as a tool to estimate biological activity in a coastal zone submitted to anthropogenic inputs. *Org. Geochem.* 31, 1765–1781. doi:10.1016/S0146-6380(00)00124-8.

Rezende, C. E., Lacerda, L. D., Ovalle, A. R. C., and Silva, L. F. F. (2007). Dial organic carbon fluctuations in a mangrove tidal creek in Sepetiba bay, Southeast Brazil. *Brazilian J. Biol.* 67, 673–680. doi:10.1590/S1519-69842007000400012.

Rios, J. H. L., Marins, R. V., Oliveira, K. F., and Lacerda, L. D. (2016). Long-Term (2002–2015) Changes in Mercury Contamination in NE Brazil Depicted by the Mangrove Oyster Crassostraea rhizophorae (Guilding, 1828). *Bull. Environ. Contam. Toxicol.* 97, 474–479. doi:10.1007/s00128-016-1855-y.

183 Rosario-Ortiz, F. L., Snyder, S. A., and Suffet, I. H. (Mel. (2007). Characterization of dissolved
184 organic matter in drinking water sources impacted by multiple tributaries. *Water Res.* 41,
185 4115–4128. doi:10.1016/j.watres.2007.05.045.
186 Santinelli, C., Nannicini, L., and Seritti, A. (2010). DOC dynamics in the meso and bathypelagic
187 layers of the Mediterranean Sea. *Deep. Res. Part II Top. Stud. Oceanogr.* 57, 1446–1459.
188 doi:10.1016/j.dsr2.2010.02.014.
189 Shin, Y., Lee, E.-J., Jeon, Y.-J., Hur, J., and Oh, N.-H. (2016). Hydrological changes of DOM
190 composition and biodegradability of rivers in temperate monsoon climates. *J. Hydrol.* 540,
191 538–548. doi:10.1016/j.jhydrol.2016.06.004.
192 Simpson, S. L., Vardanega, C. R., Jarolimek, C., Jolley, D. F., Angel, B. M., and Mosley, L. M.
193 (2014). Metal speciation and potential bioavailability changes during discharge and
194 neutralisation of acidic drainage water. *Chemosphere* 103, 172–180.
195 doi:10.1016/j.chemosphere.2013.11.059.
196 Stedmon, C. A., and Markager, S. (2005). Resolving the variability in {DOM} fluorescence in a
197 temperate estuary and its catchment unsing {PARAFAC}. *Limnol.Oceanogr.* 50, 686–697.
198 Stedmon, C. A., Markager, S., and Bro, R. (2003). Tracing dissolved organic matter in aquatic
199 environments using a new approach to fluorescence spectroscopy. *Mar. Chem.* 82, 239–254.
200 doi:10.1016/S0304-4203(03)00072-0.
201 Stephens, B. M., and Minor, E. C. (2010). DOM characteristics along the continuum from river to
202 receiving basin: A comparison of freshwater and saline transects. *Aquat. Sci.* 72, 403–417.
203 doi:10.1007/s00027-010-0144-9.
204 Stolpe, B., Guo, L., Shiller, A. M., and Hassellöv, M. (2010). Size and composition of colloidal
205 organic matter and trace elements in the Mississippi River, Pearl River and the northern Gulf
206 of Mexico, as characterized by flow field-flow fractionation. *Mar. Chem.* 118, 119–128.
207 doi:10.1016/j.marchem.2009.11.007.
208 Stolpe, B., Zhou, Z., Guo, L., and Shiller, A. M. (2014). Colloidal size distribution of humic- and
209 protein-like fluorescent organic matter in the northern Gulf of Mexico. *Mar. Chem.* 164, 25–
210 37. doi:10.1016/j.marchem.2014.05.007.
211 Waeles, M., Tanguy, V., Lespes, G., and Riso, R. D. (2008). Behaviour of colloidal trace metals
212 (Cu, Pb and Cd) in estuarine waters: An approach using frontal ultrafiltration (UF) and
213 stripping chronopotentiometric methods (SCP). *Estuar. Coast. Shelf Sci.* 80, 538–544.
214 doi:10.1016/j.ecss.2008.09.010.
215 Wang, W., Chen, M., Guo, L., and Wang, W. X. (2017). Size partitioning and mixing behavior of
216 trace metals and dissolved organic matter in a South China estuary. *Sci. Total Environ.* 603–
217 604, 434–444. doi:10.1016/j.scitotenv.2017.06.121.
218 Wang, X. C., Altabet, M. A., Callahan, J., and Chen, R. F. (2004). Stable carbon and nitrogen
219 isotopic compositions of high molecular weight dissolved organic matter from four U.S.
220 estuaries. *Geochim. Cosmochim. Acta* 68, 2681–2691. doi:10.1016/j.gca.2004.01.004.
221 Wang, Y., Zhang, D., Shen, Z., Chen, J., and Feng, C. (2014). Characterization and spacial
222 distribution variability of chromophoric dissolved organic matter (CDOM) in the Yangtze
223 Estuary. *Chemosphere* 95, 353–362. doi:10.1016/j.chemosphere.2013.09.044.
224 Wang, Z. gang, Liu, W. qing, Zhao, N. jing, Li, H. bin, Zhang, Y. jun, Si-Ma, W. cang, et al.
225 (2007). Composition analysis of colored dissolved organic matter in Taihu Lake based on
226 three dimension excitation-emission fluorescence matrix and PARAFAC model, and the
227 potential application in water quality monitoring. *J. Environ. Sci.* 19, 787–791.
228 doi:10.1016/S1001-0742(07)60132-6.
229 Weishaar, J. L., Aiken, G. R., Bergamaschi, B. A., Fram, M. S., Fujii, R., and Mopper, K. (2003).
230 Evaluation of specific ultraviolet absorbance as an indicator of the chemical composition
231 and reactivity of dissolved organic carbon. *Environ. Sci. Technol.* 37, 4702–4708.
232 doi:10.1021/es030360x.
233 Wilkinson, K. J., and Lead, J. R. (2007). *Environmental colloids and particles: behaviour,*
234 *separation and characterisation BT - IUPAC series on analytical and physical chemistry of*
235 *environmental systems v. 10*. Available at:
236 http://www.loc.gov/catdir/toc/ecip0615/2006020351.htmlhttp://www.loc.gov/catdir/enhance
237 ments/fy0741/2006020351-
238 d.htmlhttp://www.loc.gov/catdir/enhancements/fy0741/2006020351-b.html.
239 Xu, H., and Guo, L. (2017). Molecular size-dependent abundance and composition of dissolved
240 organic matter in river, lake and sea waters. *Water Res.* 117, 115–126.
241 doi:10.1016/j.watres.2017.04.006.
242 Xu, H., Houghton, E. M., Houghton, C. J., and Guo, L. (2018). Variations in size and
243 composition of colloidal organic matter in a negative freshwater estuary. *Sci. Total Environ.*
244 615, 931–941. doi:10.1016/j.scitotenv.2017.10.019.

Yamashita, Y., Maie, N., Briceño, H., and Jaffé, R. (2010). Optical characterization of dissolved organic matter in tropical rivers of the Guayana Shield, Venezuela. *J. Geophys. Res. Biogeosciences* 115. doi:10.1029/2009JG000987.

Yang, L., Chen, C. T. A., Lui, H. K., Zhuang, W. E., and Wang, B. J. (2016). Effects of microbial transformation on dissolved organic matter in the east Taiwan Strait and implications for carbon and nutrient cycling. *Estuar. Coast. Shelf Sci.* 180, 59–68. doi:10.1016/j.ecss.2016.06.021.

Yang, R., and Van Den Berg, C. M. G. (2009). Metal complexation by humic substances in seawater. *Environ. Sci. Technol.* 43, 7192–7197. doi:10.1021/es900173w.

Yi, Y., Zheng, A., Guo, W., Yang, L., and Chen, D. (2014). Optical properties of estuarine dissolved organic matter isolated using cross-flow ultrafiltration. *Acta Oceanol. Sin.* 33, 22–29. doi:10.1007/s13131-014-0451-4.

Zhou, Z., and Guo, L. (2015). A critical evaluation of an asymmetrical flow field-flow fractionation system for colloidal size characterization of natural organic matter. *J. Chromatogr. A* 1399, 53–64. doi:10.1016/j.chroma.2015.04.035.

5.3.6. Supplementary material

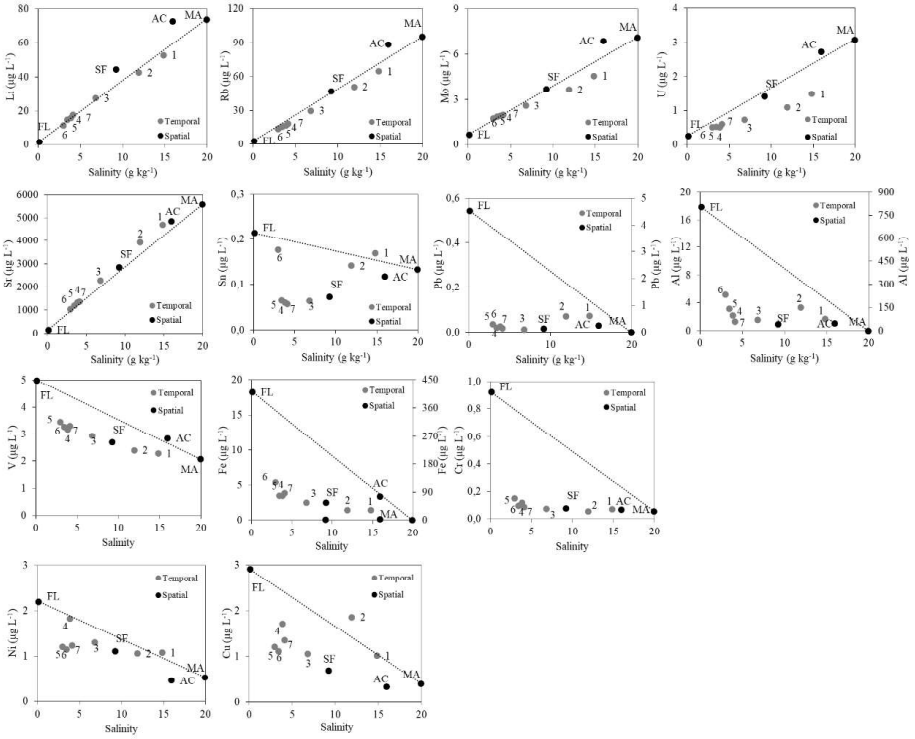

Figure S1- Concentrations of dissolved metals plotted against salinity with conservative mixing line calculated from fluvial and marine end-members.

Table S1 - Concentration factor in each cartridge to each sample.

	Concentration fator		
Sample	1	3	5
0.1µm	90.9	90.9	76.9
10kDa	75.1	75.1	108.2
1kDa	76.0	76.0	68.0

6. CONCLUSÃO GERAL

As secas e o barramento do rio Jaguaribe promoveram uma diminuição dramática do fluxo de água doce e, consequentemente, uma forte intrusão salina na região estuarina. Tais fatores levaram o sistema a condições de hipersalinidade e redução dos fluxos de carbono para a plataforma continental. O fluxo de CID e COD, no estuário do rio Jaguaribe, foi menor do que o esperado para um rio tropical, mas semelhante a outros rios chineses e sul-americanos que sofrem influência de barragens e redução da precipitação. De uma forma geral, em estuários clássicos, a exportação (fluxo positivo) de carbono sofre apenas uma redução durante períodos de baixa descarga fluvial. Enquanto que no estuário do rio Jaguaribe, o carbono fica retido (fluxo negativo) durante a estação seca devido ao represamento imposto pelas marés.

O comportamento do carbono no estuário do rio Jaguaribe foi fortemente relacionado aos parâmetros hidrodinâmicos, como o tempo de residência, vazão e percentual de água doce. Nas estações secas monitoradas, a zona de máximo de turbidez do estuário do Rio Jaguaribe atuou como retentor de matéria orgânica e CID, enquanto que durante a estação chuvosa atuou como um exportador. Correlações com a Chl-*a* mostraram que a atividade fitoplanctônica tem baixa influencia no comportamento da MOD, porém tem correlação estatisticamente significativa com a fração particulada da MO.

As análises isotópicas mostraram que a composição da MO estuarina é predominantemente terrígena, sendo as marés o principal controlador de suas concentrações. As análises de fenóis de lignina dissolvidos e de δ^{13}C-COD mostraram que a principal origem terrestre de MO para o estuário foram fragmentos de tecidos não lenhosos de plantas C_3 encontrados em sedimentos do entorno do estuário. Embora não tenha sido possível discriminar as emissões de fontes antropogênicas das naturais, por meio das análises isotópicas, as elevadas concentrações de MO e nitrogênio no canal da carcinicultura apontam esta atividade como fonte relevante de MO e nutrientes para o estuário. Durante o período estudado, foi observada uma modificação da qualidade da matéria orgânica através do aumento do aporte de MO marinha, proporcionada pelo aumento da intrusão salina, com a intensificação das secas pelo El Niño.

Os três fluóforos identificados pelo PARAFAC confirmaram a origem terrestre da MOD no estuário do rio Jaguaribe, na estação chuvosa, e mostraram que ela é composta por ácidos húmicos e fúlvicos. A MOD foi distribuída preponderantemente na fração verdadeiramente dissolvida (<1 kDa). Embora a MOD tenha sido altamente aromática, esta demonstrou ser muito reativa com a variação da salinidade através de seu comportamento não conservativo, causado provavelmente por fotodegradação e desagregação.

Através das técnicas de composição isotópica e fluorescência molecular da matéria orgânica de forma isolada, não foi possível avaliar de forma clara a contribuição autóctone da MO no estuário do rio Jaguaribe provavelmente devido à sua baixa concentração e similaridade de sinal com outras fontes, como os solos. A composição isotópica foi mais eficiente na avaliação da contribuição das principais fontes de MO, porém as técnicas ópticas caracterizaram melhor a MO, fornecendo informações sobre fontes, qualidade e idade da MO.

A análise de agrupamento e correlações de Spearman indicaram associação entre MOD e metais traço (Cu, Ni, Fe, Cr, V), sugerindo que a MOD regulou a dinâmica desses contaminantes, na estação chuvosa. A relação entre MOD e Cu e Cr é muito preocupante devido à alta toxicidade desses elementos para os organismos e o fato de que a MOD foi preponderantemente verdadeiramente dissolvida. Embora não tenha sido observada mudança da fonte da MOD espacial e temporalmente (com a variação da maré) durante a estação chuvosa, a relação entre MOD e metais ocorreu provavelmente devido à alta capacidade de ligação dos compostos húmicos com metais. Entretanto, há remoção de matéria orgânica coloidal e metais (Cu e V) associados a coloides em salinidade intermediária que indicaram floculação e estabilização de contaminantes neste instante da maré.

Embora análises estatísticas indiquem associação entre MO e metais, isto não foi possível ser avaliado quimicamente sendo necessário realizar análises da capacidade de complexação da matéria orgânica para melhor compreensão dessa interação e avaliação da biodisponibilidade dos metais traço. Logo, estudos futuros deverão contemplar uma melhor interação dos aspectos da degradação da MO pela ação microbiana e/ou fotoquímica.

7. REFERÊNCIAS ADICIONAIS

ABRANTES, K. G. et al. Importance of Mangrove Carbon for Aquatic Food Webs in Wet–Dry Tropical Estuaries. **Estuaries and Coasts**, v. 38, n. 1, p. 383–399, 2014.

ABREU, P. C. et al. Eutrophication processes and trophic interactions in a shallow estuary: Preliminary results based on stable isotope analysis (δ13C and δ15N). **Estuaries and Coasts**, v. 29, n. 2, p. 277–285, 2006.

ALMAGRO, A. et al. Projected climate change impacts in rainfall erosivity over Brazil. **Scientific Reports**, v. 7, n. 1, p. 1–12, 2017.

ATEKWANA, EL. A.; TEDESCO, L. P.; JACKSON, L. R. Dissolved Inorganic Carbon (DIC) and Hydrologic Mixing in a Subtropical Riverine Estuary, Southwest Florida , USA. **Estuaries**, v. 26, n. 6, p. 1391–1400, 2003.

BABIARZ, C. L. et al. Application of ultrafiltration and stable isotopic amendments to field studies of mercury partitioning to filterable carbon in lake water and overland runoff. **Science of the Total Environment**, v. 304, n. 1–3, p. 295–303, 2003.

BALCARCZYK, K. L. et al. Stream dissolved organic matter bioavailability and composition in watersheds underlain with discontinuous permafrost. **Biogeochemistry**, v. 94, n. 3, p. 255–270, 2009.

BARROS, G. V. et al. Stable isotopes of bulk organic matter to trace carbon and nitrogen dynamics in an estuarine ecosystem in Babitonga Bay (Santa Catarina, Brazil). **Science of the Total Environment**, v. 408, n. 10, p. 2226–2232, 2010.

BAUER, J. E. et al. The changing carbon cycle of the coastal ocean. **Nature**, v. 504, n. 7478, p. 61–70, 2013.

BAUER, J. E.; BIANCHI, T. S. Dissolved Organic Carbon Cycling and Transformation. **Treatise on Estuarine and Coastal Science**, v. 5, p. 7–67, 2011.

BEZERRA, M. F. et al. Food preferences and Hg distribution in Chelonia mydas assessed by stable isotopes. **Environmental Pollution**, v. 206, p. 236–246, 2015.

BIANCHI, T. S. et al. Carbon cycling in a shallow turbid estuary of southeast Texas: the use of plant pigment biomarkers and water quality parameters. **Estuaries**, v. 20, n. 2, p. 404–415, jun. 1997.

BIANCHI, T. S. et al. A gradient of dissolved organic carbon and lignin from Terrebonne-Timbalier Bay estuary to the Louisiana shelf (USA). **Marine Chemistry**, v. 117, n. 1–4, p. 32–

41, 2009.

BIANCHI, T. S.; BAUER, J. E. **Particulate Organic Carbon Cycling and Transformation**. [s.l.] Elsevier Inc., 2011. v. 5

BLAIR, N. E.; ALLER, R. C. The Fate of Terrestrial Organic Carbon in the Marine Environment. **Annual Review of Marine Science**, v. 4, n. 1, p. 401–423, 2012.

BRULAND, K. W.; LOHAN, M. C. Controls of Trace Metals in Seawater. In: HOLLAND, H. D.; TUREKIAN, K. K. (Eds.). . **Treatise on Geochemistry**. [s.l.] Elsevier, 2003. p. 23–47.

CAI, W.-J. Estuarine and Coastal Ocean Carbon Paradox: CO2 Sinks or Sites of Terrestrial Carbon Incineration? **Annual Review of Marine Science**, v. 3, n. 1, p. 123–145, 15 jan. 2011.

CATALÁN, N. et al. Higher reactivity of allochthonous vs. autochthonous DOC sources in a

CHIANG, J. C. H.; KOUTAVAS, A. Tropical flip-flop connections. **Nature**, v. 432, n. 7018, p. 684–685, 2004.

COBLE, P. G. Marine Optical Biogeochemistry: The Chemistry of Ocean Color. **Chemical Reviews**, v. 107, n. 2, p. 402–418, 2007.

DAI, M. et al. Evaluation of two cross-flow ultrafiltration membranes for isolating marine organic colloids. **Marine Chemistry**, v. 62, n. 1–2, p. 117–136, 1998.

DAI, M. et al. Preleminary study on the dissolved and colloidal organic carbon in the Zhujiang river estuary. **Chinese Journal of Oceanology and Limnology**, v. 18, n. 3, p. 265–273, 2000.

DAI, M. et al. Spatial distribution of riverine DOC inputs to the ocean: an updated global synthesis. **Current Opinion in Environmental Sustainability**, v. 4, n. 2, p. 170–178, maio 2012.

DEGENS, E. T.; ITTEKKOT, V. The carbon cycle--tracking the path of organic particles from sea to sediment. **Geological Society, London, Special Publications**, v. 26, n. 1, p. 121–135, 1 jan. 1987.

DIAS, F. J. D. S. et al. Physical characteristics and discharges of suspended particulate matter at the continent-ocean interface in an estuary located in a semiarid region in northeastern Brazil. **Estuarine, Coastal and Shelf Science**, v. 180, p. 258–274, 2016.

DIAS, F. J. DA S.; CASTRO, B. M.; LACERDA, L. D. DE. Continental shelf water masses off the Jaguaribe River (4S), northeastern Brazil. **Continental Shelf Research**, v. 66, p. 123–135, set. 2013.

DIAS, F. J. DA S.; MARINS, R. V.; MAIA, L. P. Impact of drainage basin changes on suspended matter and particulate copper and zinc discharges to the ocean from the Jaguaribe River in the semiarid NE brazilian coast. **Journal of Coastal Research**, v. 29, n. 5, p. 1137–1145, 30 set. 2013.

DITTMAR, T. et al. A simple and efficient method for the solid-phase extraction of dissolved organic matter (SPE-DOM) from seawater. **Limnology and Oceanography: Methods**, v. 6, p. 230–235, 1 dez. 2008.

DITTMAR, T.; KATTNER, G. The biogeochemistry of the river and shelf ecosystem of the Arctic Ocean: A review. **Marine Chemistry**, v. 83, n. 3–4, p. 103–120, 2003.

DNOCS, D. N. DE O. C. AS S. **Açude Castanhão está com apenas 3,9% da capacidade**. Disponível em: <http://www2.dnocs.gov.br/gab-cs/97-noticias-internas/3733-acude-castanhao-esta-com-apenas-3-9-da-capacidade>. Acesso em: 4 dez. 2017.

EATHERALL, A.; NADEN, P. S.; COOPER, D. M. **Simulating carbon fluxes in rivers: The first stepScience of the Total Enviroment**, 1998.

ESCHRIQUE, S. A. et al. Nutrients as indicators of environmental changes in two Brazilian estuarine systems. **Safety, Health and Environment World Congress**, n. July, p. 71–75, 2010.

ESTEVES, F. D. A. Fundamentos de Limnologia. **Interciência**, n. 2, p. 602, 1988.

EYROLLE, F.; CHARMASSON, S. Ultrafiltration of large volumes for the determination of colloidally bound artificial radionuclides in natural waters. **Applied Radiation and Isotopes**, v. 52, n. 4, p. 927–936, 2000.

FANG, K. et al. Effect of environmental factors on the complexation of iron and humic acid. **Journal of Environmental Sciences (China)**, v. 27, n. C, p. 188–196, 2015.

FEISTEL, R. A new extended Gibbs thermodynamic potential of seawater. **Progress in Oceanography**, v. 58, n. 1, p. 43–114, 2003.

FELLMAN, J. B. et al. Seasonal changes in the chemical quality and biodegradability of dissolved organic matter exported from soils to streams in coastal temperate rainforest watersheds. **Biogeochemistry**, v. 95, n. 2, p. 277–293, 2009.

FINDLAY, S. E. G.; SINSABAUGH, R. L. **Aquatic Ecosystems**. San Diego: Academic Press, 2003.

GAILLARDET, J.; VIERS, J.; DUPRE, B. Trace Elements in River Waters BT - Treatise on Geochemistry. In: **Treatise on Geochemistry**. [s.l.] Else, 2003. v. 5p. 225–272.

GIANI, M. et al. Temporal dynamics of dissolved and particulate organic carbon in the northern Adriatic Sea in relation to the mucilage events. **Science of the total environment**, v. 353, n. 1–3, p. 126–38, 15 dez. 2005.

GODOY, M. D. P.; LACERDA, L. D. DE. River-Island Morphological Response to Basin Land-Use Change within the Jaguaribe River Estuary, NE Brazil. **Journal of Coastal Research**, v. 294, n. 2, p. 399–410, 2014.

GODOY, M. D. P.; LACERDA, L. D. DE. Mangroves Response to Climate Change: A Review of Recent Findings on Mangrove Extension and Distribution. **Annals of the Brazilian Academy of Sciences**, v. 87, n. 2, p. 651–667, 2015.

GODOY, M. D. P.; MEIRELES, A. J. DE A.; LACERDA, L. D. Mangrove Response to Land Use Change in Estuaries along the Semiarid Coast of Ceará, Brazil. **Journal of Coastal Research**, v. 343, n. 3, p. 524–533, 2018.

HANSELL, D. A. et al. Dissolved organic matter in the ocean. **Oceanography**, v. 22, n. 4, p. 202–211, 2009.

HE, B. et al. Distribution, degradation and dynamics of dissolved organic carbon and its major compound classes in the Pearl River estuary, China. **Marine Chemistry**, v. 119, n. 1–4, p. 52–64, abr. 2010.

HEDGES, J. I. et al. Organic and processing of organic matter in the Amazon River as indicated by carbohydrates and amino acids. **Limnology and Oceanography**, v. 39, n. 4, p. 743–761, 1994.

HUANG, T.-H. et al. Fluvial carbon fluxes in tropical rivers. **Current Opinion in Environmental Sustainability**, v. 4, n. 2, p. 162–169, maio 2012.

HUNG, J.-J.; HUANG, M.-H. Seasonal variations of organic-carbon and nutrient transport through a tropical estuary (Tsengwen) in southwestern Taiwan. **Environmental geochemistry and health**, v. 27, n. 1, p. 75–95, fev. 2005.

IPCC. **Climate change 2014. Synthesis report.** Geneva: [s.n.].

KILLOPS, S.; KILLOPS, V. **Introduction to organic geochemistry**. [s.l.] Blackwell Publishing, 2005.

KROL, M. S.; BRONSTERT, A. Regional integrated modelling of climate change impacts on natural resources and resource usage in semi-arid Northeast Brazil. **Environmental Modelling and Software**, v. 22, n. 2, p. 259–268, 2007.

LACERDA, L. D. et al. Estimating the importance of natural and anthropogenic sources on N and P emission to estuaries along the Ceará State Coast NE Brazil. **Environmental monitoring and assessment**, v. 141, p. 149–64, 2008.

LACERDA, L. D. et al. Mercury emission factors from intensive shrimp aquaculture and their relative importance to the Jaguaribe River Estuary, NE Brazil. **Bulletin of Environmental Contamination and Toxicology**, v. 87, n. 6, p. 657–661, 2011.

LACERDA, L. D.; MARINS, R. V.; CAVALCANTE, M. S. Mercury mobilization due to global climate and regional land use changes in the Jaguaribe River Estuary. In: BOTELLO, A. . et al. (Eds.). . **El cambio del nivel del mar y eventos extremos en el Pacifico mexicano**. [s.l.] ujat,

460 unam, uac, 2017. p. 333–344.

461 LACERDA, L. D.; MIGUENS, F. C. A RESSURREIÇÃO DO METAL. **Ciência Hoje**, v. 48, p.
462 38–41, 2011.

463 LACERDA, L. D.; SANTOS, J. A.; MADRID, R. M. Copper emission factors from intensive
464 shrimp aquaculture. **Marine Pollution Bulletin**, v. 52, n. 12, p. 1823–1826, dez. 2006.

465 LEBRETON, B. et al. Origin, composition and quality of suspended particulate organic matter in
466 relation to freshwater inflow in a South Texas estuary. **Estuarine, Coastal and Shelf Science**, v.
467 170, p. 70–82, 2016.

468 LIN, H. et al. Sources and mixing behavior of chromophoric dissolved organic matter in the
469 Taiwan Strait. **Marine Chemistry**, v. 187, p. 43–56, 2016.

470 LOUIS, Y. et al. Characterisation and modelling of marine dissolved organic matter interactions
471 with major and trace cations. **Marine environmental research**, v. 67, n. 2, p. 100–7, mar. 2009.

472 LOUIS, Y.; PERNET-COUDRIER, B.; VARRAULT, G. Implications of effluent organic matter
473 and its hydrophilic fraction on zinc(II) complexation in rivers under strong urban pressure:
474 Aromaticity as an inaccurate indicator of DOM-metal binding. **Science of the Total**
475 **Environment**, v. 490, p. 830–837, 2014.

476 LU, Y. H. et al. Effects of land use on sources and ages of inorganic and organic carbon in
477 temperate headwater streams. **Biogeochemistry**, v. 119, n. 1–3, p. 275–292, 2014.

478 LUAN, H.; VADAS, T. M. Size characterization of dissolved metals and organic matter in source
479 waters to streams in developed landscapes. **Environmental Pollution**, v. 197, p. 76–83, 2015.

480 LUCIANI, X. et al. Tracing of dissolved organic matter from the SEPETIBA Bay (Brazil) by
481 PARAFAC analysis of total luminescence matrices. **Marine Environmental Research**, v. 65, n.
482 2, p. 148–157, 2008.

483 LUCIANI, X. et al. A simple correction method of inner filter effects affecting FEEM and its
484 application to the PARAFAC decomposition. **Chemometrics and Intelligent Laboratory**
485 **Systems**, v. 96, n. 2, p. 227–238, 2009.

486 MAIA, L. P. et al. **Atlas dos manguezais do nordeste do Brasil**. Fortaleza: SEMACE, 2006.

487 MARINS, R. V. et al. Efeitos da açudagem no rio Jaguaribe. **Ciência Hoje**, v. 33, n. 197, p. 66–
488 70, 2003.

489 MARINS, R. V et al. Anthropogenic sources and distribution of phosphorus in sediments from
490 the Jaguaribe River estuary, NE, Brazil. **Brazilian Journal of Biology**, v. 71, n. 3, p. 673–678,
491 2011.

492 MENDOZA, W. G.; ZIKA, R. G. On the temporal variation of DOM fluorescence on the
493 southwest Florida continental shelf. **Progress in Oceanography**, v. 120, p. 189–204, 2014.

494 MENEZES, R. S. C. et al. Biogeochemical cycling in terrestrial ecosystems of the Caatinga
495 Biome. **Brazilian Journal of Biology**, v. 72, n. 3 suppl, p. 643–653, 2012.

496 MIDDELBURG, J. J.; HERMAN, P. M. J. Organic matter processing in tidal estuaries. **Marine**
497 **Chemistry**, v. 106, p. 127–147, 2007.

498 MOLISANI, M. M. et al. The influence of Castanhão reservoir on nutrient and suspended matter
499 transport during rainy season in the ephemeral Jaguaribe river (CE, Brazil). **Brazilian journal of**
500 **biology = Revista brasleira de biologia**, v. 73, n. 1, p. 115–23, 2013.

501 MOORE, S. et al. Deep instability of deforested tropical peatlands revealed by fluvial organic
502 carbon fluxes. **Nature**, v. 493, p. 660–663, 2013.

503 MOPPER, K. et al. Effects of cross-flow filtration on the absorption and fluorescence properties
504 of seawater. **Marine Chemistry**, v. 55, n. 1–2, p. 53–74, 1996.

505 MOUNIER, S. et al. Copper complexing properties of dissolved organic matter: PARAFAC
506 treatment of fluorescence quenching. **Biogeochemistry**, v. 106, n. 1, p. 107–116, 9 ago. 2011.

507 MOURA, V. L.; LACERDA, L. D. DE. Contrasting Mercury Bioavailability in the Marine and
508 Fluvial Dominated Areas of the Jaguaribe River Basin, Ceará, Brazil. **Bulletin of Environmental**
509 **Contamination and Toxicology**, v. 101, n. 1, p. 49–54, 2018.

510 OLIVEIRA, R. C. B. DE; MARINS, R. V. Trace Metals Dynamics in Soil and Estuarine
511 Sediment as a Major Factor Controlling Contaminants Contribution to the Aquatic Environment:
512 Review. **Revista Virtual de Química**, v. 3, n. 2, 2011.

513 OURSEL, B. et al. Dynamic and fate of trace metals chronic input in a Mediterranean coastal
514 zone impacted by a large urban area. **Mar.Pollut. Bull. In press**, v. 69, p. 137–149, 2013.

515 PINCKNEY, J.; PAERL, H. W.; BEBOUT, B. M. Salinity control of benthic microbial mat
516 community production in a Bahamian hypersaline lagoon. **Journal of Experimental Marine**
517 **Biology and Ecology**, v. 187, n. 2, p. 223–237, 1995.

518 PRASAD, M. B. K.; RAMANATHAN, A. L. Organic matter characterization in a tropical
519 estuarine-mangrove ecosystem of India: Preliminary assessment by using stable isotopes and
520 lignin phenols. **Estuarine, Coastal and Shelf Science**, v. 84, n. 4, p. 617–624, 2009.

521 QUÉRÉ, C. et al. Global Carbon Budget 2018. **Earth System Science Data**, v. 10, n. 4, p. 2141–
522 2194, 2018.

523 RALISON, O. H. et al. Carbon biogeochemistry of the Betsiboka estuary (north-western
524 Madagascar). **Organic Geochemistry**, v. 39, n. 12, p. 1649–1658, dez. 2008.

525 RAY, R.; SHAHRAKI, M. Multiple sources driving the organic matter dynamics in two
526 contrasting tropical mangroves. **Science of the Total Environment**, v. 571, p. 218–227, 2016.

527 RAYMOND, P. A.; BAUER, J. E. Use of 14 C and 13 C natural abundances for evaluating
528 riverine , estuarine , and coastal DOC and POC sources and cycling : a review and synthesis.
529 **Organic Geochemistry**, v. 32, p. 469–485, 2001.

530 REZENDE, C. E. et al. Lignin phenols used to infer organic matter sources to Sepetiba Bay - RJ,
531 Brasil. **Estuarine, Coastal and Shelf Science**, v. 87, n. 3, p. 479–486, 2010.

532 SAKHO, I. et al. A cross-section analysis of sedimentary organic matter in a mangrove ecosystem
533 under dry climate conditions: The Somone estuary, Senegal. **Journal of African Earth Sciences**,
534 v. 101, p. 220–231, 2015.

535 SANTINELLI, C.; NANNICINI, L.; SERITTI, A. DOC dynamics in the meso and bathypelagic
536 layers of the Mediterranean Sea. **Deep-Sea Research Part II: Topical Studies in**
537 **Oceanography**, v. 57, n. 16, p. 1446–1459, 2010a.

538 SANTOS, J. A. et al. Hydrochemistry and trophic state change in a large reservoir in the
539 Brazilian northeast region under intense drought conditions. **Journal of Limnology**, v. 76, n. 1,
540 p. 41–51, 2017.

541 SCHETTINI, C. A. F.; VALLE-LEVINSON, A.; TRUCCOLO, E. C. Circulation and transport in
542 short, low-inflow estuaries under anthropogenic stresses. **Regional Studies in Marine Science**, v.
543 10, p. 52–64, 2017.

544 SHIN, Y. et al. Hydrological Changes of DOM Composition and Biodegradability of Rivers in
545 Temperate Monsoon Climates. **Journal of Hydrology**, v. 540, p. 538–548, 2016.

546 SIERRA, M. M. S. et al. **A utilização da espectroscopia de fluorescência no estudo da matéria**
547 **orgânica dissolvida nas águas naturais: evolução e perspectivasQuímica Nova**, 1996.

548 SIMPSON, S. L. et al. Metal speciation and potential bioavailability changes during discharge
549 and neutralisation of acidic drainage water. **Chemosphere**, v. 103, p. 172–180, 2014.

550 SOUZA, M. F. L. et al. Nutrient budgets and trophic state in a hypersaline coastal lagoon: Lagoa
551 de Araruama, Brazil. **Estuarine, Coastal and Shelf Science**, v. 57, n. 5–6, p. 843–858, 2003.

552 SPENCER, R. G. M. et al. Seasonal and spatial variability in dissolved organic matter quantity
553 and composition from the Yukon River basin, Alaska. **Global Biogeochemical Cycles**, v. 22, n.
554 4, p. 1–13, 2008.

555 SPENCER, R. G. M. et al. Photochemical degradation of dissolved organic matter and dissolved
556 lignin phenols from the Congo River. **Journal of Geophysical Research: Biogeosciences**, v.
557 114, n. 3, p. 1–12, 2009.

558 STANLEY, E. H. et al. Contemporary changes in dissolved organic carbon (DOC) in human-
559 dominated rivers: Is there a role for DOC management? **Freshwater Biology**, v. 57, n. SUPPL. 1,
560 p. 26–42, 2012.

561 STEDMON, C. A.; MARKAGER, S. Resolving the variability in {DOM} fluorescence in a
562 temperate estuary and its catchment unsing {PARAFAC}. **Limnol.Oceanogr.**, v. 50, n. 2, p. 686–
563 697, 2005.

564 STEDMON, C. A.; RASMUS, B. Characterizing dissolved organic matter fluorescence with
565 parallel factor analysis: a tutorial. **Limnology and Oceanography: Methods**, v. 6, n. 11, p. 572–
566 579, 2008.

567 STOLPE, B. et al. Colloidal size distribution of humic- and protein-like fluorescent organic
568 matter in the northern Gulf of Mexico. **Marine Chemistry**, v. 164, p. 25–37, 2014.

569 TAREQ, S. M.; TANAKA, N.; OHTA, K. Biomarker signature in tropical wetland : lignin phenol
570 vegetation index (LPVI) and its implications for reconstructing the paleoenvironment. **Science**
571 **of the Total Environment**, v. 324, p. 91–103, 2004.

572 VAZQUEZ, E. et al. Dissolved organic matter composition in a fragmented Mediterranean fluvial
573 system under severe drought conditions. **Biogeochemistry**, v. 102, n. 1, p. 59–72, 2011.

574 WANG, W. et al. Size partitioning and mixing behavior of trace metals and dissolved organic
575 matter in a South China estuary. **Science of the Total Environment**, v. 603–604, p. 434–444,
576 2017.

577 WANG, X. C. et al. Stable carbon and nitrogen isotopic compositions of high molecular weight
578 dissolved organic matter from four U.S. estuaries. **Geochimica et Cosmochimica Acta**, v. 68, n.
579 12, p. 2681–2691, 2004.

580 WANG, Z. GANG et al. Composition analysis of colored dissolved organic matter in Taihu Lake
581 based on three dimension excitation-emission fluorescence matrix and PARAFAC model, and the
582 potential application in water quality monitoring. **Journal of Environmental Sciences**, v. 19, n.
583 7, p. 787–791, 2007.

584 WILKINSON, K. J.; LEAD, J. R. **Environmental colloids and particles: behaviour,**
585 **separation and characterisation BT - IUPAC series on analytical and physical chemistry of**
586 **environmental systems v. 10**. [s.l: s.n.].

587 WORRALL, F.; BURT, T.; ADAMSON, J. Can climate change explain increases in DOC flux
588 from upland peat catchments? **Science of The Total Environment**, v. 326, n. 1–3, p. 95–112, jun.
589 2004.

590 WU, Y. et al. Biogeochemical behavior of organic carbon in a small tropical river and estuary,
591 Hainan, China. **Continental Shelf Research**, v. 57, p. 32–43, abr. 2013.

592 XU, H. et al. Variations in size and composition of colloidal organic matter in a negative
593 freshwater estuary. **Science of the Total Environment**, v. 615, p. 931–941, 2018.

594 XU, H.; GUO, L. Molecular size-dependent abundance and composition of dissolved organic
595 matter in river, lake and sea waters. **Water Research**, v. 117, p. 115–126, 2017.

596 YA, C.; ANDERSON, W.; JAFFÉ, R. Assessing dissolved organic matter dynamics and source
597 strengths in a subtropical estuary: Application of stable carbon isotopes and optical properties.
598 **Continental Shelf Research**, v. 92, p. 98–107, 2015.

599 YANG, L. et al. Effects of microbial transformation on dissolved organic matter in the east
600 Taiwan Strait and implications for carbon and nutrient cycling. **Estuarine, Coastal and Shelf**
601 **Science**, v. 180, p. 59–68, 2016.

602 YANG, R.; VAN DEN BERG, C. M. G. Metal complexation by humic substances in seawater.
603 **Environmental Science and Technology**, v. 43, n. 19, p. 7192–7197, 2009.

604 YE, F. et al. Seasonal dynamics of particulate organic matter and its response to flooding in the
605 Pearl River Estuary, China, revealed by stable isotope (δ^{13} C and δ^{15} N) analyses. **Journal of**
606 **Geophysical Research: Oceans**, v. 122, n. 8, p. 6835–6856, 2017.

607 YE, F. et al. The sources and transformations of dissolved organic matter in the Pearl River
608 Estuary, China, as revealed by stable isotopes. **Journal of Geophysical Research: Oceans**,
609 2018.

610 YI, Y. et al. Optical properties of estuarine dissolved organic matter isolated using cross-flow
611 ultrafiltration. **Acta Oceanologica Sinica**, v. 33, n. 4, p. 22–29, 2014.

612 ZHAI, W.; DAI, M. On the seasonal variation of air - sea CO2fluxes in the outer Changjiang
613 (Yangtze River) Estuary, East China Sea. **Marine Chemistry**, v. 117, n. 1–4, p. 2–10, 2009.

614 ZHANG, A. et al. ENSO elicits opposing responses of semi-arid vegetation between
615 Hemispheres. **Scientific Reports**, v. 7, p. 1–9, 2017.

616